J.E.N.379
Sp ISSN 0081-3397

Instabilities in fluid layers and in reaction-diffusion systems: Steady states, time-periodic solutions, non-periodic attractors, and related convective and otherwise non-linear phenomena.(*)

por

Manuel García Velarde

(*) Research carried out in 1976 by Prof. Velarde and collaborators, under contract with the Instituto de Estudios Nucleares.

JUNTA DE ENERGIA NUCLEAR

MADRID, 1977

CLASIFICACION INIS Y DESCRIPTORES

A14; A11
CONVECTIVE INSTABILITIES
LYAPUNOV METHOD
CHEMICAL REACTION KINETICS
LANDAU FLUCTUATIONS
HYDRODYNAMICS
NONLINEAR PROBLEMS

Toda correspondencia en relación con este trabajo debe dirigirse al Servicio de Documentación Biblioteca y Publicaciones, Junta de Energía Nuclear, Ciudad Universitaria, Madrid-3, ESPAÑA.

Las solicitudes de ejemplares deben dirigirse a este mismo Servicio.

Los descriptores se han seleccionado del Thesauro del INIS para describir las materias que contiene este informe con vistas a su recuperación. Para más detalles consúltese el informe IAEA-INIS-12 (INIS: Manual de Indización) y IAEA-INIS-13 (INIS: Thesauro) publicado por el Organismo Internacional de Energía Atómica.

Este trabajo se ha recibido para su impresión en Marzo de 1977.

Depósito legal nº M-22336-1977 I.S.B.N. 84-500-2094-8

NOTA.

El presente trabajo corresponde al Informe #1 del equipo vii) Inestabilidades Hidrodinámicas en Plasmas, del Subprograma de la J.E.N. sobre Confinamiento Inercial, proyecto Laser-Fisión-Fusión, descrito en el Informe JEN-351.

PART I

THERMOCONVECTIVE FLOWS

1. Thin horizontal fluid layers vertically heated

   1.1 Bénard's cellular patterns

   1.2 Rayleigh's convection

2. Thermohydrodynamic description, and the Boussinesq-Oberbeck approximation

   2.1 The evolution equations

   2.2 The Boussinesq-Oberbeck model applicable to a thin layer of fluid

3. The boundary conditions for a horizontal fluid layer heated from below

   3.1 Thermal boundary conditions

   3.2 Mechanical boundary conditions, and surface deflection

4. A perturbative approach to the nonlinear fields

   4.1 Landau-Hopf scheme

   4.2 Thermal fluctuations and the onset of convection

5. Convective flows in realistic situations: quantitative results

6. Bifurcation of steady states

7. Time-dependent phenomena, and transition to turbulence

   7.1 Relaxation oscillations

   7.2 The unsteady flow, and the transition to turbulence

References

PART II

REACTION-DIFFUSION SYSTEMS: THE ROLE OF BINARY COLLISIONS, AUTOCATALYSIS, AND SATURATION LAWS. PERIODIC PHENOMENA.

PART III

NON-PERIODIC ATTRACTORS

1. Thin horizontal fluid layers vertically heated

1.1 Bénard's cellular patterns

It was at the turn of the last century that Bénard [1900] reported on carefully controlled experiments of convected motions in thin horizontal liquid layers heated from below. Since his [1900,1901] two papers (based on his Ph.D. dissertation), Bénard and collaborators devoted an extensive number of publications to the same subject-seeking in the phenomena he studied a tentative explanation of a large number of apparently disparate problems.

Bénard worked with layers thinner than about a millimeter (aspect ratio of 1/100 and less with error to about 1 μm) lying on a metallic plate which was heated and maintained at a uniform temperature. The upper surface of the liquid (mostly spermaceti of whale that melts at 46°C) was free, in contact with the ambient air that was at a lower temperature than the bottom plate, on occasions at 100°C. The detailed development of the phenomena he observed occurred in two distinct phases.

Firstly, when the vertical temperature drop was large enough, a random motion of the fluid resulted. Shortly thereafter, the first phase of relatively short duration (increasing with fluid viscosity from a few seconds up to several minutes) appeared in which the fluid formed cells of almost regular shapes. In this phase, the cellular cross-sections showed nearly regular polygons of four to seven sides. During the second stage the cells became equal and regularly spaced hexagons filling up the plane. Thus, the limit of the second

phase was a steady regime of prisms with vertical boundaries and hexagonal cross-sections. The liquid rose in the core of the cell, moved outward at the top, descended at the outer periphery and moved inward at the bottom. Incidentally, Bénard made the circulation visible by pouring in the fluid a few grains of lycopod of about 20 μm diameter, whose individual motion he was able to follow in detail. He correctly characterized the spatial periodicity of the phenomenon by defining its wavelength as the distance between centers of the hexagonal parallelepipeds.

A number of other important observations were also made by Bénard, that, unfortunately, most of the workers in the field (including Lord Rayleigh) have disregarded. Bénard attributed an important role in the phenomenon to surface tension inhomogeneities without, however, elaborating deeper on this point (Bénard [1901, pp. 92, 134, 135]). He carefully studied by sophisticated means originally developed by Foucault in telescope making industry, the free surface deflection and gave quantitative estimates of the maximum values of depression and elevation from the surface level. He estimated the surface deflection at maximal 0.5 μm with a 1 mm. deep layer under his best experimental circumstances.

On the other hand, we rather expect a flattening of the free surface on increasing cell depth and eventually a transition to a deflected surface for larger cell gaps with elevation in the areas of upwelling fluid (see, however, our discussion in Section 5 below). But that depression correlates to upwelling fluid flow in surface tension-driven convection

as noted by Bénard, does not seem to be so well established. Berg et al. [1966] did find the opposite configuration on repeating one of Bénard's experiments using approximately 1 mm-thick layers of melted wax, and found elevation that occurred above cell centers.

Another result also described by Bénard is that on decreasing the thermal gradient the surface deflection is first drastically reduced, then later disappears very slowly with the temperature drop. This was achieved by merely letting the spermaceti layer cool off from 100° down to solidification (46°C). Bénard's thermal gradients were of about a degree per millimeter. Incidentally, Dauzère [1907] produced solidified Bénard cells by quickly cooling a thin layer of melted beeswax undergoing convection. At the same time he also found an analogous behavior for the convective velocity and the heat flux. The heat flux was linearly depending on the (linear) velocity field at a given point. He estimated the angular and linear convective velocities and the mean periods of circulation of suspended particles in the fluid.

Bénard heuristically and correctly attributed the surface deflection to surface tension tractions: "La tension superficielle à elle seule, provoque déja une depression au centre des cellules et un excès de pression sur les lignes de faîte qui séparent les cuvettes concaves les unes des autres" (Bénard [1901], p. 92; see also p. 134). He also gave an estimate of minimum curvature radius at both depression at the cells' center (30 cm. - 50 cm.) and elevation at the cells' edges (10 cm. - 15 cm.) at 100°C and 1 mm. layer depth.

Bénard measured carefully the surface area, s, of the cells, and compared it with the depth of the fluid layer in a number of experiments.

Lord Rayleigh [1916] investigated the dynamical origin of Bénard's cells. His analysis yielded the fundamental result that a top-heavy fluid layer was stable under the joint influence of viscosity and heat diffusion until the vertical temperature drop was large enough to overcome these two dissipative and stabilizing mechanisms. Lord Rayleigh found that the sole parameter determining stability was the temperature difference made dimensionless by a combination of parameters that yield what is now known as the Rayleigh number $Ra = \alpha g \Delta T d^3 / \kappa \nu$. This is also the product of Prandtl number times Grashof number. Thus, Lord Rayleigh discovered that convective flow sets in when the rate at which (free) energy is liberated by the uprising of the hot, less-dense fluid near the base exceeds the rate at which energy is dissipated by thermal conduction and viscous damping. This argument was later taken up to construct a variational principle (see Section below) that governs the (linear) mathematical stability problem (for historical remarks and details see Chandrasekhar [1961], Jeffreys [1956], Pellew and Southwell [1940] and Sani [1963]).

About twenty years after the publication of Lord Rayleigh's masterly analysis, several writers remarked on the inadequacy of Rayleigh's quantitative predictions, on two relevant counts. Firstly, Vernotte [1936-a,b] realized that "en recalculant les anciennes mesures de Bénard, on trouve, dans l'experience effectuée avec une epaisseur de

spermaceti égale a 1 mm., qui semble la meilleure au point de vue thermique, une valeur du nombre de Rayleigh critique, dont on que l'ordre de grandeur, mais qui se situe entre 5 et 10" ... instead of 657 as given by Rayleigh (for stress-free surfaces). As a matter of fact, Low and Brunt 1925 seem to have been the first to notice that the gradients in Bénard's experiments were at least tenfold less than required by the theory of Lord Rayleigh [1916]. Later, Bénard himself recognized the discrepancy (Bénard [1927, 1928]) and estimated the ratio at 10^{-4} or 10^{-5} , though Vernotte's estimate is roughly 10^{-2}. It is rather unlikely that so large a discrepancy arises solely from inaccurate boundary conditions. Yet a serious attack of the problem had to wait twenty years longer.

Secondly, the wavelength of the cellular pattern predicted by Lord Rayleigh was not fitting Bénard's results so well. Vernotte's arguments did not lead, however, to a more suitable and fertile theory of Bénard convection (see also Volkovisky [1939]). Though Vernotte [1936a, p. 119] asked the right question: "A-t'on le droit d'employer le principe d'Archimède et d'écrire, comme le fait Lord Rayleigh, les équations de la convection?".

It was not until the 1950's that scientists realized the necessity of incorporating surface-tension stresses in a dynamical model of Bénard convection. This became a necessity when Block [1956] found Bénard 'cellules' in horizontal layers of fluid, when the higher temperature was on the upper side. A straightforward and illuminating theoretical description of

surface-tension-driven convection was given in a paper by Pearson [1958]. Pearson's model did not adequately accomodate all of Block's findings, as we shall see below. In retrospect, it is pitiful that Bénard did not explore the role of surface-tension inhomogeneities that he however recognized as eventually important in his experiments (see also Volkovisky [1935]). A persistent misinterpretation of Bénard's hexagonal cells makes writers even today illustrate buoyancy-driven convection with some of the beautiful original pictures of Bénard.

On the side, we recall that Bénard's experiments referred to above concern the stability of fluid layers uniformly heated from below. Providing a non-uniform temperature at the bottom one is able to force the appearance of hexagonal or any other polygonal patterns. Much more so than a piece of poetry or the experimenter's signature could, in principle, be convectively constructed! (see Koschmieder [1975]).

Another remark that Bénard made and that still remains a puzzling question to us is that probably the air layer on top of the spermaceti was strongly convecting. This was one of the mechanisms that he advocated for the heat exchange between the spermaceti and the upper air. Has the convecting air layer any influence on the hexagonal tesselation? Koschmieder [1967] investigated this point. Straightforward and simple calculations, using the scanty data provided by the experimenters, permit us to think that the air layer on top of the spermaceti should have always been convecting. Bénard convection with a two-liquid layer heated from above or below would probably help clarify the issue.

Further experiments on Bénard surface tension-driven convection had been conducted by Terada [1928], Volkovisky [1939], Block [1956], Koschmieder [1966,1967] and others. Volkovisky and Terada worked with fluid layers flowing horizontally with a controlled preimposed horizontal velocity. Their results reinforce the picture already presented by Bénard and we shall not discuss them here. Block was the first to point out that Bénard's cell can be obtained by cooling a layer from below. Block was also able to suppress convection by adding tensioactive agents to the upper surface of the layer. Koschmieder was the first to remark that two bifurcations do contend to finally show up the second one. For in a finite box, the form of the boundaries impose a transient primary flow before the hexagonal tesselation develops at the steady state. Whether or not the primary phenomenon is an example of inverted bifurcation is something that remains open.

These facts together with the output from experiments conducted by astronauts on board the Apollo XIV and Apollo XVII spaceships where gravity was 10^{-6} g on Earth (see Grodzka and Bannister [1972,1975]) unambiguously manifest that gravity was rather playing a minor role, if any, in most of Bénard's original experiments. Surface tension-driven convection can be considered as a specific phenomenon qualitatively different from buoyancy-driven flows. Theories that support this view have been developed first by Pearson [1958] and later, and more realistically, by Sternling and Scriven [1959], Scriven and Sternling [1964], Smith [1966], Bentwich [1971]. There is

also the work of Nield [1964], who described the convective flows when surface tension and buoyancy are operating in the fluid layer. We shall describe Nield's predictions further below.

Lastly, we note that a standard Newtonian and Boussinesquian liquid layer, say of silicone oil, heated from below and constrained between two horizontal conducting plates accomodates patterns of rolls at and beyond a certain critical temperature difference. That agrees nicely with Rayleigh's predictions (as later improved upon by many authors; see for details Chandrasekhar [1961] or the monograph of Velarde and Pomeau [1977]). The particular orientation of these rolls is strongly influenced by the lateral geometry of the container. However, non-Newtonian and/or non-Boussinesquian fluid layers may not follow the same pattern. Symmetry-breaking mechanisms such as a kinematic viscosity strongly dependent on temperature or different b.c. at the horizontal plate boundaries may force a pattern-formation of its own. The hexagonal cell pattern under an air surface developed on a pattern of rolls. These transient circular rolls reflect the unavoidable existence of a lateral wall. Recent experiments by Hoard et al. [1970], with a rather peculiar aromatic hydrocarbon (Aroclor 1248) which has a viscosity varying exponentially with temperature, support this conjecture. No definite theoretical explanation exists, however, to account for all findings of Hoard et al. though theories seem to point in the right direction since the pioneering work of Palm [1960] (see Segel and Stuart [1962], Palm and Øiann [1964], Joseph [1971] and Velarde [1976,1977]).

1.2 Rayleigh's convection: an heuristic approach

The problem that concerns us here is the stability of a horizontal (standard) liquid layer heated from below in the presence of gravity. According to Lord Rayleigh, above a critical temperature difference the system falls away from unstable equilibrium and it may do so in several principal modes, in each of which the departure at time t may be assumed to be proportional to the small displacement of velocity supposedly present initially, and to an exponential factor $e^{\sigma t}$, where σ is positive. If the initial disturbances are small enough, that mode (or modes) of falling away will become predominant for which σ is a maximum. When it becomes difficult to prove the maximum growth of a mode, the criterion of (experimental) realizability is rather: the unstable mode that develops belongs to the minimum value of the external constraint, namely the mode corresponding to the smallest temperature difference. Both criteria are expected to provide the same answer.

Let us consider a bubble of hot fluid, of radius R, and which according to Archimedes' law moves upward with a constant velocity V in a fluid layer where a constant linear temperature gradient is maintained. An heuristic and appealing argument will show that, if the mean temperature gradient is large enough, then the upward buoyancy force on the bubble may overcome the drag force due to the viscosity of the fluid (actually it could be also proved that the downwards motion of a cold bubble may become unstable). This viscous drag force on the uprising bubble is in a first approximation (defined here by the condition $VR/\nu \ll 1$; this corresponds to low Reynolds

number, see section below) of order $-\eta RV$. With η we denote the shear viscosity of the liquid and ν is its kinematic viscosity ($\nu = \eta/\rho$, where ρ is density). On the other hand, the buoyancy force arises from the instantaneous difference between the fluid density and temperature in the bubble and its local neighborhood. The relaxation time of the bubble's temperature fluctuation, as due to heat diffusivity is $\tau \sim R^2/\kappa$, where κ denotes the thermometric conductivity (also called thermal diffusivity). This means that at a given instant of time, t, the temperature within the bubble is about that of its surroundings at an earlier instant of time, $t - \tau$; so that at time t the temperature difference T between the bubble and the fluid is $\delta T = |\text{grad } T| V\tau = |\text{grad } T\, VR^2/\kappa$, which yields an Archimedean buoyancy force $F_b = \rho\alpha\delta T R^3 g = \rho\alpha R^5 g |\text{grad } T| V/\kappa$. Here $\alpha = \frac{1}{\rho}(\partial\rho/\partial T)$. Thus, the motionless steady state approaches unstable equilibrium when this buoyancy force slightly overcomes the viscous drag. The actual ratio of buoyancy to drag obviously increases with the size of the bubble; so that instability eventually begins for bubbles of maximum size, of say height $\underline{d}$, compatible with the boundaries of the container. Thus, at the unstable equilibrium position we have $|F_b| \gtrsim R\eta|V|$ or else $Ra \gtrsim 0(1)$, with $Ra = \frac{\alpha d^4 |\text{grad } T| g}{\kappa\nu}$. With this rough estimate we cannot however claim any quantitative value of the critical temperature drop for the onset of convection. We merely single out which dimensionless combination of parameters is to be of relevant use in the mathematical stability analysis that will be given below. This result was indeed achieved by Lord Rayleigh (1916). Remarkable enough it appears that for liquids of vanishing viscosity all modes of disturbance ought to be unstable, even when we include the conduction of heat during the disturbance. Roughly speaking, it

suffices à vanishing small vertical temperature gradient to yield natural convective flows in compressible ideal liquid horizontal layers when the higher temperature is below.

Furthermore, the heuristic argument developed above also shows that if the thermometric conductivity vanishes there is always convective instability when heating a fluid layer from below; but if κ and ν are finite and large enough, a motionless steady state can be maintained for (not too large) vertical temperature differences, although a higher temperature is underneath.

The argument easily carries over to (non-Newtonian) power law fluids, and yields an important consequence. In a power law the stress-strain relation is given by a law $\omega(\frac{\partial V}{\partial y})^m$ where ω and m are two material parameters; V and the coordinate y are taken transverse to each other. Thus, we have a viscous drag of order $\omega R^2 (V/R)^m$. Then the unstable equilibrium condition is $\omega R^2 (V/R)^m \lesssim \rho\alpha R^5 Vg|\text{grad } T|/\kappa$. From which it follows

$$\left(\rho\alpha V^{1-m} R^{3+m} g\,|\text{grad } T|/\varkappa\omega\right) \gtrsim 1$$

The Newtonian fluid layer, namely the case m = 1, and $\omega = \nu$, yields back $Ra_c \gtrsim 0(1)$. It thus appears as a case where the onset of convection does not explicitly depend on the (experimentally uncontrollable) initial disturbances.

In our heuristic argument developed above, we have disregarded compressibility effects. It is instructive, however, to discuss the physical relevance of such effects as they play an important role in atmospheric circulation and the convective motions in the deep ocean.

Suppose now that the bubble is adiabatically isolated by a membrane impervious to matter, but which may freely expand if the pressure of the surrounding fluid is decreased. The fluid, for simplicity, is assumed inviscid. Let $\rho(z)$ denote the density at the bubble's center at height z, and at a temperature T. Suppose that an external weak-enough force is applied so as to slowly raise the bubble to a new height $z + \rho z$ without, however, appreciably disturbing its neighborhood. Such a slow motion is taken adiabatic, and moreover, isentropic. The bubble's adiabatic expansion will change its density to

$$\rho(z+\delta z) = \rho(z) + \chi_s \rho \, dp = \rho(z) - \chi_s \rho^2 g \, \delta z \qquad (1)$$

where use has been made of the adiabatic compressibility $\chi_S = \frac{1}{\rho}(\frac{\partial \rho}{\partial P})_S$, a derivative taken at constant entropy (or heat flux). Also, we have introduced the corresponding hydrostatic pressure variation $\delta p = -\rho g \delta z$. Accordingly, the Archimedean buoyancy force per unit mass acting on the bubble at the new height is equal to the local volume of the bubble times the (mean) local density of the surrounding fluid, called $\bar{\rho}$. Thus, the net Archimedean uprising force per unit mass is

$$\frac{g}{\rho}\left[\bar{\rho}(z+\delta z) - \rho(z+\delta z)\right] = \frac{g}{\rho}\left[\frac{\partial \bar{\rho}}{\partial z} + \chi_s \rho^2 g\right]\delta z \qquad (2)$$

This equation determines the magnitude of the external force which is required in order to maintain the bubble in equilibrium at the new height $z + \delta z$. Removal of such an external force yields an accelerated motion of the bubble, whose time evolution is

governed by Newton's law

$$\frac{d^2}{dt^2}\delta z = g\left[\frac{1}{\rho}\frac{\partial \bar{\rho}}{\partial z} + \chi_s \rho g\right]\delta z \equiv \frac{g}{\rho}\left[\frac{\partial \bar{\rho}}{\partial z} - \left(\frac{\partial \bar{\rho}}{\partial z}\right)_{adiab.}\right]\delta z \qquad (3)$$

in which $(\partial\bar{\rho}/\partial z)_{adiab.}$ denotes the (mean) adiabatic gradient. This Eq. (3) describes a vibrating motion of angular frequency N, where

$$N^2 = -\frac{g}{\rho}\left[\frac{\partial \bar{\rho}}{\partial z} - \left(\frac{\partial \bar{\rho}}{\partial z}\right)_{adiab.}\right] \qquad (4)$$

The quantity N is called the Brunt-V$\ddot{a}$is$\ddot{a}$l$\ddot{a}$ frequency (or the buoyancy frequency) in meteorology and oceanography. It corresponds to the natural frequency of oscillation of a vertical column of fluid given a small displacement from its initial equilibrium position. The corresponding periods $2\pi/N$ are typically of a few minutes in the atmosphere up to many hours in the deep ocean.

Notice that if the fluid is (almost) incompressible and the density gradients are linear then the Brunt-V$\ddot{a}$is$\ddot{a}$l$\ddot{a}$ frequency is a constant. As in a resting, isothermal fluid column there can be acoustic (or high-frequency) waves and gravity (or low-frequency) waves the quantity N yields a separation between these two classes of wave motion in the fluid.

The Brunt-V$\ddot{a}$is$\ddot{a}$l$\ddot{a}$ frequency in a fluid medium gives an indication of static stability. Real values of N mean stable, zero frequencies mean neutrally stable, and negative values of N^2, namely imaginary values of the Brunt-V$\ddot{a}$is$\ddot{a}$l$\ddot{a}$ constant would imply instability. If we move the bubble upwards a small distance, then in a stable stratified medium it would be too heavy, so it

would sink down, and if there were no friction it would overshoot, and then it would be too light, and it would oscillate with frequency N.

Stability for an incompressible fluid layer reduces according to definition (4) to the condition $\frac{\partial \bar{\rho}}{\partial z} < 0$. Thus, an incompressible inviscid (or ideal) fluid layer is unstable if its stratification is mechanically unstable. This intuitive statement is far from true in real fluid layers where cross-transport phenomena may be operating (see for instance Velarde and Schechter [1972]). The condition of instability for a compressible inviscid fluid, namely that N^2 be negative, is called in Astrophysics the Schwarzchild criterion.

Alternative expressions to (4) can be obtained by straightforward use of elementary thermodynamic relations. Let us consider the equation of state $\rho = \rho(T,p)$. Thus

$$\frac{1}{\rho}\frac{\partial \rho}{\partial z} = \chi_T \frac{dp}{dz} - \alpha \frac{dT}{dz} = -\rho g \chi_T - \alpha \frac{dT}{dz} \tag{5}$$

where $\chi_T = \frac{1}{\rho}\left(\frac{\partial \rho}{\partial p}\right)_T$ is the isothermal compressibility. Thus we have

$$N^2 = g\left[\alpha \frac{\partial \bar{T}}{\partial z} + \rho g(\chi_T - \chi_s)\right] = g\left[\alpha \frac{\partial \bar{T}}{\partial z} + \frac{\alpha^2 g T}{c_p}\right] \tag{6}$$

The Brunt-Väisälä frequency vanishes when the fluid (mean) temperature gradient is

$$\frac{\partial \bar{T}}{\partial z} = -\frac{g\rho}{\alpha}\left(\chi_T - \chi_s\right) = -\frac{gT\alpha}{c_p} \tag{7}$$

In such a case our bubble's and the surrounding fluid's density and pressure are equal. Therefore, the adiabatic temperature change

of the bubble, say T, is equal to $\frac{\partial \bar{T}}{\partial z}\delta z$, and using (7) we get

$$\frac{\delta T}{\delta z} = -\frac{g\rho}{\alpha}(\chi_T - \chi_s) = -\frac{\alpha g T}{c_p} \quad \text{or} \quad \delta\left[T + \frac{z\rho g}{\alpha}(\chi_T - \chi_S)\right] = 0 \tag{8}$$

The quantity $T + \frac{z\rho g}{\alpha}(\chi_T - \chi_S)$ is called the potential temperature in atmospheric convection analysis. We see that in the absence of dissipation and heat transfer this potential temperature is conserved. Notice that according to (8) the bubble's temperature is conserved in slow motions, when $(\chi_T - \chi_S)$ is small, namely when the speed of sound in the fluid medium is very large. The velocity of sound in a fluid is equal to

$$c = \left(\frac{\partial p}{\partial \rho}\right)_s^{1/2} = (\rho \chi_s)^{-1/2} \tag{9}$$

Hence, for a slow adiabatic process

$$\delta\rho = \left(\frac{\partial \rho}{\partial p}\right)_s \delta p \sim \rho V^2/c^2 \tag{10}$$

Thus, the condition $V \ll c$ amounts to a situation with small density contrasts $\delta\rho/\rho \ll 1$. This corresponds to the Boussinesq-Oberbeck approximation.

There remains the discussion of the stability criterion for a viscous compressible fluid layer. We shall then bridge the gap between our two previous and disconnected reasonings. At the same time, a more transparent interpretation of the Rayleigh number, as well as of the Brunt-Väisälä constant will come out.

When a dissipative transport process is introduced, it usually yields a characteristic relaxation time or say a characteristic frequency. Let viscosity and heat transport be the two dissi-

pative processes operating in our fluid layer. Let us disregard compressibility effects at present, for simplicity. We have found above that stability is governed by the condition (note that here $\frac{\partial \bar{T}}{\partial z}$ is negative when the heating is from below)

$$Ra = -\alpha g d^4 \left| \partial \bar{T}/\partial z \right| / \varkappa \nu \gtrsim 1 \qquad (11)$$

Eq. (11) can be written in terms of the Brunt-Väisälä constant, N, namely $Ra = \frac{-N^2 d^4}{\kappa \nu}$. Thus, condition (11) is equivalent to

$$-N^2 \gtrsim \varkappa \nu / d^4 \qquad (12)$$

for a viscous heat dissipating incompressible fluid layer heated from below. Notice that the introduction of dissipative dynamic mechanisms provides a lower bound value to the characteristic Brunt-Väisälä constant of the layer. One is tempted to state that dissipation rather plays a stabilizing role when a fluid layer tends to be destabilized by an external (thermal) constraint. Examples exist, however, that show viscous damping playing a dual role both stabilizing and destabilizing depending on certain conditions of operation (see for instance Lin [1967, p. 47], and Yih [1961]). If now, and according to our previous arguments we recall that incorporating compressibility merely amounts to readjusting the actual thermal (temperature or density) gradient in situ to its excess over the adiabatic value, the stability criterion for a viscous and compressible fluid layer is given by the

same criterion (11). One needs only to replace $\frac{\partial \bar{T}}{\partial z}$ by the corresponding factor appearing in the Brunt-Väisälä frequency, Eq. (6). This was the suggestion of Jeffreys [1930]. Lastly, it remains to discuss whether the upwelling fluid at the cells' centers provokes, in predominantly buoyancy-driven convection, a surelevation of an open surface to air.

2. Thermohydrodynamic description and the Boussinesq-Oberbeck approximation

2.1 The evolution equations

The governing equations of Newtonian fluid flow are the transport balance equations and the two equations of state (mechanic and caloric) which represent the field theoretic description of a continuum where we shall assume that the Gibbs local equilibrium assumption holds (see for instance Prigogine [1949], Nicolis, Wallenborn and Velarde [1969]). As a matter of fact, we shall also restrict our consideration here to the simplest realistic continuum: a standard Newtonian fluid. We are interested in the combined interplay of the basic fundamental equations of mass transport, momentum (or vorticity) transport (also called fluid flow) and energy transport (or heat). There is a straightforward analogy between all the three balance equations if one chooses the physical quantities and the (approximate) linear phenomenological laws in the proper manner. We shall, however, not dwell on this basic though rather academic question and shall merely reproduce the equations as derived for instance in the textbook of Landau and Lifshitz [1959] (see also Bird, Stewart and Lightfoot [1960]). For the time being we shall also restrict our consideration to single-component fluids. The first equation is the equation of continuity and expresses the (global) conservation of matter,

$$\frac{\partial}{\partial t}\rho + \frac{\partial}{\partial x_i}\rho V_i = 0 \quad \text{or alternatively} \quad \frac{d\rho}{dt} = -\rho \, \mathrm{div}\, V \qquad (1)$$

in which ρ and V denote respectively density and velocity.

Next we express Newton's fundamental law as set for a continuum by Euler

$$\rho \frac{\partial V_i}{\partial t} + \rho V_k \frac{\partial V_i}{\partial x_k} = \rho F_i - \frac{\partial P}{\partial x_i} + \frac{\delta \tau_{ik}}{\partial x_k} \qquad (2)$$

rate of increase of (linear) momentum per unit volume, namely the local acceleration	rate of momentum gained per unit volume by convection; inertia terms	external source of momentum or body force per unit volume	rate of momentu gained per unit volume by tractions; pressure and viscous fo ces

Here F_i, p and σ_{ik} denote external force, pressure and stress tensor.

We shall approximate the stress-strain relation by the Navier-Stokes model(*)

$$\sigma_{ik} = \eta \left(\frac{\partial V_i}{\partial x_k} + \frac{\partial V_k}{\partial x_i} - \frac{2}{3} \delta_{ik} \frac{\partial V_\ell}{\partial x_\ell} \right) + \xi \delta_{ik} \frac{\partial V_\ell}{\partial x_\ell} \qquad (3)$$

in which η and ζ denote respectively shear and bulk viscosity.

Thus, if η and ζ are taken as constants, a compact form to (2) is

$$\rho \frac{\partial V}{\partial t} + \rho V \cdot \text{grad } V = \rho F - \text{grad } P + \eta \, \text{div grad } V + (\xi + \eta/3) \, \text{grad div } V \qquad (4)$$

(*) Every time that two indices are repeated the summation convection is used. Elastic stress refers to the material's response to volume changes but it is to be noted that there are two kinds of viscous stresses: those generated by the material to oppose volume changes and the stresses generated by the material to oppose changes of shape. Real fluids with a non-vanishing bulk viscosity exhibit both viscous and elastic behaviour under isotropic pressure.

There are authors who instead of using ζ to define a bulk viscosity coefficient, use $\lambda = \zeta - 2\eta/3$. Cross-differentiating Eq. (4) in a convenient way, namely taking the curl of v in the absence of external forces or with gradient forces, the pressure field can be made to disappear and defining the vorticity $\underset{\sim}{\omega} = \text{rot}\underset{\sim}{v} = \text{curl}\ \underset{\sim}{v}$, we get

$$\frac{\partial \omega}{\partial t} = \text{rot}\,(V \wedge \omega) + \nu\ \text{div grad}\ \omega \qquad (5)$$

in which the kinematic viscosity, ν, appears as the coefficient of vorticity diffusion.

The (internal) energy balance is

$$\rho \frac{\partial \epsilon}{\partial t} + \rho V_k \frac{\partial \epsilon}{\partial x_k} = -\frac{\partial q_i}{\partial x_i} + \sigma_{ik} \frac{\partial V_i}{\partial x_k} + \rho Q \qquad (6)$$

rate of gain of (internal) energy including convective contributions	heat flow or energy increase by conduction	viscous heating due to surface tractions	energy generatin by internally di tributed sources or chemical processes, etc....

In Eq. (6) ϵ, q and Q denote respectively internal energy density, heat current and internal heat source within the fluid layer.

We shall restrict ourselves here to Fourier's heat law

$$q = -k\ \text{grad}\ T \qquad (7)$$

in which k is the coefficient of heat conductivity that we take constant.

The energy balance or heat equation can also be expressed in terms of the (local) entropy density, s,

$$\rho T \frac{ds}{dt} = \rho T\left(\frac{\partial s}{\partial t} + V.\,\mathrm{grad}\, s\right) = -\mathrm{div}\, q + \sigma : \mathrm{grad}\, V + \rho Q \tag{8}$$

Thus, entropy is a conserved quantity in the absence of viscosity, heat flow and internal sources. A more convenient and familiar equation comes with the use of the temperature field. After some elementary manipulations, a general heat equation follows from Eq. (8),

$$\rho c_v \frac{dT}{dt} + T\left(\frac{\partial p}{\partial T}\right)_\rho \mathrm{div}\, V = \mathrm{div}\, q - \sigma : \mathrm{grad}\, V + \rho Q \tag{9}$$

Alternative forms of the l.h.s. of (9) are

$$\rho T \frac{ds}{dt} = \rho c_v \frac{dT}{dt} - \frac{T}{\rho}\frac{\alpha}{\chi_T}\frac{d\rho}{dt} = \rho c_p \frac{dT}{dt} - \alpha T \frac{dp}{dt} \tag{10}$$

where α and χ_T are respectively the volumetric expansion coefficient and the isothermal compressibility, and c_v is the specific heat at constant volume.

From Eq. (9) a number of useful and more familiar approximations follow. In the absence of internal sources and with no viscous heating, and using Fourier's law (7) holding $\underline{k}$ constant, we have:

(i) for an ideal gas

$$\rho c_v \frac{dT}{dt} = k\, \mathrm{div}\, \mathrm{grad}\, T - p\, \mathrm{div}\, V \tag{11}$$

(ii) for an incompressible fluid, $\frac{d\rho}{dt} = 0$ and $c_v = c_p$

$$\rho c_p \frac{dT}{dt} = k\, \mathrm{div}\, \mathrm{grad}\, T \tag{12}$$

(iii) for a quasiincompressible fluid or a fluid at constant pressure namely a fluid with $s = s(T)$ or $\rho = \rho(T)$ and $\frac{dp}{dt} = 0$, we have

$$\rho c_p \frac{dT}{dt} = \rho c_p \frac{\partial T}{\partial t} + \rho c_p V.\text{grad}\,T = k\,\text{div grad}\,T \qquad (12)$$

The thermometric conductivity or coefficient of heat diffusivity is $\kappa = k/\rho c_p$ whose dimensions are the same as those of the kinematic viscosity, ν.

2.2 The Boussinesq-Oberbeck model applicable to a thin layer of fluid

The essential feature of the thermohydrodynamic description just given above is that the density, velocity and temperature fields are interdependent. Indeed, even though the fluid velocity may be due entirely (like in Rayleigh-Bénard convection) to the action of buoyancy (Archemedian) forces arising from density variations, this density distribution as well as the temperature field, is modified as soon as the fluid moves. Note that energy is first transported by conduction, described by the r.h.s. of Eq. (9), which induces the velocity disturbance through the buoyancy mechanism. The latter is accounted for the first term in the r.h.s. of Eq. (4) where F is taken constant and ρ varies with temperature. The extent of this coupling is affected by the Prandtl number, and for instance in liquids with small Prandtl number, like the liquid metals, the thermal conduction proceeds rapidly and the velocity also develops quickly. These facts together with the non-linearity of the inertia terms suffice to generate an

(almost) intractable differential problem. Besides, all parameters like η, k, ... are at least functions of the relevant thermodynamic independent variables, say P and T. A number of people have tried to reduce the mathematical complexity of the problem to the most extreme though relevant and useful simplification. The simplest model in the literature carries the name of Boussinesq though a number of authors had used it long before Boussinesq. We now merely state the heuristic argumentation that drastically applied yields the Boussinesq-Oberbeck model: (i) The system will consist of a thin horizontal fluid layer heated from below between two rigid plates or a fluid layer between a rigid plate and an upper surface open to ambient air. In an experimental situation at least two different length scales are involved: the vertical depth of the fluid and its lateral extent, called respectively d and L. We shall consider $(d/L) \ll 1$. d/L defines an aspect-ratio. The only external mechanical force to be considered is gravity and it will be assumed that the acceleration of gravity (g) is constant throughout the layer and is directed vertically downwards. (ii) Variations in density are assumed to be brought about only by moderate heating (the isothermal compressibility is ignored) and are taken into account only in the buoyancy term of the Navier-Stokes equations. This implies that any convective velocity is much smaller than the speed of sound in the fluid, and that any accelerations in the fluid are much less than g. Thus, density differences are considered to be much smaller than the mean density. Thus, the effects of compressibility and of adiabatic temperature gradient are

disregarded. This assumption is easily justified in standard Rayleigh-Bénard experiments, since the expected pressure contribution to the variation of density is about two orders of magnitude smaller than that due to the temperature field. Roughly, the density variation is of order of magnitude(*) $\rho\chi_T gd$. The ratio of the pressure effect to the temperature effect is $|\chi_T \rho g d/\alpha\Delta T| \sim \frac{10^2 \chi_T \rho}{\alpha}$ for a $\Delta T \sim 10$ and $d \sim 1$ CGS units. Thus, for a water layer at room temperature and atmospheric pressure, $\alpha \sim 10^4 °C^{-1}$ and $\chi_T \sim 10^{-5}$ atm$^{-1} \sim 10^{-11}$ CGS units; whereas for air $\alpha \sim 10^{-3} °C^{-1}$, $\chi_T \sim 10^{-6}$ CGS units and $\rho \sim 10^{-3}$ CGS units. Thus, for a water layer we have an estimate of $|\chi_T \rho g d/\alpha\Delta T| \sim 10^{-5}$ whereas for the layer of air it amounts to 10^{-2}. It can safely be disregarded. (iii) The fluid properties η, k, c_p and α are assumed to be constant and obviously ζ is disregarded due to condition (ii) above. On occasion in standard Rayleigh-Bénard experiments this may be one of the quantitatively less well founded assumptions. (iv) The rate of heat generation is assumed to be zero and the irreversible degradation of momentum (energy) into heat which is described by viscous dissipation is neglected (Di = 0).

With the above stated approximations the evolution equations reduce drastically though they still do not yield a simple problem. The caloric equation of state is approximated by a truncated Taylor expansion

$$\rho = \rho_0 [1 - \alpha(T - T_0)] \qquad (1)$$

(*) A pressure of 200 atm. is required to increase the density of water by one per cent; values of the order of one hundred atm. are also normal for other liquids. And even at the enormous pressures present in the extreme depths of the ocean the density does not exceed its surface value by more than five per cent. A flow would have to have a velocity of about two hundred ms.$^{-1}$ to produce a pressure rise of two hundred atm.

where ρ_o is some constant reference density at temperature T_o, and the volume expansion coefficient α is evaluated at this reference state.

The continuity equation describes a solenoidal field

$$\text{div } V = 0 \tag{2}$$

The Navier-Stokes equation reduces to

$$\frac{dV}{dt} = \frac{\partial}{\partial t} V + V \cdot \text{grad} V = -\alpha (T - T_o) g - \frac{1}{\rho_o} \text{grad } p + \nu \, \text{div grad} V \tag{3}$$

where $g = (0,0,-g)$ and $\nu = \eta/\rho_o$. Thus, we consider that the acceleration due to the buoyancy might be even larger than the inertial acceleration due to the convective term in the r.h.s. of (3).

The heat equation is merely

$$\frac{dT}{dt} = \frac{\partial}{\partial t} T + V \cdot \text{grad} T = \varkappa \, \text{div grad } T \tag{4}$$

where a second equation of state $\varepsilon = c_p T$ has been used, and here $\kappa = k/c_p \rho_o$.

For a formal derivation and details see Pérez Cordón and Velarde [1975] and Velarde and Pérez Cordón [1976].

3. The boundary conditions for a horizontal fluid layer heated from below

In the previous section, we have presented the thermohydrodynamic description of the spatial and time evolution of a fluid layer. We are dealing with a set of nonlinear partial differential equations and a discussion of initial conditions as well as boundary conditions naturally follows.

To properly fix the initial conditions in our stability problem poses a delicate problem. A realistic description of an initial state of the fluid would force us to the introduction of stochastic initial values. This is beyond the present status of the theory and surely beyond the limited scope of our paper (see, however, Newell, Lange and Aucoin [1970]). On the other hand, and at least for the first instability problem that we are considering here, our interest is restricted to steady state solutions of the time-dependent problem. This means that we are interested in the asymptotic behavior, for large intervals of time ($t \to \infty$) of the thermohydrodynamic equations for given external constraints. Thus, we may simply disregard the initial value problem here, though it is to be noted that in nonlinear problems a classification of the initial conditions may very well yield a classification of solutions.

3.1 Thermal boundary conditions

Explicit and detailed account of b.c. is indeed a matter of prime importance. A rigid conducting surface behaves in a drastically different way from a free and insulating surface.

In this subsection, we shall consider only the thermal interaction of the fluid layer with its eventual boundary.

We consider a thin fluid layer of depth d constrained between two horizontal infinitely extended "blocks" of width h and heat diffusivity κ_s. For simplicity, both blocks are taken from the same material and have the same dimensions. Note that we are only interested here in small aspect-ratio configurations for which we can disregard considering lateral boundary conditions. Lateral boundaries strongly influence, however, the possible horizontal patterns of the convective flows. This, together with any preimposed flow does indeed force a pattern of its own, say rolls along a privileged direction or with axisymmetry according to the configuration adopted in a particular Rayleigh-Bénard experiment (see Volkovisky [1939], Soberman [1958], Koschmieder [1967], Stork and Müller [1972], Bergé and Dubois [1974]). Those peculiarities are not, however, our main concern here as firstly, in small aspect-ratio configurations we may focus attention to a rather small part of the container and secondly, it does little good to fix lateral b.c. if we are not capable to solve the complete boundary value problem. It is, however, important to note that lateral boundaries do indeed tend to impose a pattern of their own even in surface tension-driven convection. In Koschmieder's experiments, there appear two symmetry breaking mechanisms, one imposed by the lateral boundaries and the other being surface tension inhomogeneities, the latter being stronger than the former and deciding the steady state convective regime at critical and slightly supercritical conditions. We shall disregard the presence of lateral boundaries (see Davis [1967,68]) where a discussion of the most

simple theoretical predictions in finite-box problems is presented.

Along each conducting block the temperature distribution is assumed to obey Fourier's law in the steady state. We have (*)

$$(D^2 - a^2)\,\theta_s = 0 \tag{1}$$

whose formal solution is

$$\theta_s = A\cosh(az) + B\sinh(az) \tag{2}$$

Here the subscript 's' denotes a point in the solid block. We have assumed separation of variables (horizontal and vertical) as a consequence of symmetry. The separation constant is a^2.

First we assume a constant and uniform temperature along the outer surface of the block, we have $\theta_s = \theta_o$ at $z = h$, where θ_o is some controlled value. We may simply take $\theta_o = 0$ and define θ_s incorporating this controlled value. The same occurs at $z = -h$ where $\theta_s = \theta_1$ and by redefining θ_s we simply write $\theta_s = 0$.

At the interface of contact between the blocks and the fluid we assume continuity of the temperature distribution and heat flux. We have, on the one hand $\theta_s = \theta_F$ at $z = 0$. Thus $\theta_F(0) = A$. On the other hand, $\kappa_s D\theta_s = \kappa_F D\theta_F$ at $z = 0$. We have $\frac{\kappa_F}{\kappa_s} D\,\theta_F = aB = -a\coth(ah)\,\theta_F$ at $z = 0$. If the vertical origen of coordinates is taken midway between the blocks, we

(*) With D we denote derivative along the z-axis: D = d/dz.

have in dimensionless form(*)

$$\theta_F = B_{\mathscr{R}} D\theta_F \tag{3}$$

in which

$$B_{\mathscr{R}} = -\frac{\mathscr{R}_F}{\mathscr{R}_s} \frac{\tanh(ah)}{ad} \tag{4.a}$$

Similarly, at the lower boundary of the fluid we have

$$\theta_F = -B_{\mathscr{R}} D\theta_F \tag{4.b}$$

Note that the formal limits $B_K \to 0$ or $B_K \to \infty$ roughly correspond to the extreme situations $\kappa_F << \kappa_s$ (a perfectly conducting boundary, e.g. a good metallic plate) and $\kappa_F >> \kappa_s$ (a perfect insulator). Different values of B delineate possible realistic situations. It is also of importance to note that h is considered finite. Two thick blocks of good conducting material constraining a thin fluid layer correspond to the simultaneous limits $\kappa_F/\kappa_s \to 0$ and $h \to \infty$. This case has been considered by Hurle, Jakeman and Pike [1967]. Boundaries of finite heat conductivity have also been considered by Sparrow, Goldstein and

(*) To distinguish this parameter B from a similar parameter to be defined in the next subsection dealing with the mechanical boundary conditions, we shall denote it here with B_K. This quantity is called a Biot number or a radiation-like parameter. Strictly speaking at $B_K \to \infty$ there is no fluctuation in the heat flux. Thus, we have a prescribed heat flux condition and this is called a Robin condition. The subscript 'F' denotes a point in the fluid itself.

Jonsson |1964|.

Quantitative, as well as qualitative differences in behavior are to be expected between the two extreme cases of highly conducting and insulating boundaries. For in the former, a fluctuation of temperature carried to the boundary soon relaxes through the block whereas at an insulating boundary it is rejected back into the fluid, and a quiescent initial linear temperature profile is more easily distorted. Thus, a lower critical temperature difference would lead to the onset of convection. On the other hand, a lowering of the critical gradient yields a smaller energy amount liberated by buoyancy and to accomodate convection the fluid rather accomodates convective cells of large wavelength. Thus, a drastic decrease in wavenumber is to be expected with insulating boundaries. As a matter of fact, the wavenumber is vanishing for an infinitely extended fluid layer. This case was first considered by Jeffreys [1926]. Vanishing of wavenumber merely means a wavenumber going to zero as the aspect ratio goes to zero, i.e., as the horizontal dimension goes to infinity. For bounded layers the lateral boundaries should provide a non-zero cut-off corresponding to the lowest mode compatible with the prescribed lateral b.c.

At the onset of convection, any motion once initiated can not be maintained, as Jeffreys pointed out. The initial linear temperature profile is distorted. At a slightly supercritical temperature difference, however, the wavenumber accomodated by the fluid layer would not necessarily be vanishing and convection would be seen. It is to be noted that a straightforward calculation yields a behavior $a \sim B^{-1/4}$, a singular be-

havior for small B. Thus, very little heat conductivity at the boundaries suffices to eliminate the vanishing of the wavenumber. This matter needs, however, further elucidation since most if not all Rayleigh-Bénard experiments are not done with insulating boundaries. However, we will not discuss the thermal boundary layer problem of such case.

Lastly, it should be mentioned the case of an open surface to air or to another fluid. From the thermal point of view, the exchange like in the case of a rigid block, demands consideration of exchange of energy through radiation, conduction and convection. The three phenomena can altogether be accounted for by a Robin condition that merely reduces to Eq. (4) with a generalized parameter B that takes into account the specific characteristics of the two fluids at the interface.

3.2 Mechanical boundary conditions and surface deflection

As we have discussed in the latter part of the previous subsection, the boundaries of the fluid layer under consideration may not be rigid metallic, plastic or crystal plates. Instead, they might be taken to be other fluid layers or a combination of rigid plates and surfaces open to ambient air as in Bénard's original experiments. In this latter case, we also have the option of whether or not to consider surface tension effects.

For large aspect ratio fluid layers, surface tension stresses should not be of prime importance and instead the dynamics is expected to be governed by buoyancy effects. Whether in a particular experiment one or the other mechanism

is dominating is an interesting question, since for surface tension-driven convection the up-welling areas of the fluid seems to correspond to the hotter points of the surface and it is then depressed. The opposite may be the case with buoyancy-driven convection in fluid layers open to air: the surface above hotter points is then elevated. We shall come back to this problem further below in this section.

The most extreme cases to be considered are rigid plates and stress-free boundaries. We shall now give a detailed description of both cases and the intermediate situation.

To make things simple, we consider a fluid layer F_1 sandwiched between two other identical fluid sublayers F_2. As before, ν denotes the kinematic viscosity and the subscript refers to each kind of fluid. Let $V_i (i = 1,2)$ be the flow velocity in layer $F_i (i = 1\text{-}2)$ in steady state.

Every fluid sublayer is dynamically controlled by the Navier-Stokes equation and the incompressibility condition. For simplicity, we shall disregard at present any thermal influence of the boundaries and the temperature is assumed uniform throughout the fluid sublayers. For the upper sublayer we have

$$\nu_2 \, \text{div grad } V_2 - \text{grad } \omega_2 = 0 \tag{1}$$

$$\text{div } V_2 = 0 \tag{2}$$

Here $v_2 = (U_2, V_2, W_2)$ and ω_2 accounts for the pressure contribution. For simplicity we shall restrict consideration to a second problem and take $U_2 = 0$. At the rigid boundary $z = h$

we have $V_2(h) = W_2(h) = 0$, whereas at the fluid-fluid interface there is continuity of the flow and momentum flux,

$$W_2(0) = W_1(0) = 0 \tag{3.a}$$

$$V_2(0) = V_1(0) \tag{3.b}$$

$$\nu_2 DV_2(0) = \nu_1 DV_1(0) \tag{3.c}$$

Symmetry allows separation of variables like in the thermal case discussed in the previous subsection. We may consider a two-dimensional problem and take quantities independent of one of the spatial coordinates, say X. We have

$$V_2(Y,z) = V_2(z)\sin aY \tag{4.a}$$

$$W_2(Y,z) = W_2(z)\cos aY \tag{4.b}$$

$$\omega_2(Y,z) = \omega_2(z)\cos aY \tag{4.c}$$

that must satisfy Eqs. (1), (2) and the b.c. Thus we have

$$(D^2-a^2)^2 V_2 = 0 \tag{5}$$

together with the explicit functions

$$V_2(z) = A\cosh az + B\sinh az + Cz\cosh az + Dz\sinh az$$

$$W_2(z) = -A\sinh az - B\cosh az - C\left(z\sinh az - \frac{z\cosh az}{a}\right) \quad (6.a)$$

$$-D\left(z\cosh az - \frac{\sinh az}{a}\right) \quad (6.b)$$

in which A, B, C and D are constants yet to be specified. From b.c. (3.a) we conclude that B = C/a. We also have $V_2(0) = V_1(0) = A$. From (3.b) and (3.c) it follows that

$$C = \frac{\nu_1}{2\nu_2} D V_1(0) \quad (7)$$

and finally

$$V_1(0) = B_\nu D V_1(0) = 2C \quad (8)$$

in which

$$B_\nu = -\frac{\nu_1}{\nu_2} \frac{\sinh(2ah) - 2ah}{\sinh^2(ah) - a^2h^2} \quad (9)$$

Thus, we find a similarity to the thermal b.c. The sublayers F_2 can be made arbitrarily thin and in the extreme case they might be reduced to boundary layers in which case a slightly

revised version of our argument holds.

Note that b.c. (9) refers to the horizontal flow field velocity and that at a strictly rigid plate we have $B_\nu = 0$, i.e. $V_1 = 0$ everywhere. We shall now discuss the b.c. to be imposed on the vertical component of the flow field $W_1(z)$ at $z = 0$.

To characterize the b.c. eventually satisfied by the vertical component of the flow field, we consider first the two extreme cases most often described in the literature. For a rigid plate, we shall have $U_1 = W_1 = 0$ everywhere on the surface boundary. Thus, the continuity equation demands

$$\left(\partial W_1 / \partial z\right) = 0 \tag{10}$$

and this corresponds to $B_\nu = 0$ as discussed above. The opposite case corresponds to a <u>level</u> surface without any stress on it. The vanishing of the horizontal components of the stress tensor means the vanishing of the viscous part of it. This condition and the fact that W_1 vanishes everywhere on the surface demands that

$$\left(\partial^2 W_1 / \partial z^2\right) = 0 \tag{11}$$

and this case corresponds to $B_\nu = \infty$. Note that considering the surface to be level amounts to neglecting all deformation effects, namely gravity waves and/or capillary ripples. We shall discuss the deformation effects a little further below. A surface may be level and yet the fluid is able to support

stress on it. For if the fluid surface is considered open to ambient air, surface tension inhomogeneities do generate surface tractions. Any non-uniform temperature (or concentration) distribution at the interface suffices to generate surface tension inhomogeneities. Usually surface tension decreases with increasing temperature. Consider the surface tension ξ to be a function of temperature alone (and thus an implicit function of horizontal coordinates). At a perturbed state we have

$$\delta\xi = -\omega\,\theta \tag{12}$$

where θ denotes the temperature fluctuation at a given point and $-\omega$ represents the slope of ξ evaluated at a given mean temperature on the plane. The balance of forces on a fluid element in the steady state that encloses a piece of the interface yields in the first order approximation,

$$\frac{\partial}{\partial x}\delta\xi = \eta\frac{\partial V}{\partial z} \tag{13}$$

On differentiating and making use of the incompressibility condition with $\Delta_2 \equiv \partial^2/\partial x^2 + \partial^2/\partial y^2$ we get

$$\Delta_2\,\delta\xi = -\eta\,\frac{\partial^2 W}{\partial z^2} \tag{14}$$

and finally

$$\frac{\partial^2 W}{\partial z^2} = \frac{\omega}{\eta}\,\Delta_2\,\theta \tag{15}$$

Except for scaling factors, ω/η is the Marangoni number.

When the restriction of a plane free surface is relaxed, the surface tension tractions and deformation in the gravitational field relax through capillary waves as well as gravity waves. As we have indicated above, to consider a level surface with surface tension stresses on it amounts to a vanishing "Crispation number". This means assuming an infinite surface tension. An important matter is to ascertain the role played by flexibility and resistance to deformation of the surface in determining stability. This matter is not as simple as it might be thought of a priori. It turns out that incorporating surface tension effects into the Rayleigh problem yields corrections to the rigid or stress-free b.c. problem that are of same order as such non-Boussinesquian effects like $\eta = \eta(T)$ or $k = k(T)$, as first emphasized by Davis and Segel [1968]. We have also neglected surface viscosity effects that are also of second order.

Finally it remains to ascertain whether the upwelling fluid flow provokes a local depression or elevation of an open surface and if there is any qualitative difference between surface tension-driven flows and buoyancy controlled convection. Bénard and Volkovisky found that hotter areas, i.e., areas of upwelling fluid flow, are depressed. However, Berg, Acrivos and Boudiart [1966] repeating Bénard's experiments with 1 mm.-thick melted wax found an opposite structure. Since Bénard's experiments were done with melted spermaceti and Berg et al. used

melted wax, non-Boussinesquian and/or non-Newtonian effects might have caused the discrepancy. The only theoretical calculations actually available refer to Newtonian liquids.

Jeffreys [1951] discusses a fluid layer with a stress-free upper interface and Scriven and Sternling [1964] use a very simple model of the interface. In this latter case, the critical wavenumber is vanishing and the direction of flow under depressed areas is determined by the inequality $(\sinh a)^2 \geq a^2$ (see also Smith [1966]).

Theoretically, the deflection of the surface can be inferred, in the simplest case, by estimating the fluctuation of vertical stress. Up to a first approximation this is

$$\delta p - 2\eta \frac{\partial W}{\partial z}$$

and is a function of the horizontal coordinates. Here δp refers to the pressure fluctuation as given by the Navier-Stokes equations. As the vertical velocity vanishes everywhere at the boundary $\frac{\partial W}{\partial z} < 0$ with the upwelling fluid. Thus, $-2\eta\frac{\partial W}{\partial z} > 0$, and this term tends to elevate the surface in buoyancy-driven convection whereas Scriven and Sternling [1964] (see also Hershey [1939]) conclude to the contrary structure in surface tension-driven flows. What we can safely say is that this matter demands further experimental research before an unambiguous result is obtained. And, if it turns out that the qualitative behavior is indeed opposite for the two driving mechanisms, there must exist a critical depth to delineate the predominancy of one over the other.

We shall not discuss here the problem of lateral boundaries for we are considering the gross phenomena that

already happen at very low aspect ratios, as originally considered by Rayleigh [1916].

4. A perturbative approach to the nonlinear fields

4.1 Landau-Hopf scheme

Following the analysis initiated by Lord Rayleigh, the motionless conductive state is not stable above some critical temperature gradient and a convective regime appears. In the following, we shall try to explain how to understand the phenomena that occur in this convective state when the Rayleigh number increases gradually beyond the critical value. In the vicinity of the bifurcation (and it turns out that this vicinity is quite large!) perturbation methods may be used. When one goes far away from the bifurcation, other methods of investigation must be used which require either extensive numerical computations or drastic simplifications. Perhaps a "simplicity" is reached in the limit of an infinite Rayleigh number, i.e., in a fully turbulent convective state. However, this is not certain at the present time.

In this section we study just the supercritical range where presumably perturbation methods are useful. Later on we shall discuss steady state transitions (i.e., the changes from a time-independent structure to another steady structure).

The perturbative scheme to be used here follows an approach originally due to Landau [1944] and Hopf [1942,1948]. The analysis goes as follows (see for recent mathematical developments Joseph [1976]). Let A be the amplitude of a fluctuation that becomes unstable when some physical parameter passes a certain critical value. Let σ be this parameter which, in the Rayleigh-Bénard case, may be taken as the difference between the actual value of the Rayleigh number, say Ra, and

the critical one, Ra_c. Thus, in the vicinity of the bifurcation, it is natural to assume an equation of evolution for A in the form

$$\dot{A} = A\sigma \tag{1}$$

When $\sigma < 0$ (i.e., $Ra < Ra_c$) the fluctuation is damped out and, when $\sigma > 0$ this fluctuation grows exponentially. In this case, when A reaches overly large values, one may no longer assume the validity of the linear equation of the motion. This is obviously true in the convection case, as the Oberbeck-Boussinesq equations are non-linear. Then, it is natural to add non-linear terms on the right hand side of (1) to account for finite amplitude fluctuations. The nature of these non-linear terms is limited by the symmetries of the system. Let us assume, for the moment, that the convection pattern is such that, by reversing all the fluid velocities, an equivalent pattern is obtained (in a rectangular box with an even number of rolls, the equivalent pattern is given by mirror symmetry). Thus, the inclusion of non-linear terms in (1) must respect the symmetry $A \leftrightarrow (-A)$, and only odd powers of A ought to be included on the right hand side of (1). Thus, we have

$$\dot{A} = A\sigma + \gamma A^3 + \beta A^5 \tag{2}$$

Let us assume first that $\gamma < 0$. For σ just slightly larger than 0, a stable steady solution of (2) exists which in expanded form is:

$$A \approx \sqrt{\frac{-\sigma}{\gamma}} \left[1 + \frac{\beta\sigma}{2\gamma^2} + \cdots\right] \qquad (3)$$

as σ approaches zero form above. This case represents a "normal bifurcation". Suppose that, on the other hand, γ is positive; then one has an "inverted bifurcation". If σ is just slightly above 0, the state $A = 0$ (i.e., the motionless state) is unstable, and another stable state exists which does not reduce to $A = 0$ at $\sigma = 0$. If $\beta > 0$ (and neglecting the higher order terms on the right-hand side of (2)), the amplitude of this new state is $\pm \beta/\gamma$ at $\sigma = 0$. This inverted bifurcation is discussed in more detail in the following subsection. But let us point out that the expansion (3) is meaningful only near $\sigma = 0$, and that a limited expansion of the right-hand side of (2) cannot really be all accurate to describe finite amplitude fluctuations, as in the case of inverted bifurcation. The Leray-Schauder topological degree theory, yields a powerful method for studying the bifurcation above a critical point, without requiring explicit details as with, for example, (2). It leads to definite statements about the existence and number of bifurcating solutions, the global properties of these solutions and their stability (see Sattinger [1973].

The Landau-Hopf theory applies to the standard Rayleigh-Bénard problem. It yields accurate quantitative predictions near the onset of convection. In this case we have a "normal bifurcation".

The perturbative approach proceeds in two directions: first, one seeks by expansion the steady solution of the hydrodynamic equations near the onset of convection. Then one studies their stability in the frame of this perturbation analysis. The search of the steady solution by expansion involves a number of non-trivial points; we shall report about that in some detail.

4.2 Thermal fluctuations and the onset of convection

Concluding our discussion of the onset of convection, let us emphasize again that the perturbation approach is meaningful only if the parameter γ in the Eq. 4.1 (2) (or the equivalent quantity derived from the perturbative solution of the fluid equations) is negative. It turns out that this is actually true in the standard Rayleigh-Bénard case of a Boussinesquian fluid layer. However, it is possible that inverted bifurcations occur in other types of convection experiments on surface-tension-driven instabilities (i.e., the original Bénard experiment, for instance). In this latter case, Koschmieder [1967] observed a change of structure at the onset of convection: an instability with a roll structure develops first, and then changes spontaneously (i.e., without any change in the external conditions) into a hexagonal structure. This denotes probably an inverted bifurcation: the rolls are marginally stable at the onset and grow spontaneously, moving toward a steady convection state with a finite amplitude and a hexagonal structure.

Another possibility of inverted bifurcation exists, if the symmetry $A \leftrightarrow (-A)$ is broken in such a way that a term of order A^2 may be inserted in the Landau equation:

$$\dot{A} = \varepsilon A + \varepsilon' A^2 + \gamma A^3 \qquad (1)$$

Just before the onset of convection the fluctuations of the fluid velocity look more or less as those of a ball in a very flat valley and a number of authors (Graham [1973], Haken [1975]) have examined if, in this situation, the thermodynamic fluctuations could be seen at a macroscopic level. Unfortunately, their order of magnitude leaves little hope for measuring these macroscopic fluctuations. Consider a velocity fluctuation with a scale of order $\ell \approx 1$ cm. in a fluid of mass density $\rho \approx 1\ g/cm^3$ at 300°K. The order of magnitude of this velocity fluctuation is

$$|V_0| \approx \left[\frac{2 k_B T}{\rho \ell^3}\right]^{1/2} \approx 2.9 \times 10^{-3}\ \mu m\, sec^{-1}$$

in which k_B is Boltzmann's constant.

Let us briefly estimate how these fluctuations are enhanced close to the Rayleigh bifurcation. They obey a Langevin equation

$$\dot{V} + \lambda V = f(t) \qquad (2)$$

The linear damping factor λ vanishes at $R = R_c$, and when the amplitude of the fluctuations becomes too large, they are limited by non-linear phenomena, as accounted for by the βA^3 term in the Landau equation (1). Thus, it is natural to expect that for R close to R_c, the fluctuations of V are described by the non-linear Langevin equation

$$\dot{V} + \lambda_o \left[(1 - R_a/R_c) + (V/V_c)^2 \right] V = f(t) \qquad (3)$$

where λ_o is the damping rate of the velocity fluctuations in the absence of any temperature gradient (i.e., at R = 0). The noise source f(t) takes its origin in the molecular fluctuations, and is unaffected (at least to a first order approximation) by the macroscopic temperature gradient; accordingly, it is a random stationary gaussian function with a white spectrum. We have written the equation (2) in order to make appear a characteristic velocity V_c, which is reached in the convection state at $R = 2R_c$, if one neglects the thermal fluctuations in this state. As already seen V_c is typically of order 100 μm/sec.

As shown for instance by Stratonovich [1963,1967] the probability distribution of the fluctuations of the solutions of a one-dimensional Langevin equation of the general form

$$\dot{V} + \phi(V) = f(t) \qquad (4)$$

where f(t) is a stationary gaussian white noise is

$$p(V) = Z^{-1} \exp\left\{-\beta \int_0^V \phi(u)\,du\right\} \tag{5}$$

where β is related to f by the fluctuation-dissipation theorem

$$\langle f(t) f(t') \rangle = \frac{2}{\beta}\,\delta(t-t') \tag{6}$$

and Z is a normalization factor.

In the present case this gives

$$p(V) = Z^{-1} \exp\left\{ \frac{-1}{2V_o^2}\left[V^2\left(1-\frac{R_a}{R_c}\right)+\frac{V^4}{4V_c^2}\right]\right\} \tag{7}$$

When R becomes very close to R_c, the dominant contribution in P(V) arises from the term $V^4/8V_o^2V_c$, which means that the fluctuations of u have (in the region $R \gtrsim R_c$) an upper bound of order

$$|V| \gtrsim (V_o V_c)^{1/2} \approx 0.54\ \mu m\, s^{-1}$$

which is somewhat smaller than the smallest measureable fluid velocity. Furthermore, in order to lie in this domain of "non-linear fluctuations" one should be very close to R_c, so the fluctuation of V reaches this limit amplitude when

$$1 - R_a/R_c \lesssim V_o/V_c \approx 2.9 \times 10^{-5}$$

It may be noted further that, very close to R_c, no term like the one represented by $\varepsilon' A^2$ should become important, although one may expect that, owing to the breaking of symmetries by non-Boussinesquian effects and/or lateral boundary

effects, these terms are present anywhere. It is also relevant to point out that in this extreme vicinity of the critical point, the typical evolution times may increase very much, and this critical "slowing down" might be a source of great experimental difficulties, as it is in many cases.

These thermal fluctuations do not seem to be a promising phenomenon for experimental studies, nor have they anything to do with the actually available experimental data.

5. Convective flows in realistic situations: Quantitative results

A concrete application of the Landau-Hopf approach to the Bénard-Rayleigh problem is due to Gor'kov [1957] and Malkus and Veronis [1958]. They investigated the case of an infinite horizontal layer with free upper and lower surfaces and two special cases of 3d convection pattern, with rectangular and hexagonal cells. Later on, Schlüter, Lortz and Busse [1965] extended this method by considering an arbitrary 3d flow with either rigid or free boundary conditions. We shall follow approximately their analysis of the steady state. The starting point is the set of the non-linear dimensionless Boussinesq-Oberbeck equations for the steady state(*)

$$\operatorname{div} V \equiv \nabla . V = 0 \tag{1.a}$$

$$P \Delta V + P \theta \underset{\sim}{k} - \nabla p = (V . \nabla) V \tag{1.b}$$

$$\Delta \theta + R W = (V . \nabla) \theta \tag{1.c}$$

where P is the Prandtl number and R the Rayleigh number. By elimination of the pressure and of the horizontal components of the velocity, one gets a sixth-order differential equation for the vertical velocity W:

(*) Eqs. (1) are obtained using the scales: κ/d for velocity, $\beta d/Ra_c$ for temperature, d^2/κ for time and κ^2/d^2 for pressure. This choice is dictated by our interest in comparing with Schlüter et al. [1965]. Δ denotes the Laplacian operator: Δ=div grad, and $\underset{\sim}{k}$ is the 3-component vector ($\delta_x=\partial^2/\partial x \partial z$, $\delta_y=\partial^2/\partial y \partial z$, $\delta_z=-\Delta_2$) and Δ_2 denotes the two-dimensional horizontal Laplacian. To simplify notation we shall indistinctly use R and Ra to denote the Rayleigh number.

$$(\Delta^3 - R\Delta_2) W = -\left(P^{-1} \underset{\sim}{\delta} \cdot \underset{\sim}{\ell} + \Delta_2 h\right) \tag{2}$$

where

$$\underset{\sim}{\ell} = (V \cdot \nabla) V \tag{3}$$

$$h = (V \cdot \nabla) \theta \tag{4}$$

The equation which relates θ to W is

$$\Delta^2 W + \Delta_2 \theta = P^{-1} \underset{\sim}{\delta} \cdot \underset{\sim}{\ell} \tag{5}$$

Near the onset of stability the rolls can be considered as exactly bidimensional, at least for containers with horizontal dimensions much larger than their height. We shall consider a system of parallel rolls with axis ox, take U = 0 and all the variables independent of the x-coordinate. Therefore, V is related to W by the continuity equation:

$$\frac{\partial}{\partial y} V + \frac{\partial}{\partial z} W = 0 \tag{6}$$

We shall consider only the simplifying case of an infinite Prandtl number fluid, which is highly realistic in many experiments. This amounts to neglecting the non-linearity arising from $|(\underset{\sim}{V} \cdot \underset{\sim}{\nabla}) \underset{\sim}{V}|$ with respect to $|(\underset{\sim}{V} \cdot \underset{\sim}{\nabla}) \theta|$. It is also convenient to introduce a field ϕ such that

$$W = -\Delta_2 \Phi \tag{7}$$

The governing equation for ϕ is in the limit $P \to \infty$:

$$(\Delta^3 - R\Delta_2)\Phi = h \tag{8}$$

The temperature and fluid velocity are related to ϕ and to the stream function $\psi \equiv \frac{\partial \phi}{\partial y}$ by:

$$W = -\partial^2\phi/\partial y^2 = -\frac{\partial \psi}{\partial y} \tag{9.a}$$

$$V = \partial^2\phi/\partial y\,\partial z = \partial\psi/\partial z \tag{9.b}$$

$$\Theta = \Delta^2 \Phi \tag{9.c}$$

We know that at $R = R_c$, together with the proper b.c., a non-vanishing solution exists for $(\Delta^3 - R\Delta_2)W = 0$. It follows from the linearized Boussinesq equations that in the neighbourhood of R_c the time-dependent fluctuations behave like $\exp\{\alpha(R-R_c)t\}$ with $\alpha > 0$. This is about the expected behaviour with the Landau equation which after linearization describes fluctuations that behave like $\exp(\sigma t)$. For a steady force field as we have considered here, the velocity growth rate is initially zero, but later it is expected to increase at a rate dependent on the Prandtl number. Non-linear terms in the Landau equation limit the growth of the amplitude fluctuations, and it turns out that at $\sigma = 0$ this amplitude is of order $\sigma^{1/2}$. Thus, it appears

natural to seek solutions of (8) in the form:

$$\underline{\Phi} = \varepsilon \underline{\Phi}^{(1)} + \varepsilon^2 \underline{\Phi}^{(2)} + \cdots \tag{10}$$

and similar expressions for V, W and θ. The basic assumption is that for R slightly above R_c the motions will develop only small amplitude: ε is assumed small. In convection problems it is usually assumed that R is set, an experimenter's figure say. However, it is not known in advance which value of R will produce a particular amplitude. Rather we may say that ε is given and we try to find the R required to produce it as a function of ε,

$$R = R_c + \varepsilon R^{(1)} + \varepsilon^2 R^{(2)} + \cdots \tag{11}$$

Note that up to second order terms and according to the arguments developed above, we should have $\varepsilon = (R - R_c)^{1/2}$.

Substituting these expansions into (8), a sequence of linear inhomogeneous equations is generated:

$$\mathcal{L}\left[\underline{\Phi}^{(1)}\right] = 0 \tag{12.a}$$

$$\mathcal{L}\left[\underline{\Phi}^{(2)}\right] = h^{(2)} - R^{(1)} W^{(1)} \tag{12.b}$$

$$\mathcal{L}\left[\underline{\Phi}^{(n)}\right] = h^{(n)} - \sum_{p=1}^{n-1} R^{(p)} W^{(n-p)} \qquad \cdots\cdots$$

$\cdots\cdots$

where the linear operator $\mathcal{L}$ is

$$\mathcal{L} \equiv \Delta^3 - R_c \Delta_2 \tag{13}$$

and

$$h^{(n)} \equiv \sum_{p=1}^{n-1} (V^{(p)} \cdot D)\, \theta^{(n-p)} \tag{14}$$

From the existence theorems of solutions at each order, one gets the unknown parameter $R^{(n)}$ by requiring that the right-hand side be orthogonal to the solutions of the adjoint homogeneous equation:

$$\mathcal{L}[\theta^{(1)}] = 0 \quad ; \quad \mathcal{L} = \mathcal{L}^+ \tag{15}$$

with corresponding b.c. on θ.

The small parameter ε can be determined as a function of the relevant quantity, i.e., $|R - R_c|$, if the procedure is ended after a given number of iteration steps. Note that to the first order the amplitude of the motion which is identified with ε remains unknown.

Before solving the 2nd order equation for $\theta^{(2)}$, the parameter $R^{(1)}$ must be determined from the solubility condition:

$$\langle h^{(2)} \theta^{(1)} \rangle - R^{(1)} \langle W^{(1)} \theta^{(1)} \rangle = 0 \tag{16}$$

where by definition:

$$\langle f g \rangle = \frac{a}{2\pi} \int_0^{2\pi/a} dy \int_{-1/2}^{+1/2} dz\, f(y,z)\, g(y,z) \tag{17}$$

$2\pi/a$ being the horizontal wavenumber, and the fluid layer being between the planes $z = -1/2$ and $z = +1/2$. We can easily verify that all quantities of the form:

$$\langle \Phi' (V \cdot \nabla) \Phi \rangle \tag{18}$$

vanish, provided the functions ϕ and ϕ' satisfy the boundary conditions and have the same horizontal dependence. This is the case for

$$\langle \theta^{(1)} h^{(2)} \rangle = \langle \theta^{(1)} (V^{(1)} \cdot \nabla) \theta^{(1)} \rangle = 0 \tag{19}$$

Since:

$$\langle \theta^{(1)} W^{(1)} \rangle \neq 0 \tag{20}$$

$R^{(1)}$ must vanish.(*)

(*) It is of interest to note that this argument is no longer valid if the plane-form is made of more than one wavenumber. In this case $\langle \theta^{(1)} h^{(2)} \rangle$ may vanish owing to the $(z) \Leftrightarrow (-z)$ symmetry, that leaves $\theta^{(1)}$ invariant and changes the sign of $h^{(2)}$. Again this argument breaks down when the latter symmetry does not exist, as it is the case, for instance, with a rigid boundary at the bottom and a stress-free boundary at the top (Busse [1962,1967]) or if non-Boussinesquian effects are to be considered (Palm [1960]). In all of these cases, the non-vanishing of $R^{(1)}$ is realized for an hexagonal pattern only (for an infinite horizontal planform at least). This comes from quite general arguments and could explain what happens in some of Bénard-like experiments. For we first note that the above defined scalar product is no longer valid in the case of an arbitrary horizontal planform and must be replaced with

$$\langle fg \rangle = \frac{1}{S} \int_S d\underset{\sim}{x} \int_{-1/2}^{+1/2} dz \, f(\underset{\sim}{x}, z) g(\underset{\sim}{x}, z)$$

in which $\underset{\sim}{x}$ is a two-dimensional vector, and S the surface of the layer. If this is infinite, one has just to set $\lim_{S \to \infty} 1/S \int_S d\underset{\sim}{x}$ instead of $1/S \int_S d\underset{\sim}{x}$. The quantity $R^{(1)}$ depends on the third power of the first order solutions. Let us assume that it involves only a finite number of wave vectors,

$$\Phi^{(1)}(\underset{\sim}{x}, z) = \sum_i \Phi_i^{(1)}(z) \cos(\pi \underset{\sim}{a_i} \cdot \underset{\sim}{x})$$

each one of the a_i's having the same length which is defined by the linear theory at $R = R_c$. Thus, the expression of $R^{(1)}$ is of the form:

$$R^{(1)} = \lim \frac{1}{S} \int_S d\underset{\sim}{x} \left[\sum_{ijk} R_{ijk}^{(1)} \cos(\pi \underset{\sim}{a_i} \cdot \underset{\sim}{x}) \cos(\pi \underset{\sim}{a_j} \cdot \underset{\sim}{x}) \cos(\pi \underset{\sim}{a_k} \cdot \underset{\sim}{x}) + \dots \right]$$

where $R_{ijk}^{(1)}$ is obtained summing over z. In the limit $S \to \infty$ the integration over x vanishes, except if $\underset{\sim}{a_i} + \underset{\sim}{a_j} + \underset{\sim}{a_k} = 0$. As the three vectors $\underset{\sim}{a_i}$, $\underset{\sim}{a_j}$ and $\underset{\sim}{a_k}$ have the same length, this can only be realized if these vectors from a regular triad which yields a hexagonal pattern. In the case of a two-dimensional roll, the horizontal integral that defines $R^{(1)}$ may not be vanishing due to lateral boundary conditions which break the invariance under translation. The situation where $R^{(1)}$ differs from zero is more complicated from the point of view of the stability of the bifurcating solutions.

To find the second-order approximation, we look for a particular solution of Eq. (12.b) with $R^{(1)} = 0$. The inhomogeneous term $h^{(2)}$ is made of two parts: a y-independent term and a term proportional to cos(2ay) to which we will refer as the second harmonic.

Values of $R^{(2)}$ are given in Table 5.1(*). $R^{(2)}$ is obtained from the solubility condition of the third-order approximation in Eq. (15). For $B_\nu = \infty$ (free b.c.) we recover the result of Malkus and Veronis ($R^{(2)} = \frac{9\pi^2}{16} a_c^4 = 135.2$) and for $B_\nu = 0$ (rigid boundaries), we find the result of Schlüter et al. ($R^{(2)} = 1014.6$).

Bergé and Dubois [1976] have recently made accurate measurements of the fluid velocity close to the onset of convection. In order to compare their results with the results of the ε-expansion, it is necessary to use the parameter $\tilde{\varepsilon} = (\frac{R}{R_c} - 1)$. V, W and θ expand like:

$$V = \tilde{\varepsilon}^{1/2} \tilde{V}^{(1)} + \tilde{\varepsilon} \tilde{V}^{(2)} \qquad (21.a)$$

$$W = \tilde{\varepsilon}^{1/2} \tilde{W}^{(1)} + \tilde{\varepsilon} \tilde{W}^{(2)} \qquad (21.b)$$

$$\theta = \tilde{\varepsilon}^{1/2} T^{(1)} + \tilde{\varepsilon} T^{(2)} \qquad (21.c)$$

(*) When $R^{(2)} > 0$ as it is the case here, then from $R = R_c + \varepsilon^2 R^{(2)}$ it follows that to order ε^2, $\varepsilon^2 = (R-R_c)/R^{(2)}$ which is valid only if $R \geq R_c$. If it turns out that $R^{(2)} < 0$, there is an indication of sub critical instability (or inverted bifurcation). To conclusively assess the existence or not of such metastable states, a more rigorous and complete technique is to be used, like, way, the energy method (Joseph [1976]).

The quantities $V^{(1)}$, $V^{(2)}$, $W^{(1)}$, ... are functions of z which depend on B_ν and B_κ. For the numerical comparison with experimental data, it is convenient to take the maximum of these functions of z, that we shall call $V^{(1)}_{max}$, $V^{(2)}_{max}$, ... In the case $B_\nu = B_\kappa = 0$, the dimensionless numerical value of maxima are:

$$\widetilde{W}^{(1)}_{max} = 11.82,\ \widetilde{W}^{(2)}_{max} = 0.2279,\ \widetilde{V}^{(1)}_{max} = 11.67,\ \widetilde{V}^{(2)}_{max} = 0.2603,$$

$$T^{(1)}_{max} = 945.6,\ T^{(2,0)}_{max} = 459.1,\ T^{(2,2)}_{max} = 50.37$$

Here, $T^{(2,0)}$ accounts for a y-independent contribution, whereas $T^{(2,2)}$ belongs to the second harmonic.

For the ensemble of conditions:

$$\epsilon = 1,\quad B_\kappa = B_\nu = 0,\quad \frac{\varkappa}{d} = 1.14 \times 10^{-3}\ cm\,s^{-1}$$

chosen to reproduce data of Bergé and Dubois [1976] the corresponding values of the dimensional velocities are:

$$\frac{\varkappa}{d}\,\widetilde{W}^{(1)}_{max} = 135\ \mu m\,s^{-1} \quad \underline{and} \quad \frac{\varkappa}{d}\,\widetilde{V}^{(1)}_{max} = 133\ \mu m\,s^{-1}$$

The comparison with experimental values, 140 $\pm$ 10 µm/s and 132 $\pm$ 4 µm/s respectively, shows good agreement.

With the same values of the physical parameters, the theoretical result for the second harmonic is

$$\frac{\varkappa}{d}\,\widetilde{V}^{(2)}_{max} = 2.9\ \mu m\,s^{-1} \quad \underline{and} \quad \frac{\varkappa}{d}\,\widetilde{W}^{(2)}_{max} = 2.6\ \mu m\,s^{-1}$$

These figures, though of the same order of magnitude as those measured by Bergé and Dubois ($\widetilde{V}^{(2)} = 5 \pm 0.3$ µm/s), are smaller than the experimental values.

We must point out that for each order there is a relation between the maxima of $\tilde{V}$ and $\tilde{W}$, illustrating the conservation of flux in a roll:

$$\int_0^{z_o/2} \tilde{V}(0,z)dz = \int_0^{y_o/2} \tilde{W}(y,0)\,dy \qquad (22)$$

A rough estimate of each integral allows us to replace the previous equality by:

$$y_o \tilde{W}_{max} \approx z_o \tilde{V}_{max} \qquad (23)$$

For instance, in the first order approximation where $y_o = \frac{\pi}{2a_c}$ and $z_o = 1/2$, we have $\tilde{V}^{(1)}_{(max)} \approx \frac{\pi}{a_c} \tilde{W}^{(1)}_{(max)}$. (0,0) locates the center of a roll and y_o and z_o its horizontal and vertical extent.

Bergé and Dubois [1976] have also measured a third harmonic mode in the flow. This comes from the splitting of the third-order approximation to (15). We have:

$$\Phi^{(3)} = \Phi^{(3,1)} \cos(ay) + \Phi^{(3,3)} \cos(3ay) \qquad (24)$$

in which $\phi^{(3,1)}$ adds higher-order contribution to the first harmonic and $\phi^{(3,3)}$ belongs to the third one. Accordingly, the velocity and temperature fields also split into two mode contribution

$$\tilde{V}^{(3)} = \tilde{V}^{(3,1)} \cos(ay) + \tilde{V}^{(3,3)} \cos(3ay) \qquad (25.a)$$

$$\tilde{W}^{(3)} = \tilde{W}^{(3,1)} \cos(ay) + \tilde{W}^{(3,3)} \cos(3ay) \qquad (25.b)$$

$$T^{(3)} = T^{(3,1)} \cos(ay) + T^{(3,3)} \cos(3ay) \qquad (25.c)$$

It is to be noted that the solubility condition of the fourth-order approximation yields $R^{(3)} = 0$. Furthermore, $R^{(n)} = 0$ whenever n is odd.

With $B_\nu = B_\kappa = 0$, the maximum amplitude of the velocity and temperature are for the third harmonics

$$\tilde{V}^{(3,3)}_{(max)} = 0.06826$$
$$\tilde{W}^{(3,3)}_{(max)} = 0.1943$$
$$T^{(3,3)}_{(max)} = 20.87$$

The vertical velocity is three times greater than the horizontal one, expressing the flux conservation in an elementary roll.

This corresponds to the dimensional velocity (with $R = 2R_c$, $\frac{\kappa}{d} = 1.14$ cm/s):

$$W^{(3,3)}_{max} = 2.2\ \mu m/s$$
$$V^{(3,3)}_{max} = 0.77\ \mu m/s$$

$W^{(3,3)}_{max}$ is of the same order as $W^{(2)}_{max}$, and this has been observed experimentally (Bergé and Dubois, private communication).

The value of $R^{(4)}$ is needed to give the amplitude and the z-dependence of the quantities (3,1). This has been done by solving the 4th order approximation and thus writing the solubility condition for the 5th order.

Table 5.1 Quantitative predictions for various values of Biot number in mechanical b.c.:

$$B_\nu \frac{dV}{dz} = V;\ W = \theta = 0.$$

B_ν	a_c	R_c	$R^{(2)}$	$R^{(4)}$	$\tilde{W}^{(1)}_{max}$	$\tilde{V}^{(2)}_{max}$
0	3.116	1707.7	1014.6	849.79	11.82	0.2603
0.05	2.942	1355.9	668.1	347.43	11.74	0.1795
0.1	2.824	1186.0	514.4	149.36	11.64	0.1363
0.5	2.489	843.3	247.6	3.30	11.24	0.0459
1	2.381	761.2	194.7	- 2.68	11.10	0.0250
100	2.223	658.6	135.8	- 4.625	10.88	0.0003
50000	2.221	657.5	135.2	- 4.626	10.88	0.0
(∞)						

****

Table 5.2 Quantitative predictions for various values of Biot number in thermal b.c.:

$$B_\kappa \frac{d\theta}{dz} = \theta;\ W = V = 0$$

$a_c xB_\kappa$	a_c	R_c	$R^{(2)}$	$R^{(4)}$	$\tilde{W}^{(1)}_{max}$	$\tilde{V}^{(2)}_{max}$
0	3.116	1707.7	1014.6	849.79	11.82	0.2603
0.5	2.669	1415.1	920.48	241.90	8.65	0.4504
1	2.398	1267.5	699.85	142.02	6.98	0.5092
5	1.629	955.1	198.69	15.24	3.68	0.5383
50	0.803	772.8	13.54	- 0.126	1.54	0.3807
1000	0.300	727.2	0.21	-8×10^{-4}	0.54	0.1606
50000	0.082	720.5	0.6×10^{-3}	-10^{-7}	0.15	0.0445
(∞)						

6. Bifurcation of steady states

When the Rayleigh number increases beyond the critical value R_c (1707.8 in the standard case), the horizontal dependence of both the velocity field and the temperature field become more and more anharmonic, although these quantities remain time independent. Of course, this analysis was based upon an expansion in the "small" parameter $\varepsilon \propto (R - R_c)$, and it is likely that this fails to describe the phenomena when ε becomes too large.

The experiments have clearly established (see further below) that, beyond some value of R, say R_t, the flow becomes time dependent. It is also of interest to notice that, in the steady state when Ra increases from R_c to R_t, $R_c < Ra < R_t$, the wavelength of the two-dimensional pattern increases and then there is (generally) a transition toward a three-dimensional steady flow. Let us discuss this matter in some detail.

i) Wavelength increase

Koschmieder and Pallas [1974] and Bergé and Dubois [1974] (see also Bergé [1976] and Dubois [1976]) have shown in carefully controlled experiments that a number of rolls disappear when the Rayleigh number increases beyond R_c. That means unambiguously that the wavelength of the convective pattern increases.

In the experiments conducted by Bergé and Dubois the "boat" is rectangular shaped, the axis of the rolls being parallel to the shorter side. Beyond some value of the Rayleigh number, say R_1, one of two extreme lateral rolls (i.e., one of

the rolls closer to the shorter side) disappears completely. Thus, two states of convection rolls are well defined: the N-rolls pattern (N integer), which is stable at $R_a < R_1$, and a (N-1)-rolls state which is stable at Ra $\gtrsim R_1$. There does not seem to be any stable intermediate steady state as would be expected on intuitive grounds. Furthermore, and contrary to Koschmieder's [1969] findings with an (axisymmetric) cylindrical geometry, Bergé and Dubois [1974] find an hysteresis in this transition: when Ra slowly decreases from R_1, the (N - 1)-rolls state, disappears only when Ra becomes smaller than some $R_2 < R_1$. This finding has some similarity to what Burkhalter and Koschmieder [1973] find in the Taylor vortices problem. Is this hysteresis in the Rayleigh-Bénard problem just a spurious result of the experimental conditions of Bergé and Dubois or a consequence of the rectangular geometry? According to Koschmieder (private communication), the values of R_1 and R_2 are clearly dependent on geometry. By changing the aspect ratio of the apparatus, say to make room for more rolls, then R_1' as well as R_2' would be different, and $R_1' < R_1$. If, on the other hand, the aspect ratio is made very small, then rolls would be dropped from the pattern at very small steps in Rayleigh number. That means, that in the end, for an infinite layer a steady increase of the wavelength would be observed.

Following a 'principle of minimum complexity, we may describe the inverted or first-order bifurcation in finite containers by the following dynamical model system with one degree of freedom:

$$\dot{A} = (Ra - R_1)A + A^3 - \beta A^5 \quad \text{with } \beta > 0 \qquad (1)$$

Let us take $\Delta = Ra - R_1$; the stationary solutions are:

a) if $\Delta < -1/4\beta$: $A = 0$, which is stable. It may be viewed as the N-rolls state.

b) if $-1/4\ \beta < \Delta < 0$: five steady states exist namely $A = 0$ and the four roots

$$A_{\varepsilon\eta} = \varepsilon\sqrt{\frac{1+\eta\sqrt{1+4\beta\Delta}}{2}} \quad \text{with } \varepsilon = \pm 1;\ \eta = \pm 1$$

Here, the states $A = 0$ and $A_{\pm 1,+1}$ are linearly stable, but the states $A_{\pm 1,-1}$ are unstable. The stable states $A_{\pm 1,+1}$ may be viewed as the two (N-1)-rolls stable state; there is a pair of such states since they can be obtained from the N-rolls state by deleting any one of the two extreme lateral rolls.

c) If $\Delta > 0$, three steady states exist: $A = 0$ which is linearly unstable and $A_{+1,+1}$ and $A_{-1,+1}$, which are stable. The time evolution of any solution of Eq. (1) may be obtained at once. Each stable steady state has its own "domain of attraction" in the plane (Ra,A) starting from a point in the domain of attraction of a stable solution, the representative point moves towards this stable solution along a vertical in the plane (A, R_c). One may also notice that in the present case that there is a locus of points for which the evolution is ambiguous. In the terminology of the catastrophy theory [Thom, 1974], this kind of bifurcation is called Whitney's cusp (in French, fronce). The model equation (1) describes also quite well one other feature observed in the experimental time dependence of the bifurcation (Bergé and Dubois, private

communication). Starting from a situation with N rolls (A = 0 in our picture and Ra just slightly larger than R_1), the end roll disappears in two well defined time steps: first a very slow motion (half an hour) then a rapid destruction followed by a rearrangement of the convective pattern to accomodate the new (N-1) rolls steady state (a relaxation time of a few minutes).

Close to R_1, the instability that drives the system away from the A = 0 state has a small growth (since this increment vanishes at $R = R_1$, assuming some regularity, it remains small close to R_1). Once A has grown sufficiently, however, the instability is governed by the non-linearity and the non-linear dynamics appear with a finite time constant (rate) even at $R' = R_1$ since it does not suffer any qualitative change at R_1.

This first order bifurcation has been observed in rectangular containers only. Koschmieder and Pallas [1974] have also reported that in a circular box the wavelength of the concentric annular rolls increases with the increase of the Rayleigh number. However, in their case the flow pattern changes continuously. The axisymmetric central roll disappears progressively when the Rayleigh number is slowly increased. Actually, there is nothing like the transition observed by Bergé and Dubois [1974]. It is possible that, in their geometry, the structural change is of first order, although the critical numbers R_1 and R_2 are very close to each other, and that the two structures, namely those corresponding to A = 0 and $A_{\pm 1,+1}$, are very much alike; which in

our picture means that β is very large. With the axisymmetric geometry the bifurcation cannot be described by a one-degree-of-freedom system, as there is a single final state which is the original state without the central roll.

Krishnamurti has also observed a wavelength increase in her experiments, but does not report on any detail of the phenomenon that we discuss here. Schlüter, Lortz and Busse [1965] and Busse [1967] have determined the range of wavenumbers for which the roll pattern remains stable under super-critical conditions. They find that rolls are stable for wavenumbers lying on a finite band that collapses to the single value of Pellew and Southwell [1940] at Ra_c. This finding does not yield, however, a reason for the spectacular selection of a single wavenumber that shows up in every experiment. In our opinion, to account properly for this fact we ought to consider the initial value problem disregarded here. On the one hand, a classification of initial allowable conditions may very well provide a classification of patterns to be found at the steady state, i.e., as the asymptotic solution. On the other hand, we will show in Appendix II that a simple model (Lorenz [1963]) may yield either a steady or a time-dependent regime depending on the initial condition.

The reader will have noticed that in the above discussion no simple intuitive explanation has been proposed for the quite general fact of wavelength increase. A striking feature of this is of geometric nature: in every case, the roll that disappears is a rather "peculiar" one of the convective structure: the central roll in the axisymmetric container and the two far extreme lateral ones in a rectangular

box. We believe that the "hot spot-instability" to be discussed below might appear first in this roll which causes its destruction. Again it should be interesting to assess or dismiss our conjecture by conducting experiments where "practically" all rolls play identical role, as we have suggested above.

ii) Eckhaus instability

Though the stability of two-dimensional rolls has been studied by a number of authors, we shall describe now an elegant analysis developed by Eckhaus [1965,1971] to delineate the range of stability of the primary steady convection to longitudinal perturbations. Later on (see Section 7.2) we shall come back to further interesting predictions made by Clever and Busse [1974].

Restricting our consideration to a small enough neighbourhood of critical Rayleigh number, let $\gamma(k,R)$ be the linear growth rate of a perturbation with wavenumber k at Rayleigh number R. Thus, neutral stability at $R = R_c$ and $k = k_c$ demands $\gamma(k_c,R_c) = 0$, and that for $R < R_c$ the perturbation be damped (Rayleigh [1916], Pellew and Southwell [1940], Joseph [1965]). For slightly super-critical conditions, we expect the following approximate description to hold

$$\gamma(k,R) \approx \alpha_0 \left[\lambda (R-R_c) - (k-k_c)^2 \right] \qquad (2)$$

in which $\alpha_0 > 0$, and $\lambda > 0$ are some unknown, though constant parameters. The absence of linear terms in $(k - k_c)$ in Eq. (2)

comes from the necessary damping of all modes below the critical Rayleigh number. Above R_c, however, there is a band of expected unstable perturbations with horizontal wave number belonging to the open set $(k_c - \Delta_o, k_c + \Delta_o)$ with $\Delta_o = \frac{R-R_c}{\lambda}$. The actual growth of these unstable modes is limited by non-linear effects, so that a finite amplitude convective regime is eventually reached.

Let A(X,t) be an expected temperature fluctuation at the onset of convection. It can be expanded in Fourier components as follows:

$$A(X,t) = \sum_j A_{k_j} e^{ik_j X} \tag{3}$$

with $A_{-k} = A_k^*$. According to the symmetries of the non-linear Boussinesq-Oberbeck description of a fluid layer heated from below, and under similar boundary conditions on top and bottom, the system is invariant under translations and has also the mirror symmetry $(\delta\underset{\sim}{V}, \delta T, Z) \leftrightarrow (-\delta\underset{\sim}{V}, -\delta T, -Z)$; Z=0 defines the mid-plane of the contained. Thus, above R_c the simplest non-linear Landau-Hopf equation (see Section 4) that describes the time evolution of a Fourier mode of the temperature perturbation is

$$\dot{A}_k = \alpha_o \left[\Delta_o^2 - \Delta_k^2\right] A_k - \beta_o \sum_{\substack{j,l,m \\ k_j + k_l + k_m = k}} A_{k_j} A_{k_l} A_{k_m} \tag{4}$$

For simplicity, and without any real loss of generality, we take β_o real and k-independent. Note that we are restricting

consideration to horizontal wavenumbers in a single direction. Otherwise, β_o would depend on the angles between different wavenumbers.

In the case of a single wavenumber, Eq. (4) reduces to

$$\dot{A}_k = \alpha_o \left[\Delta_o^2 - \Delta_k^2\right] A_k - 3\beta_o |A_k|^2 A_k \qquad (5)$$

The factor 3 in front of β_o accounts for the three possible choices with the triplet $\{k_j, k_\ell, k_m\}$ when $k_j, k_\ell, k_m = k$ and $k_j + k_\ell + k_m = k$.

A steady solution of (5) is

$$|A_k|^2 = \frac{\alpha_o \left[\Delta_o^2 - \Delta_k^2\right]}{3\beta_o} \qquad (6)$$

provided $\beta_o > 0$ and $\Delta_o > |\Delta_k|$. That $\beta_o > 0$ follows from the absence of subcritical instabilities (Joseph [1965]).

The stability of (6) to infinitesimal perturbations of wavenumber $k + q$ $(q \neq 0)$ is governed by Eq. (5)

$$\delta \dot{A}_{k+q} = (\gamma_{k+q} - 2\gamma_k)\delta A_{k+q} - 3\beta_o \delta A^*_{k-q} A_k^2 \qquad (7.a)$$

in which δA already represents a perturbation on (6), and $\gamma_{k'} = \alpha_o [A_o^2 - (k'-k_c)^2]$. We also have the coupled equation of motion

$$\delta \dot{A}^*_{k-q} = (\gamma_{k-q} - 2\gamma_k)\delta A_{k-q} - 3\beta_o \delta A_{k+q} \dot{A}^{*2}_k \qquad (7.b)$$

Exponentially growing solutions of (7) with time constant μ yield

$$[\mu - (\gamma_{k+q} - 2\gamma_k)][\mu - (\gamma_{k-q} - 2\gamma_k)] = \gamma_k^2 \qquad (8)$$

In which, as usual, the time constant μ determines stability. Solution (6) is stable if given any q, μ is negative (or at least has negative real part). One of the two solutions of (8) has an extremum $\mu = 0$ at $q = 0$. Note that the occurrence of this neutrally stable solution at $q = 0$ is an obvious consequence of the translation invariance of the equations of motion. Close to this extremal point, we may neglect q^4 with respect to q^2 and q^2 with respect to Δ_o^2 and Δ_k^2. Thus, Eq. (8) becomes

$$\mu^2 - 2\mu\gamma_k + 2\alpha_o q^2(\gamma_k - 2\Delta_k\alpha_o) = 0 \qquad (9)$$

As $\gamma_k - 2\Delta_k\alpha_o =$ at $\Delta_k = \pm \frac{\Delta_o}{3}$, the range of stability of the solution of Eq. (4) is the open set $(K_c - \frac{\Delta_o}{3}, K_c + \frac{\Delta_o}{3})$. This result is particularly interesting as it delineates the range of non-linear stability of the steady roll pattern to longitudinal perturbations with no need, however, to appeal to any explicit calculations of such non-linear contributions as the β_o term in (4). This result of Eckhaus [1965,1971] points in the right experimental direction as discussed in the previous subsection. More general two-dimensional perturbations in the neighbourhood of R_c have been considered by Schlüter et al. [1965] but we shall turn now to the problem of transition to three-dimensionality.

iii) Transition to a three-dimensional still steady convection

Let us now turn our attention to another problem also belonging to the supercritical regime: the transition from predominantly two-dimensional convection to a three-dimensional convective pattern. This non-linear regime called "bimodal convection" by Busse and Whitehead [1974] has been explored experimentally by Krishnamurti [1970], Koschmieder and Pallas [1974] and Bergé and Dubois [1976], and has been studied theoretically by Busse [1972].

At a Rayleigh number depending on the Prandtl number, a secondary set of rolls appears with an axis orthogonal to the axis of the rolls of the first bifurcation. The wavelength of the transverse rolls is approximately half the wavelength of the primary pattern. According to Krishnamurti there is hysteresis in the formation of this three-dimensional structure. However, recent experiments conducted by Bergé and Dubois [1976] indicate a continuous transition as the first bifurcation is, except that the growth rate of the new structure of the velocity field is much slower than at the primary onset of predominantly two-dimensional convection. (Needless to note that convection is always three-dimensional with a real experiment in a finite box!). Owing to such a slow growth, it is rather tricky to measure accurately the secondary critical Rayleigh number associated with "bimodal convection". Busse [1967] has shown by computer analysis that for infinite Prandtl number fluids, the two-dimensional roll planform for an unbounded layer becomes linearly unstable whenever Ra is larger than $22{,}600 \pm 100$. Actually, Busse has defined a domain of "linear"

stability in the plane (Ra, a) bounded by Ra_c and 22,600 respectively from below and above. As a matter of fact, Koschmieder and Pallas [1974] find a well developed three-dimensional pattern at $Ra \approx 8\ Ra_c \approx 13{,}660$. A very similar figure has recently been found by Bergé and Dubois (private communication) using a rectangular container. These results contrast with the reported figure of 22,000 by Busse and Whitehead [1971].

This super-critical instability may be considered responsible for the occurrence of three-dimensional convection. Busse has noted that, in every case, the second instability comes first for perturbations with a wavevector orthogonal to the primary one. Furthermore, the wavelength of the perturbation is also found by Busse to be noticeably smaller than the wavelength of the primary flow: a result in qualitative agreement with the experimental findings.

Lastly, following Clever and Busse [1974], we may understand aspects of the secondary instability as follows. Let us assume first that the primary flow is absent. At a given super-critical Rayleigh number there is, among all the unstable convective patterns, a horizontal wavenumber with the highest growth rate which would tend to appear first. The primary flow stabilizes this secondary flow, but with an efficiency which is minimum when the two flows are orthogonal. This supports that the secondary flow is orthogonal to the primary one and has a wavenumber close to that corresponding to a maximum growth rate in the absence of primary flow.

7. Time-dependent phenomena and transition to turbulence

7.1 Relaxation oscillations

A number of experiments have shown that the convection flow becomes time-dependent when the Rayleigh number increases beyond a certain critical value. This unsteadiness may be due either to instabilities taking place inside the convection cell or to relaxation oscillation arising from the coupling between the heating system and the fluid. Of course, only the first kind of phenomenon is of intrinsic interest, as it does not depend on any particular experimental arrangement and reflects basic properties of the fluid equations. However, the occurrence of relaxation oscillations may lead to misunderstandings in the interpretation of experiments and we shall briefly explain how they may be triggered.

Consider an inverted bifurcation. At $R = R_1$ or slightly above, the parameter A (which may be viewed as the convection velocity, for instance) changes its value from $A = 0$ to another one, say $\pm A_1$. At the same time, the net heat flux through the cell changes from say ϕ_o in the state $A = 0$, to ϕ_1 in the state $\pm A_1$. Suppose now that heat is supplied at a constant rate, or that owing to the presence of poorly conducting boundaries, it may vary only very slowly. Thus, heat is taken by the convective flow in the state $\pm A_1$ in a time shorter than the scale of supply from boundary. Thus, the Rayleigh number may decrease from R_1 to R_2, and if flux in the $\pm A_2$ state is larger than ϕ_o it overshoots the $\pm A_2$ state and falls again in the $A = 0$ state with $R < R_2$. At this stage,

due to the constant heat supply, the Rayleigh number starts again to increase from R_2 to R_1 where the A = 0 state again becomes unstable, jumps to A_1, and so on. This explains the basic phenomenon by which relaxation oscillation may take place in a fluid heated at a constant power. Using a perturbation expansion around the critical number, Busse [1967] has obtained a system of equations describing these relaxation oscillations. Description of the gross features of the phenomenon will permit us to emphasize the differences between normal and inverted bifurcation. In the spirit of the Landau approach, let us consider first an equation of motion for A that describes an inverted bifurcation:

$$\dot{A} = \varepsilon A + A^3 - \beta A^5 \quad \text{with } \beta > 0 \tag{1}$$

The parameter ε describes approximately the temperature difference across the cell. This is proportional to $R - R_1$, where R_1 is the critical Rayleigh number at which the state A = 0 becomes linearly unstable.(*) This temperature difference is maintained by a constant external source, say S, and it tends to be lowered by the convective motion. Let μ be the typical rate of evolution of ε, then a model equation for the time dependence of ε is:

$$\dot{\varepsilon} + \mu\varepsilon = \mu(s - kA^2) \quad \text{with } k > 0 \tag{2}$$

(*) The state A = 0 does not need to be the motionless steady state; the whole discussion applies to an inverted bifurcation that can emerge from any steady state, convective or not.

The system (1) - (2) has A = 0 as a steady solution. This solution is stable for S < 0 and unstable for S > 0. Another steady state may exist, which is given by the solution of

$$\beta A^4 + A^2(k-1) = S = \tag{3}$$

The linear stability of this steady state is studied by considering a perturbation like $\delta A e^{\sigma t}$. The characteristic equation for σ is

$$\sigma^2 + \sigma\left[\mu + 4S + 2A^2(1-2k)\right] + 2\mu\left(S + \beta A^4\right) = 0 \tag{4}$$

if $k > 1/2$, the perturbation grows in an oscillatory way when $\mu + 4S + 2A^2(1-2k)$ becomes negative. They are two critical values of S if $1 > 4\beta\mu$:

$$S_{\pm} = -\frac{\mu}{4} + \frac{2k-1}{8\mu}\left(1 \pm \sqrt{1-4\beta\mu}\right) \tag{5}$$

the unstable region being $S_- < S < S_+$.

The upper bound of this unstable region, S_+, can be positive, for instance if k is large enough. This means that, in a range of values of S, μ, k and β, no stable steady solution exists.

It may be readily shown that no solution can go to infinity: consider the quantity $K = \varepsilon\dot{\varepsilon} + A\dot{A}$, when ε and A tend to infinity: From (1) and (2),

$$K \approx -\mu\varepsilon^2 - (k-1)A^2\Sigma - \beta A^6 = \\ = -\mu\left[\Sigma - \frac{(k-1)}{2\mu}A^2\right]^2 + \frac{(k-1)^2}{4\mu^2}A^4 - \beta A^6 \tag{6}$$

As A^4 becomes negligible in front of A^6 as A increases, this shows that K becomes certainly negative if ε and A are too large. This proves that, beyond some large circle in the plane (ε,A), the motion is always directed inwards; thus, according to general theorems on the continuous vector fields on a plane, this shows that the motion of the point (ε,A) tends to a limit cycle at least in the range of values of S for which no stable fixed point exists.

Concluding, we note that if steady oscillations (or perhaps even more complicated time dependent phenomena!) occur in a convection experiment where the heat flux is kept fixed, no definite statements should be made before a careful analysis rules out possible relaxation oscillations. This observation might help to clarify a recent dispute concerning oscillations in a two-component Bénard problem, in which the Soret effect is involved (see Hurle and Jakeman [1975], Platten [1975] and Caldwell [1974,1975]).

7.2 The unsteady flow and the transition to turbulence

Let us turn now to unsteadiness due to instabilities taking place in the fluid itself. The experimental investigation concerning this point is not fully satisfactory. A number of authors (Deardorff and Willis [1965], Rossby [1969], Hurle [1966], Krishnamurti [1970], Busse and Whitehead [1974], Ahlers [1974]) have observed that beyond a certain Rayleigh number, say R_t, the convection flow is no longer steady. We shall not go into a detailed analysis of these experiments, but merely indicate a number of questions that we think have

not yet received a sensible answer and demand further clarification:

i) How does R_t depend on the Prandtl number? Krishnamurti [1970] claims that at $P \gtrsim 50$, R_t reaches an almost constant value. This disagrees with the findings of Busse and Whitehead [1974]. There seems to be a serious experimental difficulty, as the first occurrence of a time-dependent flow is associated with regions of strong inhomogeneities in the convection pattern, which are caused mainly by experimental imperfections. Furthermore, it is not at all clear whether the bifurcation at R_t is of the normal or inverted type, i.e., whether the time-dependent part of the flow has or hasn't a vanishing amplitude at R_t.

ii) Does a periodic (or eventually a multiperiodic stage) precede a more complicated (or turbulent) stage? A number of authors have reported the occurrence of oscillation close to R_t; however, the coherence time of these oscillations is still unknown. This is unfortunate, since as explained below, there is a sharp distinction from the theoretical point of view between periodic motions with an infinite coherence time and aperiodic motions with a finite coherence time. And it turns out that, even in this latter case, the motion may very well look periodic, although it is not. Ahlers [1974] has measured the total heat flux in a convection experiment conducted with liquid helium. He has found that there was a quite well-defined jump from a steady flow to an unsteady one with irregular time dependence. But this does not imply that the flow has jumped

at the same time from a steady pattern to an unsteady one, since Koschmieder and Pallas [1974] have shown that well-defined transitions in the convective pattern might have no measurable influence on the heat flow. The white noise spectrum described by Ahlers [1974] may very well be due to the appearance of 'thermals' (or small regions of hot/cold fluid) in the layer. They originate in the two thermal boundary layers close to each rigid horizontal boundary where the temperature gradient experiences the greatest deformation under the extreme conditions observed in the turbulent regime in Ahlers' case. The sporadic and random 'thermals' move rapidly throughout the cell carrying a finite amount of (heat) energy to be released at the opposite plate. Can this be the origin of the shot-noise in certain time-dependent thermoconvective phenomena? (This remark was suggested by J. M. Normand; see also Rossby [1969]. The thermal boundary layer problem clearly demands a theoretical analysis, but this has not been done so far).

iii) What is the basic mechanism of unsteadiness? As far as we know, there are different suggestions which we shall discuss below.

iv) Is it possible to describe, with reasonable accuracy, the bifurcation toward an unsteady convection by keeping a finite (and hopefully, not too large) number of degrees of freedom? In other words, does the unsteady flow involve fluctuations with an arbitrary large band of wavenumbers?

To explain the basic mechanism of unsteadiness there are several theories that we shall describe now (see

for a more detailed account, Velarde and Pomeau [1977]). The first explanation of the onset of oscillations in Rayleigh convection seems to be that of Rossby [1969]. It is an adaptation of the large Rayleigh number theory developed by Howard [1963] and goes as follows. Let us assume that, at some instant of time, say t = 0, convection has made the temperature field almost uniform throughout the layer, with however the obvious exception of two thin boundary layers near the horizontal plates. Near the horizontal plates conduction is the basic mechanism of heat transport. Let T_1 be the "uniform" temperature distribution and T_2 be the temperature at the bottom plate. We take $T_2 > T_1$. The diffusive boundary layer that develops near each plate has a thickness $\delta(t_c) \sim d/Pe^{1/2} \sim (\kappa t_c)^{1/2}$, in which t_c denotes some characteristic time interval. The temperature drop across the boundary layer is $T_2 - T_1$, and if T_1 does not vary in an appreciable way it would in turn become unstable when $(T_2 - T_1) g\alpha\delta^3(t_c)/\kappa\nu$ exceeds some critical Rayleigh number, so that convection develops in the boundary layer itself. This yields an "explosive" instability as convection tends to increase the thickness of the layer which in turn increases the growth rate. Then a "bubble" or "thermal" of temperature T_2 progresses in a convective fluid of mean temperature T_1. This thermal leaves the lower plane to move upwards. This motion would in turn destroy the boundary layer setting the fluid back to the initial configuration. The mean period τ of this oscillation is approximately the time delay needed to build a new unstable boundary layer, and it is given by

$$(\alpha\tau)^{3/2}(T_2 - T_1) \sim 1 \qquad (1)$$

from which we have

$$\tau \sim (T_2 - T_1)^{-2/3} \qquad (2)$$

The power dependence given by Eq. (2) fits quite well with the results of Rossby [1969]. Rossby's theory has not as yet been proven invalid, it uses rather general arguments and it is not really known whether a given unsteady convective pattern fits Rossby's theory or not. Measurements close to the upper and lower boundaries should be very useful.

Another mechanism to secondary instability was suggested by Welander [1967]. Consider a temperature fluctuation (or "hot spot") which is convected by the flow. To a first approximation we may assume that this hot spot rotates within the roll with a mean period that is approximately proportional to the convective time delay imposed by the velocity field. Welander noticed an accelerating mechanism for this periodic motion. His reasoning goes as follows. A hot spot moves upwards faster than the average flow, and downwards slower. As it is cooled in its rising motion, the cooling stage may become less efficient than the warming one, and there is a tendency for this hot spot to become hotter and hotter as it keeps on each rotation a boost which is not balanced during the cooling stage. Of course, this mechanism has to struggle against heat and vorticity diffusion.

Let us however come back to the known experimental facts. In the high Prandtl number limit, Krishnamurti has observed oscillations of the convection pattern which she attributes to the instability described by Welander. On

the other hand, Willis and Deardorff [1970] see no important difference between the unsteady patterns at low (air, σ = .71) and large (silicon oil, σ = 57) Prandtl number. Furthermore, they have studied the temperature fluctuations at low Prandtl number and shown that the oscillations are almost independent on depth, which is in sharp disagreement with the Welander picture. The more recent measurement of Busse and Whitehead [1974] results are essentially in qualitative agreement with those of Willis and Deardorff: with large Prandtl number they observe first an oscillatory instability whose general structure closely resembles the one of the low Prandtl number case. They also observed that, when the amplitude of the oscillations exceeded some level, a transition to a much more irregular phenomenon, which they call "spoke pattern", took place.

Except for the measurements of the temperature field in the convection cell made by Willis and Deardorff, and various measurements of the time period, there are actually no quantitative data available about the structure of the periodic flow, so that it is not clear yet whether the oscillations predicted by Welander have been seen or not. However, recent results of Clever and Busse [1974] are of interest. In their stability study of an infinite away from two-dimensional parallel rolls to infinitesimal time-dependent perturbations at super-critical Rayleigh numbers. They have predicted a number of instabilities, two of which we shall now briefly describe. These are called the zig-zag instability and the oscillatory instability. Both have equal spacial periodicity to the primary roll pattern and along the latter's axis (say x). In addition, they also have a

non-vanishing wavenumber component, b, along a perpendicular direction (say y) to the primary structure. The growth rate and periodicity, b, of the zig-zag mode tends to the shortening of the effective rolls wavelength and thus merely represents a small shift of the roll pattern in the y-direction. The growth rate of the oscillatory instability, however, does not vanish with vanishing b. This oscillatory instability corresponds to a bending of the primary rolls that propagate in time along the roll axis. Nearly perfect agreement between the theoretically predicted frequency of this oscillatory instability and the experimental findings of Willis and Deardorff [1970] is claimed by Clever and Busse [1974].

Though Welander also gave a model that yielded some quantitative results, we shall turn now to describe Saltmann's [1962] and Lorenz' [1963] theory of the transition to time-dependent convection. These works procede Welander's but according to Malkus [1972] they essentially refer to a similar phenomenon.

REFERENCES

AHLERS, G., 1974, Phys. Rev. Letters 33, 1185.

BÉNARD, H., 1900, Rev. Gen. Sci. 11, 1261.

BÉNARD, H., 1901, Ann. Chim. Phys. [7] 23, 62.

BÉNARD, H., 1927, C. R. Acad. Sci. Paris 185, 1109.

BÉNARD, H., 1928, Bull. Soc. Franc. Phys., 112 S.

BENTWICH, M., 1971, Appl. Sci. Res. 24, 305.

BERG, J. C., A. ACRIVOS and M. BOUDIART, 1966, Adv. Chem. Eng. 6, 61

BERGÉ, P. and M. DUBOIS, 1976, "Fluctuation, Instabilities and Phase Transitions", NATO Advanced Study Institute, Vol. B11 (Plenum, New York) 323.

BERGÉ P. and M. DUBOIS, 1974, Phys. Rev. Letters 32, 1041.

BERGÉ, P., 1976, J. Physique 37, Colloq. C1, 23.

BIRD, R. B., W. E. STEWART and E. N. LIGHTFOOT, 1960, Transport Phenomena (Wiley, New York).

BLOCK, M. J., 1956, Nature 178, 650.

BURKHALTER, J. E. and E. L. KOSCHMIEDER, 1973, J. Fluid Mech. 58, 547.

BUSSE, F., 1962, Ph.D. Thesis (Munich) unpublished.

BUSSE, F., 1967, J. Fluid Mech. 28, 223.

BUSSE, F., 1972, J. Fluid Mech. 52, 97.

BUSSE, F. and J. A. WHITEHEAD, 1974, J. Fluid Mech. 66, 67.

CALDWELL, D. R., 1974, J. Fluid Mech. 64, 347.

CALDWELL, D. R., 1975, J. Phys. Chem. 79, 1882.

CHANDRASEKHAR, S., 1961, Hydrodynamic and hydromagnetic stability (Clarendon Press, Oxford).

CLEVER, R. M. and F. H. BUSSE, 1974, J. Fluid Mech. 65, 625.

DAUZERE, C., 1907, J. Physique 6, 892.

DAVIS, S. H., 1967, J. Fluid Mech. 30, 465.

DAVIS, S. H., 1968, J. Fluid Mech. 32, 619.

DAVIS, S. H. and L. A. SEGEL, 1968, Phys. Fluids 11, 470.

DEARDORFF, J. W. and G. E. WILLIS, 1965, J. Fluid Mech. 23, 337.

DUBOIS, M., 1976, J. Physique 37, Colloq. C1, 137.

ECKHAUS, W., 1965, Studies in Nonlinear Stability Theory (Springer-Verlag, New York).

ECKHAUS, W., 1971, in "Instability of Continuous Systems", H. Leipholz, editor (Springer-Verlag, Berlin) 194.

GOR'KOV, L. P., 1957, J.E.T.P. 33, 402 (English transl. 1958 Soviet Phys. J.E.T.P. 6, 311).

GRAHAM, R., 1973, Springer Tracts Mod. Phys., Vol. 66.

GRODZKA, P. G. and T. C. BANNISTER, 1972, Science 176, 506.

GRODZKA, P. G. and T. C. BANNISTER, 1975, Science 187, 165.

HAKEN, H., 1975, Revs. Mod. Phys. 47, 67.

HERSHEY, A. V., 1939, Phys. Rev. 56, 204.

HOARD, C. Q., C. R. ROBERTSON and A. ACRIVOS, 1970, Int. J. Heat Mass Transfer 13, 849.

HOPF, E., 1942, Ber. Math. Phys. Akad. (Leipzig) 94, 1.

HOPF, E., 1948, Comm. Pure Appl. Math. 1, 303.

HOWARD, L., 1963a, J. Fluid Mech. 17, 333.

HOWARD, L., 1963b, J. Fluid Mech. 17, 405.

HURLE, D. T. J., E. JAKEMAN and R. E. PIKE, 1967, Proc. Roy. Soc. London A296, 469.

HURLE, D. T. J. and E. JAKEMAN, 1975, Adv. Chem. Phys. 32, 277.

JEFFREYS, H., 1926, Phil. Mag. |7|, 2, 833.

JEFFREYS, H., 1930, Proc. Camb. Phil. Soc. 26, 170.

JEFFREYS, H., 1951, Quart, J. Mech. Appl. Math. 4, 283.

JEFFREYS, H., 1956, Quart. J. Mech. Appl. Math. 9, 1.

JOSEPH, D. D., 1965, Arch. Rat. Mech. Anal. 20, 59.

JOSEPH, D. D., 1971, J. Fluid Mech. 47, 257.

JOSEPH, D. D., 1976, Stability of Fluid Motions (Springer-Verlag, Berlin, Heidelberg and New York).

KOSCHMIEDER, E. L., 1966, Beit. Z. Phys. Atmos. 39, 1

KOSCHMIEDER, E. L., 1967, J. Fluid Mech. 30, 9.

KOSCHMIEDER, E. L., 1969, J. Fluid Mech. 35, 527.

KOSCHMIEDER, E. L., 1975, Adv. Chem. Phys. 32, 109.

KOSCHMIEDER, E. L. and S. G. PALLAS, 1974, Int. J. Heat Mass Transfer 17, 991.

KRISHNAMURTI, R., 1970, J. Fluid Mech. 42, 295, 309.

LANDAU, L. D., 1944, C. R. Acad. Sci. USSR 44, 311.

LANDAU, L. D. and E. M. LIFSHITZ, 1959, Fluid Mechanics (Pergamon Press, Oxford).

LIN, C. C., 1967, The Theory of Hydrodynamic Stability (Univ. Press, Cambridge).

LORENZ, E. N., 1963, J. Atmos. Sci. 20, 130.

MARKUS, W. V. R., 1972, in Proc. 4th Liege Symposium on Ocean Hydrodynamics, Mem. Soc. Soy. Sci. Liege 4, 125.

MALKUS, W. V. R. and G. VERONIS, 1958, J. Fluid Mech. 4, 225.

NEWELL, A. C., C. G. LANGE and P. J. AUCOIN, 1970, J. Fluid Mech. 40, 513.

NICOLIS, G., J. WALLENBORN and M. G. VELARDE, 1969, Physica 43, 263.

NIELD, D. A., 1964, J. Fluid Mech. 19, 341.

PALM, E., 1960, J. Fluid Mech. 8, 183.

PALM, E. and H. ØIANN, 1964, J. Fluid Mech. 19, 353.

PEARSON, J. R. A., 1958, J. Fluid Mech. 4, 489.

PELLEW, A. and R. V. SOUTHWELL, 1940, Proc. Roy. Soc. London A176, 312.

PEREZ-CORDÓN, R. and M. G. VELARDE, 1975, J. Physique, Paris 36, 591.

PLATTEN, J. K. and G. CHAVEPEYER, 1975, Adv. Chem. Phys. 32, 281.

PRIGOGINE, I., 1949, Physica, 15, 272.

RAYLEIGH (Lord), 1916, Phil. Mag. 32, 529.

ROSSBY, H. T., 1969, J. Fluid Mech. 36, 309

SALTZMAN, B., 1962, J. Atmos. Sci. 19, 329.

SANI, R., 1963, Convective Instability, Ph.D. Thesis (Minnesota) unpublished.

SATTINGER, D. H., 1973, Topics in Stability and Bifurcation Theory (Springer-Verlag, New York).

SCHLÜTER, A., D. LORTZ and F. BUSSE, 1965, J. Fluid Mech. 23, 129.

SCRIVEN, L. E. and C. V. STERNLING, 1964, J. Fluid Mech. 19, 321.

SEGEL, L. A. and J. T. STUART, 1962, J. Fluid Mech. 13, 209.

SMITH, K. A., 1966, J. Fluid Mech. 24, 401.

SOBERMAN, R. K., 1958, J. Appl. Phys. 29, 872.

STERNLING, C. V. and L. E. SCRIVEN, 1959, A. I. Ch. E. Journal 5, 514.

STORK, K. and U. MÜLLER, 1972, J. Fluid Mech. 54, 599.

STRATONOVICH, R. L., 1963, 1967, Topics in the Theory of Random Noise, Vols. I and II (Gordon and Breach, New York).

TERADA, T. and Second year students of Physics, 1928, Tokyo Imp. Univ., Aero. Res. Inst. Rept. 3, 3.

THOM, R., 1974, Stabilité structurelle et Morphogénèse (Union Gén. Eds., Paris).

VELARDE, M. G., 1976, in "Mathematical and Numerical Methods in Fluid Dynamics" (IAEA, Vienna) 489.

VELARDE, M. G., 1977, in "Fluid Dynamics" (Les Houches, 1973), R. Balian and J. L. Peube, editors (Gordon & Breach, New York) 469.

VELARDE, M. G. and R. PEREZ-CORDÓN, 1976, J. Physique, Paris, 37,17

VELARDE, M. G. and Y. POMEAU, 1977, Thermohydrodynamic Instabilities: An Introduction (Springer-Verlag, New York) in preparation.

VELARDE, M. G. and R. S. SCHECHTER, 1972, Phys. Fluids 15, 1707.

VERNOTTE, P., 1936a, C. R. Acad. Sci. Paris 202, 119.

VERNOTTE, P., 1936b, C. R. Acad. Sci. Paris 202, 733.

VOLKOVISKY, V., 1935, C. R. Acad. Sci. Paris 200, 1285.

VOLKOVISKY, V., 1939, Pub. Sc. Tech. Ministère de l'Air, Vol. 151.

WELANDER, P., 1967, J. Fluid Mech. 29, 17.

WILLIS, G. E. and J. W. DEARDORFF, 1970, J. Fluid Mech. 44, 661

YIH, C. S., 1961, Phys. Fluids 4, 808.

1. Model equations and stability analysis: one-dimensional problems

In this part of the 1976 Report we shall discuss the role of nonlinearity, and bifurcation to limit cycle and nonlinear steady structures in simple reaction-diffusion systems. We shall, however, restrict ourselves here to isothermal, non-convecting media, leaving for the 1977 Report a detailed discussion of the coupling of convection, and convective instability to non-idothermal reaction-diffusion mechanisms. Nonlinearity may be brought either by spatially local strong interaction or by non-local processes in kinetic phenomena. For motivation, the reader is referred to the book of Aris [1976]. On the other hand, we are also interested in understanding the role of binary and ternary collision processes in dense media, i.e. bimolecular and trimolecular reaction steps /

The following models of global processes have been of our interest: We consider two intermediate reactions in an open container where strong non-equilibrium reaction takes place:

(i) $$A \longrightarrow Y \tag{1.a}$$

$$X + Y \longrightarrow 2X \tag{1.b}$$

$$X \xrightarrow{\text{SAT.}} P \tag{1.c}$$

To this scheme we associate the following differential problem in dimensionless form

$$\frac{\partial}{\partial t}X = XY - \left(X/1+qX\right) + D_X \Delta X \qquad (2.a)$$

$$\frac{\partial}{\partial t}Y = A - XY + D_Y \Delta Y \qquad (2.b)$$

in which the saturation law is called the first-order Hinshelwood-Langmuir [Michaelis-Menten] law. Note that A, P, are products whose concentration can be externally controlled. q yields a measure of the strength of the saturation law. X,Y, A denote concentrations of the respective reactant that we shall take positive definite. All reaction constants, besides q, have been normalized to one (see for details IBAÑEZ, FAIRÉN and VELARDE [1976.a]). D_X,D_Y are respectively the dimensionless diffusion constants of X and Y and Δ denotes the Laplacian operator. We shall consider either fixed concentrations on the boundary (Dirichlet problem) or fixed fluxes (Neumann problem).

(ii)

$$A \longrightarrow Y \qquad (3.a)$$

$$B \rightleftharpoons X \qquad (3.b)$$

$$X + Y \xrightarrow{\text{INHIB.}} P \qquad (3.c)$$

to which we associate the following evolution problem in dimensionless form

$$\frac{\partial}{\partial t} X = B - X - \left(XY / 1 + q X^2 \right) + D_x \Delta X \tag{4.a}$$

$$\frac{\partial}{\partial t} Y = A - \left(XY / 1 + q X^2 \right) + D_Y \Delta Y \tag{4.b}$$

The symbols have the same meaning as above. For motivation and details see IBAÑEZ, FAIRÉN and VELARDE [1976.b].

(iii)

$$A \longrightarrow Y \tag{5.a}$$

$$Y + q X \longrightarrow (q+1) X \quad [q > 0; q = 1, q = 2] \tag{5.b}$$

$$X \longrightarrow P \tag{5.c}$$

to which we associate the following dimensionless problem

$$\frac{\partial}{\partial t} X = X^q Y - X + D_x \Delta X \tag{6.a}$$

$$\frac{\partial}{\partial t} Y = A - X^q Y + D_Y \Delta Y \tag{6.b}$$

Here the cases q = 1 and q = 2 correspond respectively to binary and ternary collision processes. For motivation and details see BALSLEV and DEGN [1975].

Fixed points (i.e., steady solutions) of these models are easily found in the homogeneous case. Once the fixed points are located we are interested in their stability. We shall discuss model after model:

(i) Model (1)

Fixed point (homogeneous)

$$X_s = A/Y_s \tag{7.a}$$

$$Y_s = 1 - qA \tag{7.b}$$

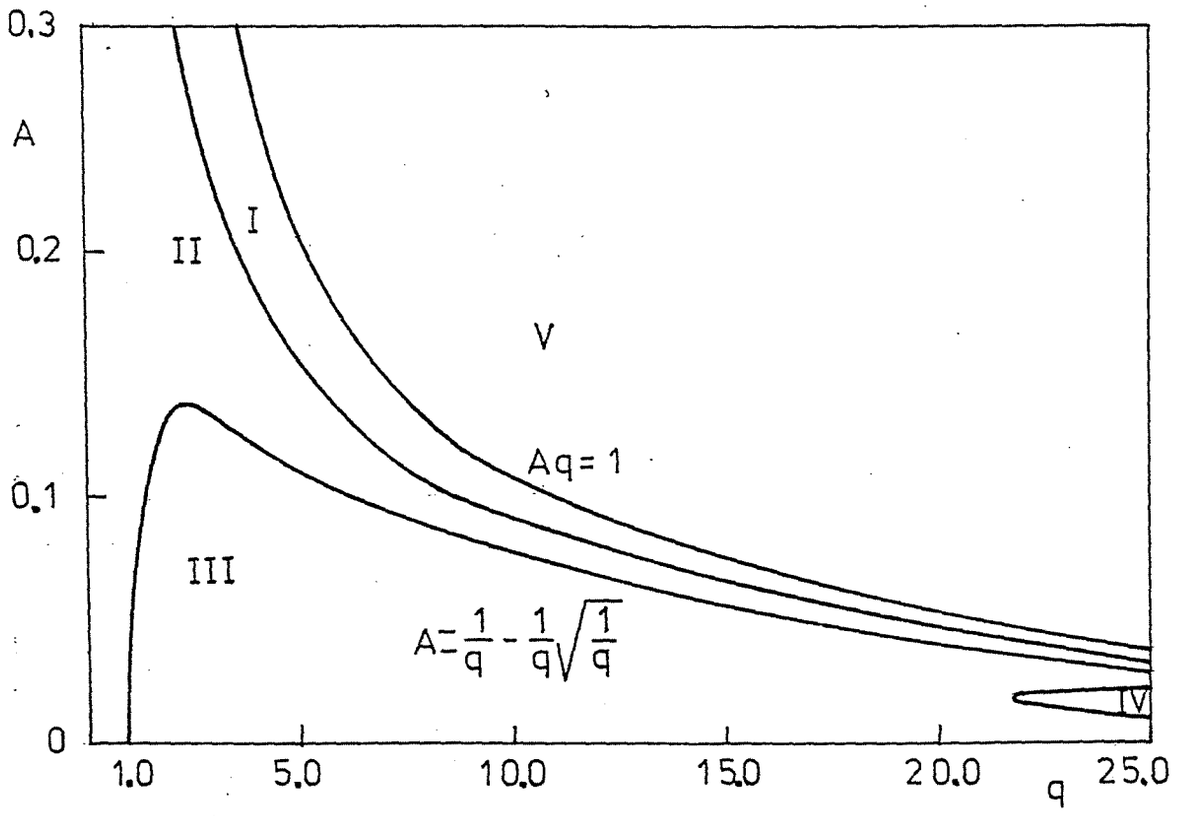

FIG. 1

Figure 1 describes the linear stability portrait.

Regions I and II correspond to asymptotic stability of the steady state (X_s, Y_s), with characteristics of stable node (region I) and stable focus (region II). All

other regions (III through V) yield instability of the steady state.

Regions III and IV correspond, respectively, to unstable focus and unstable node. Provided the nonlinear solution is bounded, limit cycle behaviour is to be expected in these two regions. We have located the limit cycle for $q = 2.0$ and $A = 0,1$. It is to be noted that the limit cycle is orbitally asymptotically stable. For a given value of q with decreasing A($A < 1/q$ the limit cycle appears as a Hopf bifurcation at $A_o = 1/q - (1/q)^{3/2}$. Its amplitude viz. the distance separating (X_s, Y_s), at every instant of time, from the moving point with same Y_s) on the orbit, is a continuous function of A. Region V is such that $Aq > 1$, and corresponds to saddle point. We have also studied the influence of molecular diffusion of the intermediate reactants, X and Y. It suffices to add to the r.h.s. a term $D_x \partial^2 X/\partial r^2$ and correspondingly to the r.h.s. a term $D_y \partial^2 Y/\partial r^2$. Here D_x and D_y denote the two molecular diffusivities involved. For simplicity we limit ourselves here to a one-dimensional problem. The system is thought to be enclosed in a box of length $L(0 < r < L = 1)$.

For fixed concentrations (f.c.) or fixed fluxes (f.f.) on boundary, the system still possesses one homogeneous steady solution and the same given above: (x_s, y_s). Linear stability analysis with diffusion yields the following major results: (i) for $D_x > D_y$ and f.f. on boundaries the regions I and II are unchanged. (ii) For $D_x > D_y$ and f.c. on boundaries, diffusion tends to play a

stabilizing role; that is, region II increases at the expense of region III. (iii) For $D_x < D_y$ and f.f. on boundaries, diffusion plays a destabilizing role. Region III is enlarged at the expense of region II. (iv) For $D_x < D_y$ and f.c. on boundaries, diffusion acts both as a stabilizing and destabilizing mechanism with not too dramatic a role to be of interest to us here.

In cases (iii) and iv) instability first arises from saddle point-type linear eigenvalues λ_m that depend on non-vanishing wave-numbers ($m \neq 0$). It is to be noted that on demanding which linear normal mode comes with fastest growth all we find is that $D_y > D_x$ if a mode is to grow at all. Thus to define a critical value of A, A_c, we follow the prescription given by Segel and Jackson [1972]. A_c should belong to the range of A such that $A_c > 1/q - (1/q)^{3/2}$ in which the steady homogeneous solution is stable if diffusion is absent.

Furthermore A_c should also be smaller than the values of A which yield a region of asymptotic stability to the homogeneous solution. Thus for A in the range $1/q - (1/q)^{3/2} < A < A_c$ the homogeneous solution is unstable. Dissipative structures (i.e. asymptotically stable steady inhomogeneous solutions) appear in such region. Two examples are described in Fig. 2. In Fig. 2 (bottom) the dissipative structure corresponds to a single mode excitation at $q = 10.0, D_x = 1.0 \times 10^{-4}$, $D_y = 5.0 \times 10^{-4}$, and $A = 0.07565$. Fig. 2 (top) depicts a dissipative structure when four modes are excited at once. This corresponds to $A = 0.07365$, and all other quantities as above. The phase difference of 180° between the X and Y distributions, corresponds to regions where alternatively the substrate or the product accumulate.

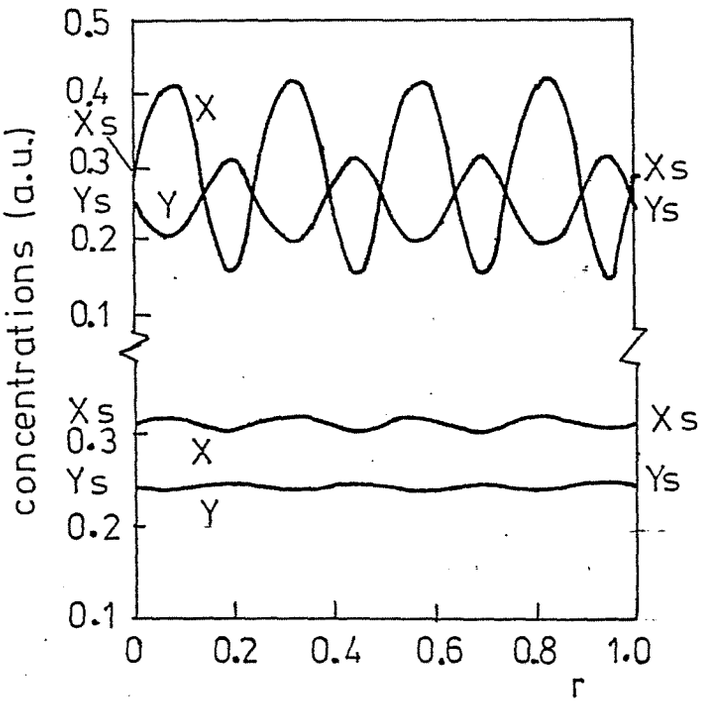

FIG. 2

(ii) Model (3)

Fixed point

$$X_s = B - A \tag{8.a}$$

$$Y_s = \left\{ A \left[1 + q(B-A)^2 \right] \right\} / (B-A) \tag{8.b}$$

Fig. 3 depicts the linear stability portrait.

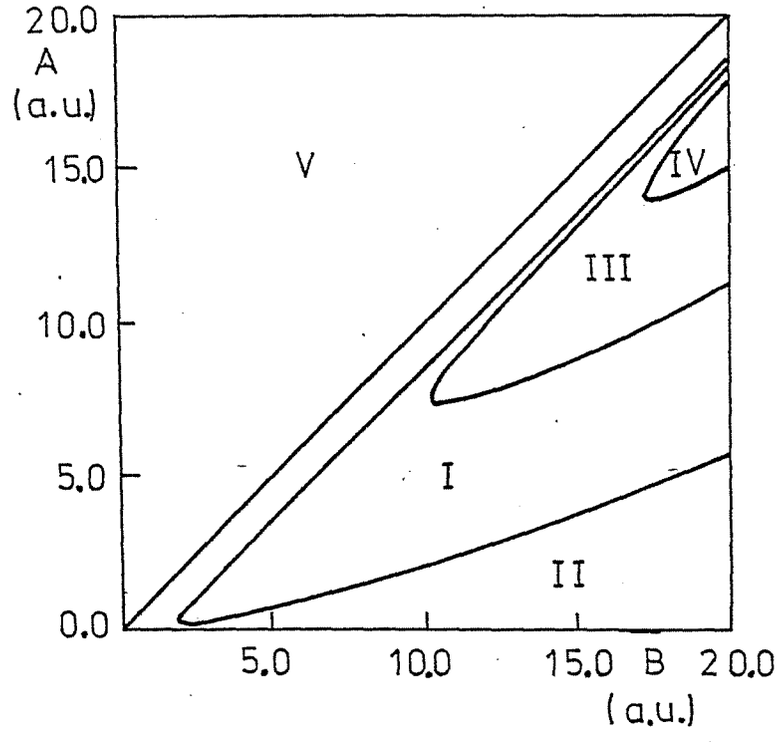

FIG. 3

Regions I and II correspond respectively to stable focus (I) and stable node (II). Regions III and IV yield instability of the steady state. Here we have respectively unstable focus (III) and unstable node (IV) with a Poincaré index (+1) (which is a necessary condition for the appearance of limit cycle around the steady state). Region V is of no interest here as it yields negative or undefined values of concentrations. On the other hand, it corresponds to saddle point behavior with a Poincaré index (-1). No limit cycle is to be expected here.

In regions III and IV, the system does satisfy the necessary and sufficient conditions for the existence of

limit cycle (Poincaré-Bendixon theorem in dimension two). As an illustration, the limit cycle can be drawn with the computer for the triplet A = 14.0, B = 20.0 and q = 0.5.

To study the influence of diffusion of the intermediate reactants we simply add to the r.h.s. a term $D_X \partial^2 X/\partial r^2$ and correspondingly to the r.h.s. a term $D_Y \partial^2 Y/\partial r^2$. Here D_X and D_Y respectively denote the mass diffusivity of X and Y. For simplicity we limit consideration here to a one-dimensional box of length $L (0 \leq r \leq L = 1)$. The new differential system with either fixed concentrations or fixed fluxes still posseses a unique homogeneous steady solution given by (8). Linear stability of (8) in (4) to inhomogeneous perturbations is governed by a wave-dependent eigenvalue polynomial equation in $\lambda_k = \lambda(k)$

$$\lambda_k^2 + \delta_k \lambda_k + \Delta_k = 0 \qquad (9)$$

in which k denotes the inverse of a characteristic length of the perturbation. In Eq. (9), $\delta_k = \delta + (k\pi/L)^2 (D_X + D_Y)$ and

$$\Delta_k = \Delta + D_X D_Y \left(\frac{k\pi}{L}\right)^4 +$$

$$+\left(\frac{k\pi}{L}\right)^2 \left\{ D_Y \left(1 + \frac{A[1 - q(B-A)^2]}{(B-A)[1 + q(B-A)^2]}\right) + D_X \frac{(B-A)}{1 + q(B-A)^2} \right\}$$

For a given triplet (D_X, D_Y, q), and varying A and B, we may cross from the asymptotic stability region of the steady solution (i.e., $Re\lambda_k < 0$ for all admissible k) to a region of instability. Assuming that in the unstable region, bifurcation of secondary solutions corresponds to a single critical wavenumber k_c (with all other $k \neq k_c$), and $Re\lambda_k < 0$), the following cases are of interest.

i) $\lambda_k(k = k_c)$ is purely imaginary. With fixed fluxes (f.f.) on boundaries, bifurcation occurs with a vanishing wavenumber. Thus, diffusion does not play any role. However, with fixed concentrations (f.c.) on boundaries bifurcation appears with $k_c = 1$. Here, diffusion plays a stabilizing role.

ii) $\lambda_k(k = k_c)$ is real. In this case $k_c \neq 0$ and diffusion may play a destabilizing role. However, not all values of the triplet (D_X, D_Y, q) yield bifurcation. Bifurcation with λ_k real is only possible provided the following two conditions are satisfied.

$$D_Y > D_X \tag{10.a}$$

$$T(D_X, D_Y, q) \equiv$$
$$\equiv \left(1 - \frac{4 D_X D_Y}{(D_X + D_Y)^2}\right) - 64 \frac{(D_X D_Y)^2 q}{(D_X + D_Y)^4} > 0 \tag{10.b}$$

(it is to be noted that if $D_Y < D_X$ or $T < 0$ there is bifurcation to a time-dependent solution from purely imaginary eigenvalues). For f.c. diffusion plays a destabilizing role in the system whereas for f.f. diffusion plays no role.

When conditions (10) are satisfied with λ_k real, the homogeneous steady solution (8) yields way to an inhomogeneous steady solution. An asymptotically stable inhomogeneous steady solution is called a dissipative structure . Computer solution of the nonlinear system with diffusion, shows the appearance of dissipative structures that we have plotted in Fig. 4 for the case $\{D_X = 10^{-4}$, $D_Y = 10^{-3}$, q = 0.5, A = 8.916, B = 11.0 and L - 1.0$\}$.

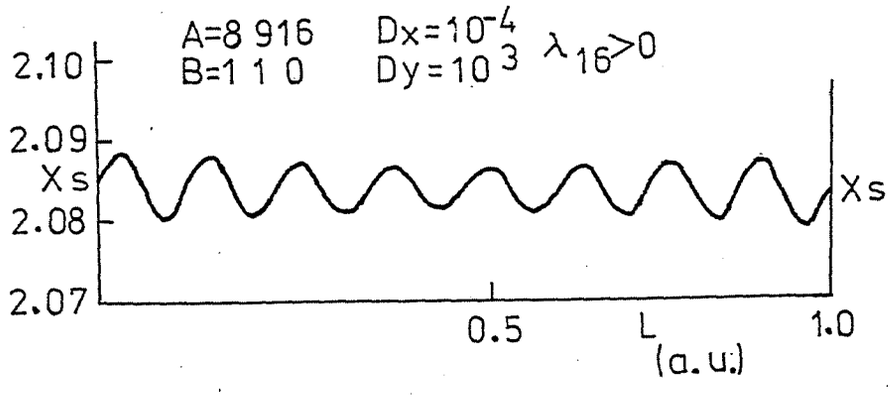

FIG. 4

(iii) Model (5)

Fixed point

$$X_s = A \tag{11.a}$$

$$Y_s = A^{(1-q)} \quad (q>0\,;\ q=1\,,\ q=2) \tag{11.b}$$

There is also the possibility of an unbounded solution

$$X(t) = 0 \tag{12.a}$$

$$Y(t) = At + Y(t=0) \tag{12.b}$$

The linear portrait of stability around (11) is pictorially described in Fig. 5.

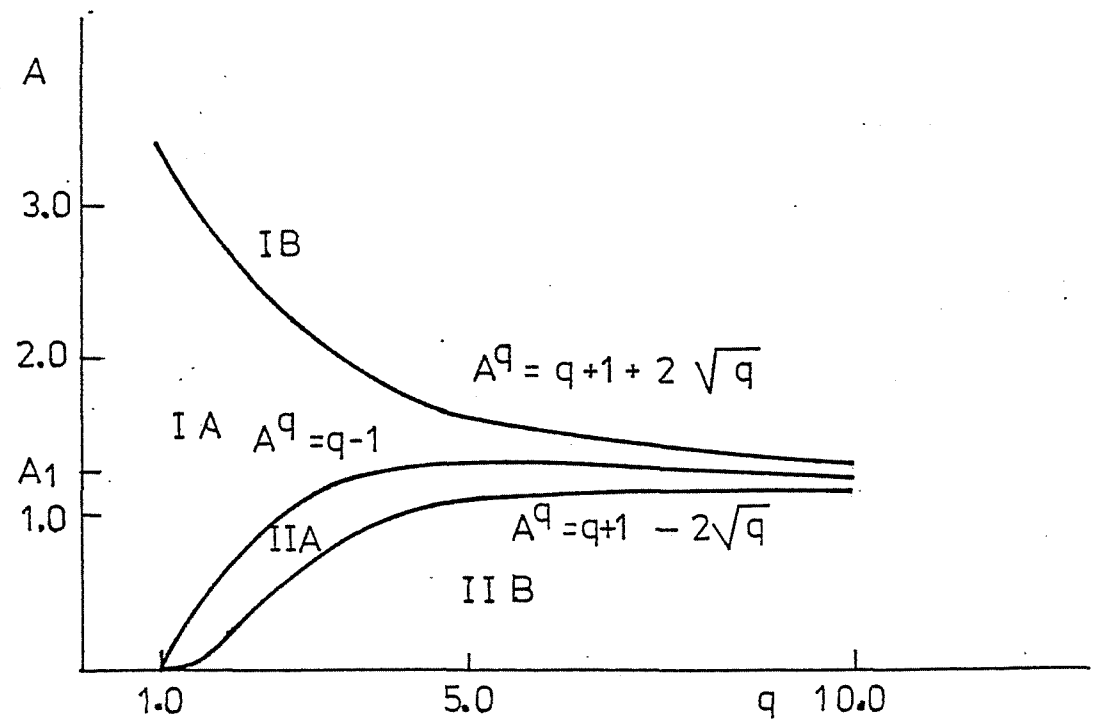

FIG. 5

Regions IA and IB are of local asymptotic stability of (11) with characteristics of stable focus (IA) and stable node (IB) respectively. In region II the steady state is unstable with characteristics of unstable focus (IIA), and unstable node (IIB) respectively.

According to a theorem proved by Tyson [1973] and Hanusse [1972] there is no possibility of limit cycle for $q = 1$. This result follows from our computer-aided representation (Fig. 5). For if $q < 1$, the steady state (11) is stable for all values of $A > 0$. The two instability areas (II) described in Fig. 5 just collapse to a point as q approaches one from above.

On the other hand, the maximum of $A^q = (q - 1)$ occurs at $q \approx 4.59$, and $A = A_1 \approx 1.3$. Thus, for $A > A_1$ the steady state (11) is asymptotically stable for all values of $q > 0$.

At $A = A_c = (q - 1)^{1/q}$, there is a Hopf bifurcation for all $q > 1$. The following two conditions are satisfied: (i) the roots $\lambda_1(A) \pm i\lambda_2(A)$ are such that $\lambda_1(A_c) = 0$, and $\lambda_2(A_c) \neq 0$, and (ii) the transversality condition $\frac{\partial \lambda_1(A)}{\partial A}\Big|_{A=A_c} \neq$ These two conditions ensure the existence of a time-periodic solution in at least a small neighborhood of A_c. If $\{X_p(t), Y_p(t)\}$ denote the periodic solution of frequency $\omega = \omega(A)$, Hopf bifurcation theorem yields that $\sup|X_p(\tau) - X_s| \to 0$, $\sup|Y_p(\tau) - Y_s$ and $\omega \to \lambda_2(A_c)$ for $\tau \in |0, \frac{2\pi}{\omega}|$ as $A \to A_c$.

The stability of $\{X_p, Y_p\}$ is related to the Floquet exponents . It appears that if the solution exists for $A < A_c$ it is orbitally asymptotically stable, whereas for $A > A_c$, if there is one it is unstable.

The analytical form of this time-periodic solution

can be obtained by the Poincaré-Linstedt method. We take

$$A_p = A_c + \sum_{n=2}^{\infty} \epsilon^n A_n \tag{13.a}$$

$$X_p = X_s + \sum_{n=1}^{\infty} \epsilon^n X_n \tag{13.b}$$

$$Y_p = Y_s + \sum_{n=1}^{\infty} \epsilon^n Y_n \tag{13.c}$$

$$\omega = \lambda_2(A) + \sum_{n=2}^{\infty} \epsilon^n \lambda_n' \tag{13.d}$$

It is to be noted that the vanishing value of the new unknown ϵ yields back the primary solution (11). Substituting (13) in (6) and solving up to third order gives $A_2 = -\frac{1}{4} A_c^{-1}(q-1) < 0$, and $A_p < A_c$. Thus, the bifurcated solution is orbitally asymptotically stable.

That Hopf bifurcation theorem only ensures the existence of a periodic solution in a small enough neighborhood of A_c it is clear. For we have found that for $A \leq \bar{A}_c$ with $0.90 < \bar{A}_x < 0.91$ and $q = 2$ the periodic solution $\{X_p, Y_p\}$ is no longer valid, and the system (6) takes on the unbounded solution (12). This behaviour is to be expected as there is no saturation law in Eq. (6). Nor is there more than the $(q+1)$-molecular step and this is just not enough to stop an unlimited growth of the intermediate reactants. The transition is illustrated in Fig. 6 where $\sup|X_p(\tau)-X_s|$ is plotted against A. $A_c = 1$ is the point where the steady solution (11) loses stability, and the system (6) takes on the limit cycle $\{X_p, Y_p\}$.

We have also studied the role of diffusion in (6), and the results are qualitatively similar to those found in the two models previously discussed by the present authors. Thus, we merely give here the relevant features of the phase diagram shown in Fig. 7 . If D_x, D_y denote the respective diffusion coefficients of reactants X and Y, for fixed fluxes on the boundary (Neumann problem), there is bifurcation to asymptotically stable inhomogeneous steady state for $q \geq Q$ ($Q = 2.25$ with $D_y/D_x = 5$). There is bifurcation to time-periodic solution for $1 < q < Q$ ($Q = 2.25$ with $D_y/D_x = 5$). No bifurcation exists for $q \leq 1$. It is to be noted that with $D_y/D_x \to \infty$ we have $Q \to 1$.

FIG. 6

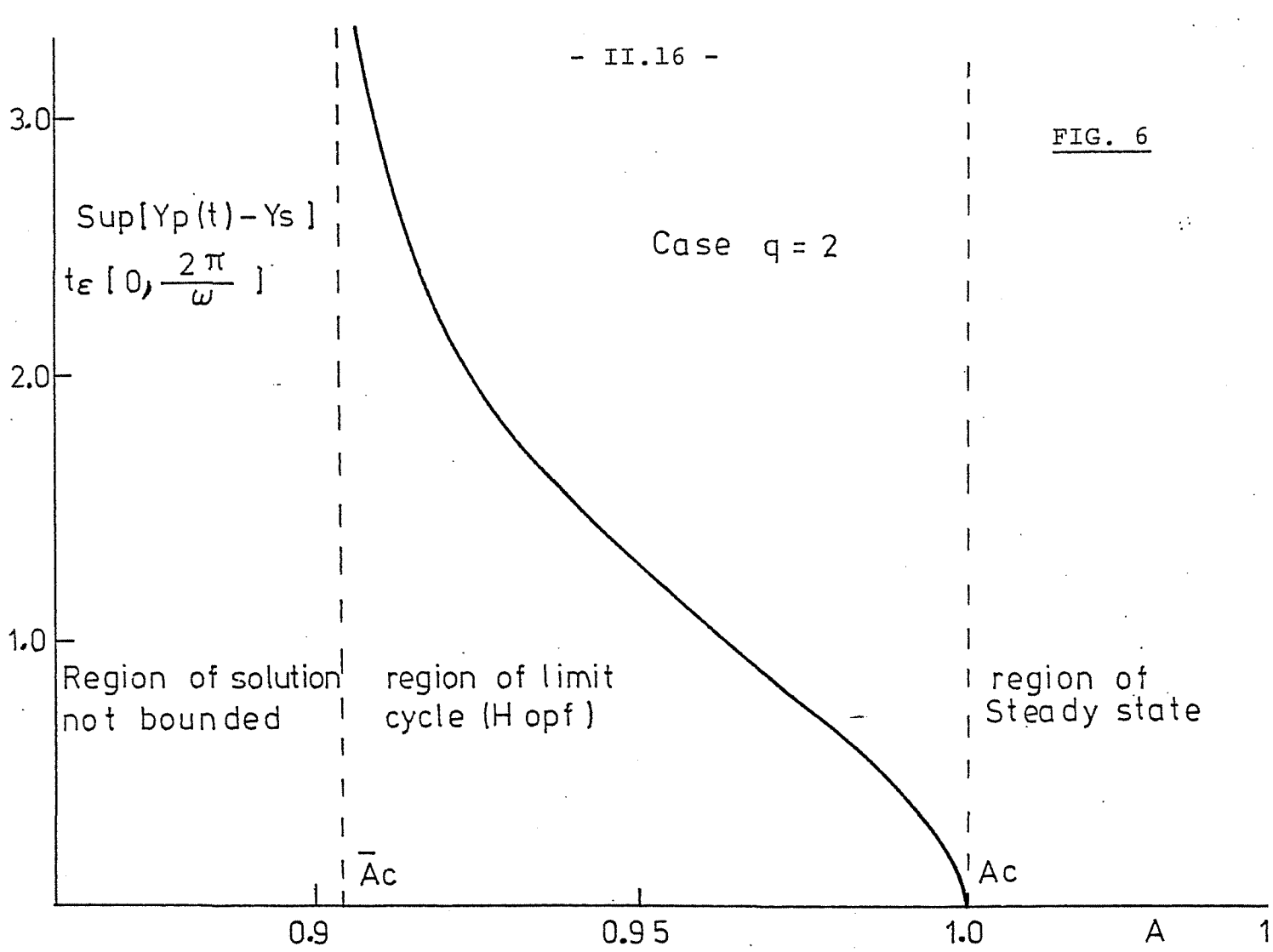
3.0
2.0
1.0
Sup[Yp(t) - Ys]
t ε [0, 2π/ω]
Case q = 2
Region of solution not bounded
region of limit cycle (H opf)
region of Steady state
Ac
Ac
0.9
0.95
1.0
A
1

FIG. 7

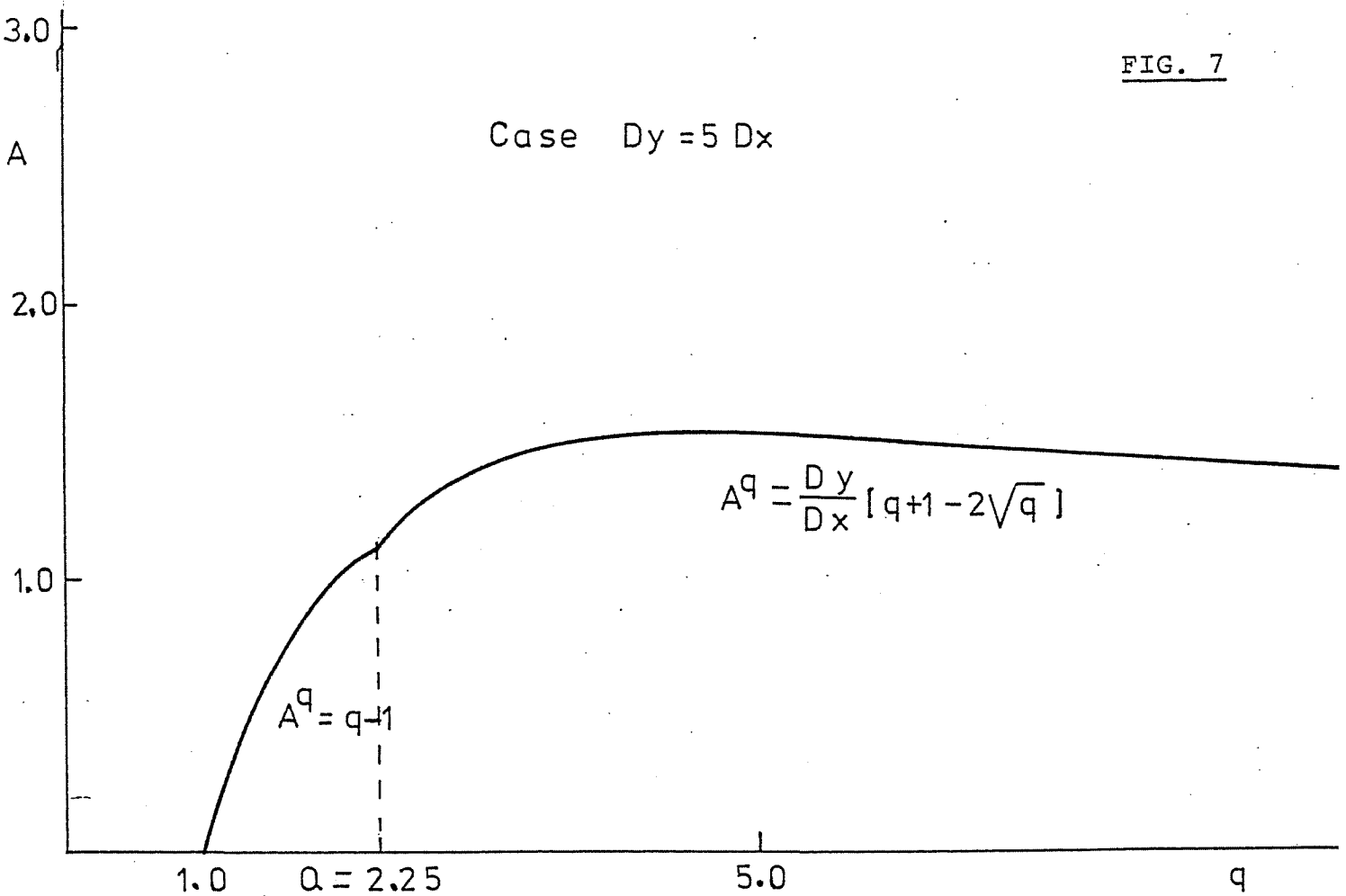
3.0
A
2.0
1.0
Case Dy = 5 Dx
$A^q = \frac{Dy}{Dx}[q+1-2\sqrt{q}]$
$A^q = q-1$
1.0
Q = 2.25
5.0
q

2. Nonlinear structures on a sphere

2.1. Fixed point and its stability

In Section II.1 we have considered the stability of non linear structures (steady states and limit cycle) in a simple autocatalytic reaction-diffusion scheme involving the Michaelis-Menten (first-order Hinshelwood-Langmuir) saturation law with restriction, however, to a one-dimensional problem. We shall consider here the same process as above (for motivation see Aris [1976]), but in the case of a spherical surface. In dimensionless differential form, the model is

$$\frac{\partial}{\partial t} X = XY - \frac{X}{1+qX} + D_X \Delta X \qquad (1.a)$$

$$\frac{\partial}{\partial t} Y = A - XY + D_Y \Delta Y \qquad (1.b)$$

in which X, Y and A denote dimensionless concentration of reactants that we take positive. D_X and D_Y are the respective dimensionless diffusion coefficients of X and Y, and $q > 0$ yields the relative strength of the saturation law in (1).

Let us consider the spherical surface, S, defined by (R, θ, ϕ) respectively radial at fixed R, polar, and azimuthal coordinates. In this geometry, the Laplacian operator takes the form

$$\Delta = \frac{1}{\sin\theta} \frac{\partial}{\partial\theta} \left(\sin\theta \frac{\partial}{\partial\theta}\right) + \frac{1}{\sin^2\theta} \frac{\partial^2}{\partial\varphi^2} \qquad (1.c)$$

In the dimensionless form of the problem we have taken R = 1.

The (fixed point) steady homogeneous solution of (1) is

$$X_s(\theta,\varphi) = A/(1-qA) \tag{2.a}$$

$$Y_s(\theta,\varphi) = 1-qA \tag{2.b}$$

For later convenience, we displace this solution to the origin of coordinates and the system (1) becomes in compact form

$$\frac{\partial}{\partial t}u = L(\gamma)u + N(\gamma,u) \tag{3.a}$$

in which u is the two-dimensional vector $u = \binom{X}{Y}$ and γ accounts for the four parameters involved in the problem $\gamma \equiv (A, q, D_X, D_Y)$. $L(\gamma)$ is the linear operator

$$L \equiv \begin{pmatrix} qA(1-qA)+D_X\Delta & A(1-qA)^{-1} \\ qA-1 & -A(1-qA)^{-1}+D_Y\Delta \end{pmatrix} \tag{3.b}$$

and $N(\gamma,u)$ describes the non linear contributions to (1),

$$N = \begin{pmatrix} XY + \sum_{n=2}^{\infty} (-)^n q^{n-1}(1-qA)^{n+1}X^n \\ -XY \end{pmatrix} \tag{3.c}$$

The stability of the fixed point in (3) is related to the eigenvalues, λ, of L

$$L(\gamma)\,\phi = \lambda\,\phi \tag{4}$$

The eigenfunctions of (4) can be expressed in terms of the eigenfunctions of the Laplacian. We have

$$\Delta Y_{\ell m}(\theta,\varphi) = -\ell(\ell+1)\,Y_{\ell m}(\theta,\varphi) \tag{5}$$

in which $Y_{\ell m}$ are spherical harmonics. Thus, the eigenfunctions ϕ are

$$\phi_{\ell m} = \begin{pmatrix} \phi^1_{\ell m} \\ \phi^2_{\ell m} \end{pmatrix} Y_{\ell m}(\theta,\varphi) \tag{6}$$

in which $\phi^i_{\ell m}$ (i = 1,2) are complex numbers.

The eigenvalue characteristic equation that describes the stability of the fixed point is

$$\lambda^2_{\ell m} - T(\gamma,\ell)\,\lambda_{\ell m} + D(\gamma,\ell) = 0 \tag{7.a}$$

with

$$T(\gamma,\ell) = qA(1-qA) - A(1-qA)^{-1} - \ell(\ell+1)(D_x + D_y) \tag{7.b}$$

$$D(\gamma,\ell) = A(1-qA) - \ell(\ell+1)\left[D_Y qA(1-qA) - D_X A(1-qA)^{-1}\right] + \ell^2(\ell+1)^2 D_X D_Y \qquad (7.c)$$

For a given triplet of $\{q, D_X, D_Y\}$ and variable A the fixed point may become unstable at some critical value, A_c, in one of the two following ways

(i) At a given A_c there is $\gamma_c = (A_c, q, D_X, D_Y)$ for which the eigenvalue $\lambda_{\ell m}$ cross the imaginary axis with non-vanishing imaginary part. This defines a ℓ_c and we must have

$$T(\gamma_c, \ell_c) = 0 \qquad (8.a)$$

$$D(\gamma_c, \ell_c) > 0 \qquad (8.b)$$

On the other hand, for all $\ell \neq \ell_c$ it must be

$$T(\gamma_c, \ell) < 0 \qquad (9.a)$$

$$D(\gamma_c, \ell) > 0 \qquad (9.b)$$

Thus, the only eigenvalues that bring instability to the fixed point correspond to the critical values ℓ_c, and all other eigenvalues have negative real parts. From (8.a) and (9.a) together with (7.b) we find $\ell_c = 0$. The only one spherical harmonic that brings instability belongs to $\ell = m = 0$.

(ii) The eigenvalues that bring instability are real and cross the imaginary axis from left to right. Then we must have

$$T(\gamma_c, \ell_c) < 0 \tag{10.a}$$

$$D(\gamma_c, \ell_c) = 0 \tag{10.b}$$

together with

$$T(\gamma_c, \ell) < 0 \tag{11.a}$$

$$D(\gamma_c, \ell) > 0 \tag{11.b}$$

for all $\ell \neq \ell_c$. The critical eigenvalue is associated with the minimum of D in (11.b) which is given by

$$\ell_c(\ell_c+1) = \frac{D_Y q A_c (1-qA_c) - D_X A_c (1-qA_c)^{-1}}{2 D_X D_Y} \tag{12.a}$$

$$D_X A_c (qA_c-1)^{-1} + D_Y q A_c (1-qA_c) = 2\left[D_X D_Y A_c (1-qA_c)\right]^{1/2} \tag{12.b}$$

According to (10.b) and (7.c) it must be $\ell_c \neq 0$. Thus, we have $(2\ell_c + 1)$ eigenfunctions branching at once at ℓ_c. Besides, from (11.a) and (12.a) we also obtain the necessary condition $D_Y > D_X$ for a non linear structure to bifurcate at A_c.

A few remarks are now pertinent:

(a) If $q < 1$ and $D_X > D_Y$ the fixed point (2) is asymptotically stable for all values of A: there is no $A_c > 0$ that satisfies (8) and (9) or (10) and (11) for $q < 1$.

(b) With $D_X > D_Y$, there exists $\gamma_c = (A_c, q, D_X, D_Y)$ such that for all $q > 1$, the fixed point (2) is asymptotically stable for all $A > A_c$. The fixed point becomes unstable for $A < A_c$ with the eigenvalues λ_{oo}. These eigenvalues have vanishing real parts at $A = A_c$. A_c is given by the relation $T(\gamma_c, 0) = 0$.

(c) With $D_Y > D_X$ there are two possible bifurcation pictures. Either the fixed point becomes unstable for values A_c satisfying $T(\gamma_c, 0) = 0$ with purely imaginary eigenvalues λ_{oo} or becomes unstable satisfying (12.b) with eigenvalues $\lambda_{\ell_c m}$, real and vanishing at A_c.

Figure 1 accounts for the case $D_Y = 5D_X$. Region I denotes values for which the fixed point is stable. At $A_c = \frac{1}{q} - \frac{1}{q\sqrt{q}}$ there is instability and bifurcation to periodic solutions, and at A_c as given by (12.b) to spatially inhomogeneous structures as we shall explain below.

It is to be noted that in case (a) there is only one eigenfunction $\phi_{oo}(\theta, \varphi)$ at bifurcation; in case (b) the null-eigenvalue of (4) has $(2\ell_c + 1)$ degeneracy (with $\ell_c \neq 0$) and this is not a minor difference with respect to the one-dimensional case discussed above.

FIG. 1

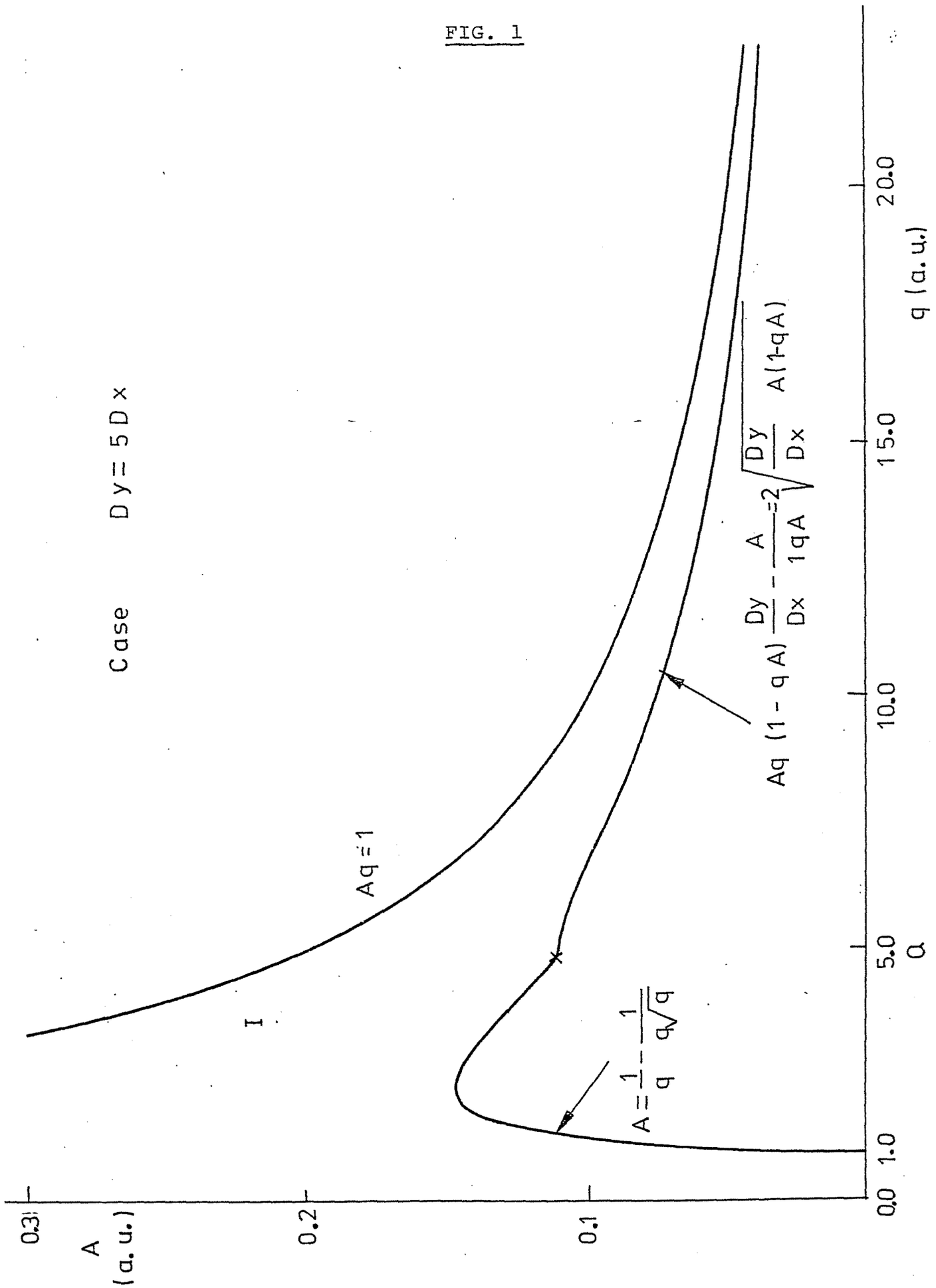
Case Dy = 5 Dx
I
Aq = 1
$Aq\,(1 - qA)\frac{Dy}{Dx} - \frac{A}{1qA} = 2\sqrt{\frac{Dy}{Dx}\,A(1-qA)}$
$A = \frac{1}{q} - \frac{1}{q\sqrt{q}}$
A (a. u.)
0.3
0.2
0.1
0.0
1.0
5.0
10.0
15.0
20.0
Q
q (a. u.)

2.2. Non linear steady (inhomogeneous) structure and its stability

In the following we shall restrict consideration to values of $D_Y > D_X$, $q > 0$ and $A < A_c$, with A_c given by (12.b), such that (i) $L(\gamma)$ possesses eigenfunctions belonging to the vanishing eigenvalue at A_c,

$$L(\gamma_c)\,\phi_{\ell_c m} = 0 \quad ; m = -\ell_c, -\ell_c+1, \ldots, \ell_c-1, \ell_c \tag{1}$$

Here ℓ_c is given by (12.a) and the corresponding eigenfunction is

$$\Phi_{\ell_c m} = \begin{pmatrix} 1 \\ C \end{pmatrix} Y_{\ell_c m}(\theta,\varphi) \tag{2.a}$$

with

$$C = -A_c^{-1}\,(1-qA_c)\left[qA_c(1-qA_c) - D_X\,\ell_c(\ell_c+1)\right] \tag{2.b}$$

We shall seek solutions in the space of complex-valued functions with continuous second derivatives on the spherical surface S^2. The following scalar product of functions u and $\tilde{u}$ belonging to the space is introduced

$$\langle u, \tilde{u} \rangle = \int_{\Omega} \left(X^* \tilde{X} + Y^* \tilde{Y}\right) d\Omega \tag{3}$$

in which $d\Omega$ accounts for the angular integration.

The adjoint operator L^+ of L is

$$L^+(\gamma) = \begin{pmatrix} qA(1-qA) + D_x \Delta & qA - 1 \\ A(1-qA)^{-1} & -A(1-qA)^{-1} + D_y \Delta \end{pmatrix} \quad (4)$$

The eigenfunctions belonging to the vanishing eigenvalue are

$$\phi^+_{\ell_c m} = \begin{pmatrix} 1 \\ D \end{pmatrix} Y_{\ell_c m}(\theta, \varphi) \quad (5.a)$$

with

$$D \equiv (1-qA_c)^{-1}\left[qA_c(1-qA_c) - D_x \ell_c(\ell_c+1)\right] \quad (5.b)$$

(ii) The following <u>transversality</u> condition is satisfied

$$\langle \phi^+_{\ell_c m}(\Omega), L'(\gamma_c)\phi_{\ell_c m}(\Omega) \rangle \neq 0 \quad (6)$$

in which $L'(\gamma)$ denotes the derivative of L with respect to A

$$L'(\gamma) = \begin{pmatrix} q(1-2qA) & (1-qA)^{-2} \\ q & -(1-qA)^{-2} \end{pmatrix} \quad (7)$$

With the above conventions and restrictions we shall use the Poincaré-Linstedt method and set

$$L(\gamma)\,u + N(\gamma, u) = 0 \tag{8.a}$$

$$A = A_c + \sum_{n=1}^{\infty} \epsilon^n A_n \tag{8.b}$$

$$u = \sum_{n=1}^{\infty} \epsilon^n u_n \tag{8.c}$$

in which ϵ is a new unknown that we shall fix by the solvability conditions (Fredholm alternative) to be imposed upon (8).

The stability of (8.c) is related to the eigenvalues of the linearized approximation to (8.a) in the neighborhood of (8.c). This linearized eigenvalue problem is

$$L(\gamma)\,\phi + M(\gamma, u)\,\phi = \lambda\,\phi \tag{9.a}$$

in which M, a linear operator, accounts for the derivative of N with respect to u.

In accordance to (8), we seek solutions to (9) in the form

$$\phi = \sum_{n=0}^{\infty} \epsilon^n \phi_n \tag{9.b}$$

$$\lambda = \sum_{n=1}^{\infty} \epsilon^n \lambda_n \tag{9.c}$$

We now introduce (8.b), (8.c) and (9.b), (9.c) respectively in (8.a) and (9.a), and we get

$$L(\gamma) = L(\gamma_c) + \epsilon A_1 L'(\gamma_c) + \\ + \epsilon^2 \left[A_2 L'(\gamma_c) + \frac{1}{2} A_1^2 L''(\gamma_c) \right] + O(\epsilon^3) \tag{10.a}$$

$$N(u,\gamma) = \epsilon^2 N_2(\gamma_c, u_1) + \epsilon^3 N_3(\gamma_c, u_1, u_2, A_1) + O(\epsilon^4) \tag{10.b}$$

$$M(u,\gamma) = \epsilon M_1(\gamma_c, u_1) + \epsilon^2 M_2(\gamma_c, u_1, u_2, A_1) + O(\epsilon^3) \tag{10.c}$$

We shall equate terms of same power in ϵ both in (8) and (9).

(i) <u>First-order approximation</u>

The terms in ϵ^0 and ϵ yield

$$L(\gamma_c) u_1 = 0 \tag{11.a}$$

$$L(\gamma_c) \phi_0 = 0 \tag{11.b}$$

Thus, the solutions belong to the kernel of $L(\gamma_c)$. From (1) we have

$$u_1 = \sum_{m=-\ell_c}^{\ell_c} a_m \left(\frac{1}{C}\right) Y_{\ell_c m}(\theta,\varphi) \qquad (12.a)$$

$$\phi_o = \sum_{m=-\ell_c}^{\ell_c} b_m \left(\frac{1}{C}\right) Y_{\ell_c m}(\theta,\varphi) \qquad (12.b)$$

in which a_m, b_m are complex numbers. As u_1 must be real, and $Y_{\ell m}(\theta,\phi) = (-)^m Y^*_{\ell,-m}(\theta,\phi)$ in which the star denotes the complex conjugate, we have $a_m = (-)^m a^*_m$ with $m = 1, \ldots, \ell_c$, and a_o real.

(ii) Second-order approximation

Equating second-order powers in (8) and (9) we get

$$L(\gamma_c)u_2 = -A_1 L'(\gamma_c)u_1 - N_2(\gamma_c,u_1) \qquad (13.a)$$

$$L(\gamma_c)\phi_1 = -A_1 L'(\gamma_c)\phi_o - M_1(\gamma_c,u_1)\phi_o + \lambda_1\phi_o \qquad (13.b)$$

with

$$N_2(\gamma_c,u_1) = \begin{pmatrix} X_1Y_1 + (1-qA_c)^3 q X_1^2 \\ -X_1Y_1 \end{pmatrix} \qquad (13.c)$$

$$M_1(\gamma_c,u_1) = \begin{pmatrix} Y_1 + 2q(1-qA_c)^3 X_1 & X_1 \\ -Y_1 & -X_1 \end{pmatrix} \qquad (13.d)$$

and $u_1 = (X_1, Y_1)$.

Secular terms in (13) are eliminated with the use of Fredholm's alternative, namely the following orthogonality condition is imposed,

$$A_1 \langle \phi^+_{\ell m}, L'(\gamma_c) u_1 \rangle + \langle \phi^+_{\ell m}, N_2(\gamma_c, u_1) \rangle = 0 \tag{14}$$

with $m = -\ell_c, \ldots, \ell_c$. We now use the relation

$$Y_{\ell m}(\theta,\varphi)\, Y_{\ell' m'}(\theta,\varphi) = \sum_{L=|\ell-\ell'|}^{\ell+\ell'} \sum_{M=-L}^{L} (-)^M \times$$

$$\times \left[\frac{(2\ell+1)(2\ell'+1)(2L+1)}{4\pi}\right]^{1/2} \begin{pmatrix} \ell & \ell' & L \\ 0 & 0 & 0 \end{pmatrix} \begin{pmatrix} \ell & \ell' & L \\ m & m' & M \end{pmatrix} Y_{L,-M}(\theta,\varphi) \tag{15}$$

in which the Wigner "3j" coefficients have been introduced (4). Thus, (14) yields

$$A_1 G a_{m''} + F \sum_{m=-\ell_c}^{\ell_c} \sum_{m'=-\ell_c}^{\ell_c} a_m a_{m'} (-)^{m''} \times$$

$$\times \left[\frac{(2\ell_c+1)^3}{4\pi}\right]^{1/2} \begin{pmatrix} \ell_c & \ell_c & \ell_c \\ 0 & 0 & 0 \end{pmatrix} \begin{pmatrix} \ell_c & \ell_c & \ell_c \\ m & m' & -m'' \end{pmatrix} = 0 \tag{16.a}$$

with m" = 0, 1, ..., ℓ_c, and

$$G = \langle \phi^{+}_{\ell_c m} , L'(\gamma_c)\phi_{\ell_c m} \rangle \neq 0 \qquad (16.b)$$

$$F = C + (1 - q A_c) q^3 - DC \qquad (16.c)$$

System (16) together with condition $a_m = (-)^m a_m^*$ (m = 1,...,ℓ_c) yields $(2\ell_c + 1)$ equations with $(2\ell_c + 2)$ unknowns: (a_{ℓ_c}, $a_{-\ell_c+1}$, ..., a_{ℓ_c}, A_1). On the other hand, Fredholm's alternative yields $(2\ell_c + 1)$ equations with $(2\ell_c + 2)$ unknowns: ($b_{-\ell_c}$, ...,b_{ℓ_c}, λ_1),

$$-A_1 G\, b_{m''} - 2F \sum_{m=-\ell_c}^{\ell_c} \sum_{m'=-\ell_c}^{\ell_c} (-)^{m''} a_m b_{m'} \left[\frac{(2\ell_c+1)^3}{4\pi}\right]^{1/2} \times$$

$$\times \begin{pmatrix} \ell_c & \ell_c & \ell_c \\ 0 & 0 & 0 \end{pmatrix} \begin{pmatrix} \ell_c & \ell_c & \ell_c \\ m & m' & -m'' \end{pmatrix} + \lambda_1 (1 + CD)\, b_{m''} = 0 \qquad (17)$$

with m" = $-\ell_c$, ..., ℓ_c.

It is to be noted that when the null-eigenvalue of $L(\gamma_c)$ is not simple the equations relating a_m, b_m, A_1 and λ_1 are not linear, and at A_c bifurcation of several branches is possible (see below for further details).

We have now the following alternative: Either (i) ℓ_c is <u>even</u> with $\begin{pmatrix} \ell_c & \ell_c & \ell_c \\ 0 & 0 & 0 \end{pmatrix} \neq 0$ and the equations (16) and (17) have a non trivial solution, or

(ii) ℓ_c is <u>odd</u>, with $\begin{pmatrix} \ell_c & \ell_c & \ell_c \\ 0 & 0 & 0 \end{pmatrix} = 0$ and the solution of (16), (17) yields $A_1 = \lambda_1 = 0$. In this latter case, we ought to go to higher orders once the equations (13) are solved. They reduce here to

$$L(\gamma_c) u_2 = - N_2(\gamma_c, u_1) \tag{18.a}$$

$$L(\gamma_c) \phi_1 = - M_2(\gamma_c, u_1)\, \phi_0 \tag{18.b}$$

With the use of (15) we get

$$u_2 = \sum_{L=0}^{2\ell} \sum_{M=-L}^{L} \sum_{m=-\ell_c}^{\ell_c} \sum_{m'=-\ell_c}^{\ell_c} \begin{pmatrix} V_1(L) \\ V_2(L) \end{pmatrix} (-)^M \times$$

$$\times a_m a_{m'} \left[\frac{(2\ell_c+1)^2 (2L+1)}{4\pi} \right]^{1/2} \begin{pmatrix} \ell_c & \ell_c & L \\ 0 & 0 & 0 \end{pmatrix} \times \tag{19.a}$$

$$\times \begin{pmatrix} \ell_c & \ell_c & L \\ m & m' & -M \end{pmatrix} Y_{LM}(\theta, \varphi)$$

with L even, and

$$\phi_1 = 2 \sum_{L=0}^{2\ell} \sum_{M=-L}^{L} \sum_{m=-\ell_c}^{\ell_c} \sum_{m'=-\ell_c}^{\ell_c} \begin{pmatrix} V_1(L) \\ V_2(L) \end{pmatrix} a_m b_{m'} (-)^M \times$$

$$\times \left[\frac{(2\ell_c+1)^2 (2L+1)}{4\pi} \right]^{1/2} \begin{pmatrix} \ell_c & \ell_c & L \\ 0 & 0 & 0 \end{pmatrix} \begin{pmatrix} \ell_c & \ell_c & L \\ m & m' & -M \end{pmatrix} Y_{LM}(\theta, \varphi) \tag{19.b}$$

with L even, in which

$$V_1(L) = \frac{C D_Y L(L+1) + A_c q (1-qA_c)^2 + (1-qA_c)^3 q D_Y L(L+1)}{D_X D_Y \left[L(L+1) - \ell_c(\ell_c+1) \right]} \qquad (19.c)$$

$$V_2(L) = \frac{C q A_c (1-qA_c) - D_Y C L(L+1) -}{D_X D_Y \left[L(L+1) - \ell_c(\ell_c+1) \right]}$$

$$\underline{- C(1-qA_c) - (1-qA_c)^4 q} \qquad (19.d)$$

(iii) Third-order approximation

As for ℓ_c odd, we have $A_1 = \lambda_1 = 0$ the equations to this order are

$$L(\gamma_c) u_3 = - A_2 L'(\gamma_c) u_1 - N_3(\gamma_c, u_1, u_2) \qquad (20.a)$$

$$L(\gamma_c)\phi_2 = -A_2 L'(\gamma_c)\phi_0 - M_2(\gamma_c, u_1, u_2)\phi_0 - \\ - M_1(\gamma_c, u_1)\phi_1 + \lambda_2 \phi_0 \qquad (20.b)$$

with

$$N_3(\gamma_c, u_1, u_2) = \begin{pmatrix} X_1 Y_2 + X_2 Y_1 + 2q(1-qA_c)X_1X_2 - (1-qA_c)^4 q^2 X_1^3 \\ -X_1 Y_2 - X_2 Y_1 \end{pmatrix} \quad (20.c)$$

and

$$M_2(\gamma_c, u_1, u_2) = \begin{pmatrix} Y_2 + 2q(1-qA_c)^3 X_2 - 3q^2(1-qA_c)^4 X_1^2 & X_2 \\ -Y_2 & -X_2 \end{pmatrix} \quad (20.d)$$

Using Fredholm's alternative in (20.a), we get $(2\ell_c + 1)$ equations with $(2\ell_c + 2)$ unknowns: $(a_{-\ell_c}, \ldots, a_{\ell_c}, A_2)$,

$$A_2 G a_{m''} + \sum_{L=0}^{2\ell} \sum_{M=-L}^{L} \sum_{m=-\ell_c}^{\ell_c} \sum_{m'=-\ell_c}^{\ell_c} \sum_{m''=-\ell_c}^{\ell_c} a_m a_{m'} a_{m''} \times$$

$$\times \frac{(2\ell_c+1)^2(2L+1)}{4\pi} \left[(-)^m W(L) - (1-qA_c)^4 q^2 \right] \times \quad (21.a)$$

$$\times \begin{pmatrix} \ell_c & \ell_c & L \\ 0 & 0 & 0 \end{pmatrix}^2 \begin{pmatrix} \ell_c & \ell_c & L \\ m''' & -m & -M \end{pmatrix} \begin{pmatrix} \ell_c & \ell_c & L \\ m' & m'' & -M \end{pmatrix} = 0$$

with L <u>even</u>, and $m''' = 0, 1, \ldots, \ell_c$, $a_m = (-)^m a^*_{-m}$, $m = 1, \ldots, \ell_c$, and

$$W(L) = \left[V_2(L) + c V_1(L) \right](1-D) + 2q(1-qA_c)^3 V_1(L) \quad (21.b)$$

Using again Fredholm's alternative in (20.b) we get $(2\ell_c + 1)$ equation, with $(2\ell_c + 2)$ unknowns: $(b_{-\ell_c}, \ldots, b_{\ell_c}, \lambda_2)$,

$$A_2 G b_{m'''} + \sum_{L=0}^{2\ell_c} \sum_{M=-L}^{L} \sum_{m=-\ell_c}^{\ell_c} \sum_{m'=-\ell_c}^{\ell_c} \sum_{m''=-\ell_c}^{\ell_c} \times$$

$$\frac{(2\ell_c+1)^2(2L+1)}{4\pi} \times \begin{pmatrix} \ell_c & \ell_c & L \\ 0 & 0 & 0 \end{pmatrix}^2 \begin{pmatrix} \ell_c & \ell_c & L \\ m''' & -m & -M \end{pmatrix} \begin{pmatrix} \ell_c & \ell_c & L \\ m' & m'' & -M \end{pmatrix} \times \quad (22)$$

$$\times \left[2a_m a_{m'} b_{m''} (-)^m W(L) + b_m a_{m'} a_{m''} (-)^m W(L) - 3q^2(1-qA_c)^4 a_m a_{m'} b_{m''} \right] -$$

with L even, and $m''' = -\ell_c, \ldots, \ell_c$. $\qquad - \lambda_2 (1+CD) b_{m'''} = 0$

2.3. Further discussion of a particular case

We shall illustrate here the salient differences between the spherical problem treated above and the one-dimensional case. For the sake of simplicity, we take $\ell_c = 1$. As ℓ_c is odd, we have $A_1 = \lambda_1 = 0$, and thus, to obtain A_2 and λ_2 we make use of (21) and (22). To get A_2 from (21), we have

$$A_2 G a_0 + a_0^3 \left(M - \frac{qN}{20\pi} \right) - 2 a_0 a_1 a_{-1} \left(M + \frac{3N}{20\pi} \right) = 0 \quad (1.a)$$

$$A_2 G a_1 + a_1 a_0^2 \left(M - \frac{3N}{20\pi} \right) - 2 a_1^2 a_{-1} \left(M + \frac{qN}{20\pi} \right) = 0 \quad (1.b)$$

with $a_{-1} = -a_1^*$, and

$$M = \frac{1}{4\pi} W(L=0) + \frac{1}{5\pi} W(L=2) \tag{1.c}$$

$$N = (1 - q A_c)^4 q^2 \tag{1.d}$$

in which W(L) and G have already been defined.

There are two solutions to (1).

$$\text{(i)}\quad a_0 \neq 0,\ \mathrm{Re}\, a_1 = \mathrm{Im}\, a_1 = 0\ ,\ A_2 = a_0^2 A_2' \tag{2.a}$$

with corresponding branches

$$u(\theta,\varphi) = \pm\left[\frac{3(A-A_c)}{4\pi A_2'}\right]^{1/2}\begin{pmatrix}1\\ c\end{pmatrix}\cos\theta + \tag{2.b}$$

$$+\left(\frac{A-A_c}{A_2'}\right)\frac{1}{4\pi}\left[\begin{pmatrix}V_1(0)\\ V_2(0)\end{pmatrix}+\begin{pmatrix}V_1(2)\\ V_2(2)\end{pmatrix}\left(3\cos^2\theta - 1\right)\right] + O(A-A_c)^{3/2}$$

and

$$\text{(ii)}\quad a_0 = 0\ ;\ a_1 = m e^{i\delta}\ ,\ A_2 = m^2 A_2' \tag{3.a}$$

with corresponding branches

$$u(\theta,\varphi) = \pm\left[\frac{3(A-A_c)}{2\pi A_2'}\right]^{1/2}\begin{pmatrix}1\\C\end{pmatrix}\sin\theta\cos(\varphi+\delta)+$$

$$+\left(\frac{A-A_c}{A_2'}\right)\left[\frac{1}{2\pi}\begin{pmatrix}V_1(0)\\V_2(0)\end{pmatrix}+\begin{pmatrix}V_1(2)\\V_2(2)\end{pmatrix}\frac{3}{4\pi}\sin^2\theta\cos 2(\varphi+\delta)-\right. \tag{3.b}$$

$$\left.-\frac{1}{4\pi}\begin{pmatrix}V_1(2)\\V_2(2)\end{pmatrix}(3\cos^2\theta-1)\right]+O(A-A_c)^{\frac{3}{2}}$$

It is to be noted that solution (2) has no ø-dependence. On the other hand, solution (3) depends on a parameter δ to be determined from initial conditions: thus, (3) defines a one-parameter family of solutions.

Stability of the bifurcated branches is related to λ_2, and this quantity is given by the following equations

$$A_2 G b_0 + 3a_0^2 b_0\left(M-\frac{9N}{20\pi}\right)-2a_1a_{-1}b_0\left(M+\frac{9N}{20\pi}\right)- \tag{4.a}$$
$$-2b_1a_0a_{-1}M-2b_{-1}a_0a_1M+b_0\lambda_2(1+CD)=0$$

$$A_2Gb_1-4a_1a_{-1}b_1\left(M+\frac{9N}{20\pi}\right)+b_1a_0^2\left(M-\frac{9N}{20\pi}\right)- \tag{4.b}$$
$$-2b_{-1}a_1a_{-1}\left(M+\frac{9N}{20\pi}\right)+2a_0a_1b_0M+\lambda_2b_1(1+CD)=0$$

$$A_2Gb_{-1}-4b_{-1}a_{-1}a_1\left(M+\frac{9N}{20\pi}\right)+2a_{-1}a_0b_0M+ \tag{4.c}$$

$$+b_{-1}a_0^2\left(M-\frac{9N}{20\pi}\right)-2a_{-1}^2b_1\left(M+\frac{9N}{20\pi}\right)+$$

$$+\lambda_2b_{-1}(1+CD)=0 \tag{4.d}$$

in which M, N, and G are as above.

With solution (2), we have the following alternative: Either

$$\text{(i)}\quad \lambda_2^{(1)} = 0\,,\ b_0 = 0\,,\ b_1 \neq 0\,,\ b_{-1} \neq 0 \tag{5.a}$$

or

$$\text{(ii)}\quad \lambda_2^{(2)} = 2a_0^2\left(M - \frac{qN}{20\pi}\right)\Big/(1+CD)\,,\ b_0 \neq 0, \tag{5.b}$$

$$b_1 = b_{-1} = 0$$

Thus, if $\lambda_2^{(2)} > 0$, there appears a positive eigenvalue of $L(\gamma) + M(\gamma,u)$ in the ε^2-approximation, and the branch (2) is unstable. If, however, $\lambda_2^{(2)} < 0$, we cannot establish stability as $\lambda_2^{(1)}$ yields a vanishing eigenvalue to $L(\gamma) + M(\gamma,u)$ in the ε^2-approximation. Thus, higher order terms are needed to assess the stability properly.

We note that $\operatorname{sgn} \lambda_2^{(2)} = \operatorname{sgn}(A_2)$, and the following relations hold

$$1 + CD = (D_Y - D_X)/D_Y \ > 0 \tag{6.a}$$

$$G = \langle \phi^+_{\ell_c m}, L'(\gamma_c)\phi_{\ell_c m} \rangle \ < 0 \tag{6.b}$$

Thus, solution (2) is unstable when it appears subcritical ($A > A_c$), whereas if supercritical ($A < A_c$) its stability is decided in at least the ε^3-approximation, and so on. We shall not carry further, however, our analysis here.

With solution (3) the alternative is: Either

$$\text{(i)}\quad \lambda_2^{(2)} = 0\,,\quad b_0 \neq 0,\quad b_1 = b_{-1}\, e^{2i\alpha} \tag{7.a}$$

or

$$\text{(ii)}\quad \lambda_2^{(2)} = 4m^2 \frac{\left(M + \frac{9N}{20\pi}\right)}{(1+CD)}\,,\quad b_0 = 0,\ b_1 = -b_{-1}\, e^{2i\alpha} \tag{7.b}$$

Again we find a situation encountered in the previous case. When solution (3) shows subcritical it is unstable but if it appears supercritical its stability analysis demands higher order approximations, and so on. Figure 2 displays the various bifurcations that are possible: three different cases appear in accordance to the range of values of $\lambda_2^{(2)}$ in either solution (2) or (3).

2.4. Bifurcation to a limit cycle

When q, D_X and D_Y are such that <u>either</u> $q > 1$ and $D_X > D_Y$ <u>or</u> $D_Y > D_X$ and q is such that bifurcation of the steady solution (1.2) occurs for purely imaginary eigenvalues of (1.4), then there exists a critical value, A_c,

$$A_c = \frac{1}{q} - \frac{1}{q\sqrt{q}} \tag{1}$$

FIG. 2

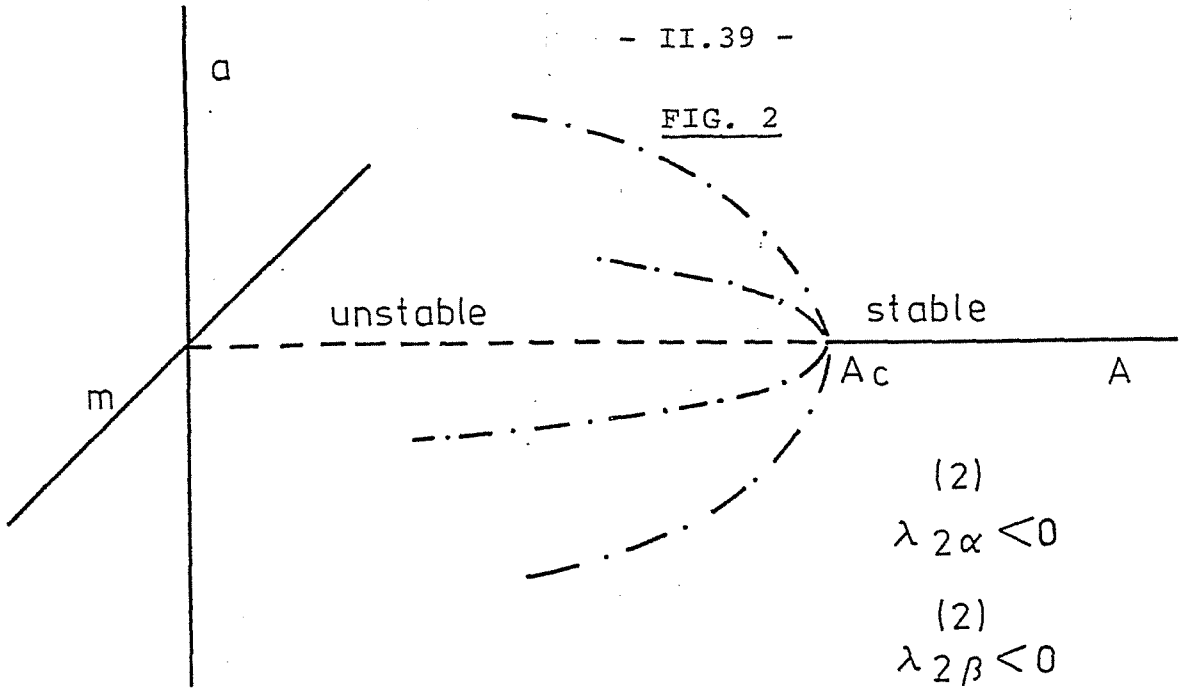
a
unstable
stable
m
Ac
A
(2)
$\lambda_{2\alpha} < 0$
(2)
$\lambda_{2\beta} < 0$

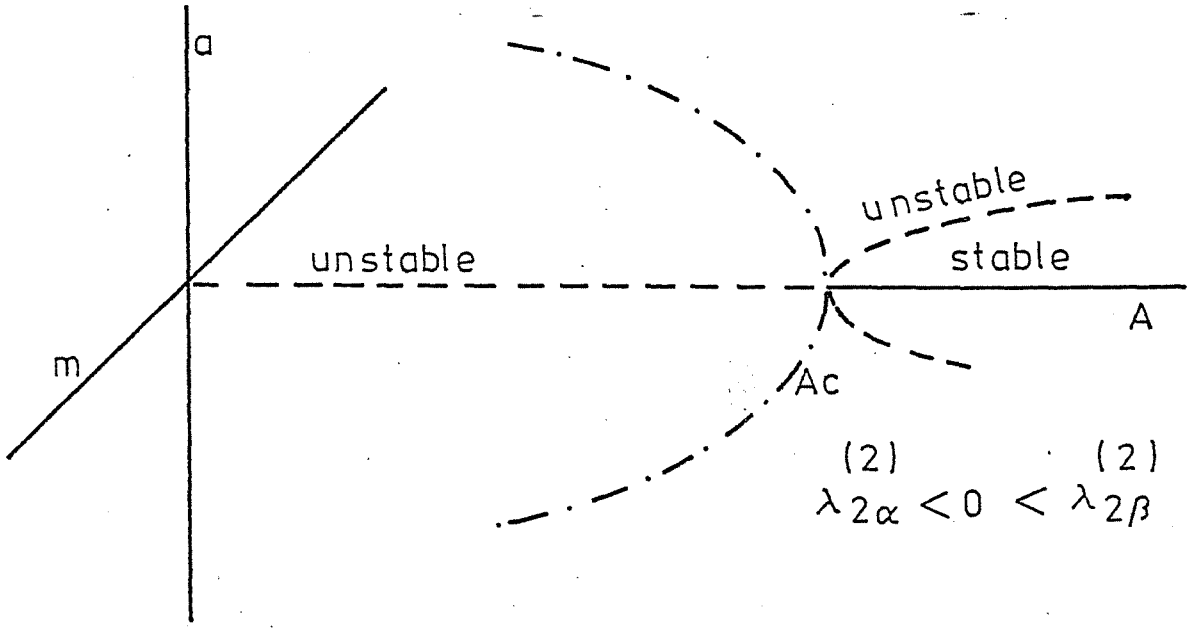
a
unstable
unstable
stable
m
A
Ac
(2)
$\lambda_{2\alpha} < 0$
(2)
$< \lambda_{2\beta}$

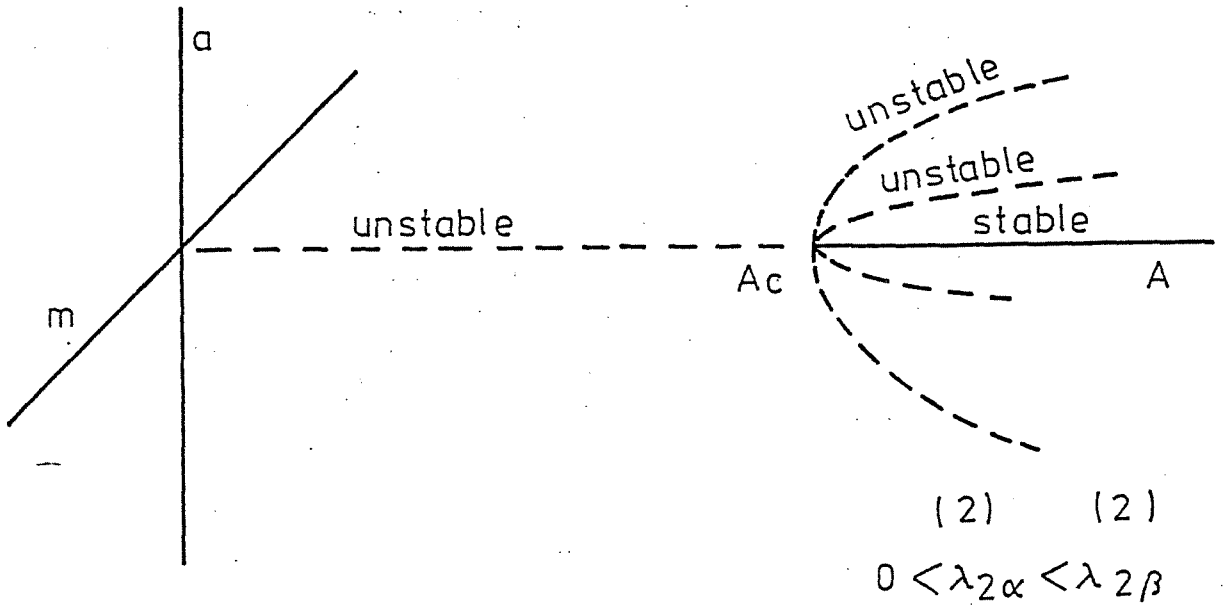
a
unstable
unstable
unstable
stable
m
Ac
A
(2)
$0 < \lambda_{2\alpha}$
(2)
$< \lambda_{2\beta}$

such that the fixed point is asymptotically stable in the range $\frac{1}{q} > A > A_c$ and unstable at $A = A_c$ with a branch emanating for $\ell_c = 0$. Thus, $L(\gamma_c)$ has purely imaginary eigenvalues $\pm i\omega_o$

$$L(\gamma_c)\,\varphi_o = +i\omega_o\,\varphi_o \tag{2.a}$$

$$L(\gamma_c)\,\varphi_o^* = -i\omega_o\,\varphi_o^* \tag{2.b}$$

with

$$\omega_o = \frac{(\sqrt{q}-1)^{1/2}}{q} \tag{2.c}$$

$$\varphi_o = \begin{pmatrix} 1 \\ -\left[\sqrt{q}/\sqrt{q}-1\right]^{1/2} e^{-i\alpha} \end{pmatrix} \tag{2.d}$$

and

$$\sin\alpha = q^{-1/4}\,, \quad \frac{\pi}{2} \geq \alpha \geq 0\,. \tag{2.e}$$

Then the following two conditions of Hopf bifurcation theorem are satisfied :

(i) in the neighborhood of A_c the eigenvalues of $L(\gamma_c)$ are of the form

$$\lambda_1(A) \pm i\lambda_2(A) \tag{3.a}$$

With both λ_1, λ_2 real, $\lambda_1(A_c) = 0$ and $\lambda_2(A_c) \neq 0$,
(ii) the transversality condition

$$\left.\frac{\partial \lambda_1(A)}{\partial A}\right|_{A=A_c} \neq 0 \qquad (3.b)$$

which leads to bifurcation to a limit cycle at A_c. We shall construct this periodic solution in the neighborhood of A_c by the Poincaré-Linstedt method.

We shall look for 2π-periodic functions with first time differential continuous and with continuous spatial second-differentials on the spherical surface S :

$$\left\{ u(\theta,\varphi,0) = u(\theta,\varphi,2\pi)\ ;\ u(\theta,\varphi,t) = \left[X(\theta,\varphi,t), Y(\theta,\varphi,t)\right];\right.$$
$$\left. X, Y \in C^1[0,2\pi]\ ;\ X, Y \in C^2(S) \right\}$$

In the above defined space of functions, we consider the following inner product

$$\langle \tilde{u}, u \rangle = \int_0^{2\pi} d\tau \int_S d\Omega \left[\tilde{X}(\theta,\varphi,\tau) X^*(\theta,\varphi,\tau) + \tilde{Y}(\theta,\varphi,\tau) Y^*(\theta,\varphi,\tau) \right] \qquad (4)$$

for a pair of functions u and $\tilde{u}$ belonging to the space; the star on quantities denotes complex conjugation.

For later convenience, we change the time variable to

$$\tau = \omega t \qquad (5)$$

Thus, $u = u(\tau)$ obeys the following equation

$$\omega \frac{\partial}{\partial \tau} u = L(\gamma) u + N(\gamma, u) \tag{6}$$

We define

$$J(\gamma_c) = \omega_0 \frac{\partial}{\partial \tau} - L(\gamma_c) \tag{7.a}$$

with its adjoint

$$J^+(\gamma_c) = -\omega_0 \frac{\partial}{\partial \tau} - L^+(\gamma_c) \tag{7.b}$$

with $L^+(\gamma)$ given in (2.4). Thus it follows

$$J(\gamma_c)\,\psi_0 = 0 \quad , \quad J(\gamma_c)\,\psi_0^* = 0 \tag{8.a}$$

$$J^+(\gamma_c)\,\psi_0^+ = 0 \quad , \quad J^+(\gamma_c)\,\psi_0^{+*} = 0 \tag{8.b}$$

with

$$\psi_0 = \begin{pmatrix} e^{i\tau} \\ -\left[\sqrt{q}/\sqrt{q}-1\right]^{1/2} e^{i(\tau-\alpha)} \end{pmatrix} \tag{8.c}$$

$$\psi_0^+ = \frac{i}{2\pi \sin\alpha} \begin{pmatrix} e^{i(\tau-\alpha)} \\ \left[\frac{\sqrt{q}-1}{\sqrt{q}}\right]^{1/2} e^{i\tau} \end{pmatrix} \tag{8.d}$$

For simplicity we have chosen constants such that

$$\langle \psi_0^+ , \mathrm{Re}\, \psi_0 \rangle = 1 \qquad (8.e)$$

Note that the transversality condition (3.b) reduces to

$$\mathrm{Re} \langle \psi_0^+ , L'(\gamma_c)\, \psi_0 \rangle \neq 0 \qquad (9)$$

in which $L'(\gamma_c)$ accounts for the linear differential operator of L with respect to A (2.7).

We now set

$$A = A_c + \sum_{n=1}^{\infty} \epsilon^n A_n \qquad (10.a)$$

$$u = \sum_{n=1}^{\infty} \epsilon^n u_n \qquad (10.b)$$

$$\omega = \omega_0 + \sum_{n=1}^{\infty} \epsilon^n \omega_n \qquad (10.c)$$

together with corresponding ε-expansions for L and N (2.10). Inserting (10) and (2.10) in (6) and equating same powers in ε we get an hierarchy of equations that we solve up to the first few orders.

(i) First-order approximation

Equating first powers in ε from (6) we get

$$J(\gamma_c) u_1 = 0 \qquad (11)$$

U_1 is a linear combination of ψ_o and ψ_o^*, and on physical grounds it is taken real only. Thus we have

$$u_1 = \mathrm{Re}\,\psi_o = \begin{pmatrix} \cos\tau \\ -\left[\frac{\sqrt{q}}{\sqrt{q}-1}\right]^{1/2}\cos(\tau-\alpha) \end{pmatrix} \tag{12}$$

Note that considering $\mathrm{Im}\psi_o$ merely amounts to a displacement of the time origin and as the system (6) is autonomous it is irrelevant.

(ii) Second-order approximation

Equating now second-order powers in ε from (6) we get

$$J(\gamma_c)u_2 = -\omega_1 \frac{\partial}{\partial\tau}u_1 + A_1 L'(\gamma_c)u_1 + N_2(\gamma_c, u_1) \tag{13}$$

To (13) and (11) we apply Fredholm's alternative. This yields A_1 and ω_1

$$A_1 = -\frac{\mathrm{Re}\langle \psi_o^+, N_2(\gamma_c, u_1)\rangle}{\mathrm{Re}\langle \psi_o^+, L'(\gamma_c)u_1\rangle} \tag{14.a}$$

$$\omega_1 = -\mathrm{Im}\langle \psi_o^+, N_2(\gamma_c, u_1)\rangle - A_1\,\mathrm{Im}\langle \psi_o^+, L'(\gamma_c)u_1\rangle \tag{14.b}$$

Note that the transversality condition (9) demands that A_1 and ω_1 be finite. It follows

$$A_1 = \omega_1 = 0 \tag{14.c}$$

Thus, u_2 is given by the equation

$$J(\gamma_c)u_2 = N_2(\gamma_c, u_1) \tag{15.a}$$

We now seek solutions to (15.a) in the following form

$$u_2 = \begin{pmatrix} m_1 \cos(2\tau + \Omega_1) + n_1 \\ m_2 \cos(2\tau + \Omega_2) + n_2 \end{pmatrix} \tag{15.b}$$

in which m_1, m_2, n_1, n_2, Ω_1, Ω_2 are all real constants.

Substitution of (15.b) in (15.a) yields

$$m_1 = \frac{1}{3(\sqrt{q}-1)}\left[q^2\sqrt{q} - \frac{11}{4}q^2 + \frac{7}{2}q\sqrt{q} - \frac{3}{4}q\right]^{1/2} \tag{16.a}$$

$$\cos\Omega_1 = \frac{1}{6m_1}\frac{q+\sqrt{q}}{\sqrt{q}-1} \quad , \quad 0 \leq \Omega_1 \leq \pi/2 \tag{16.b}$$

$$m_2 = \frac{q}{3(\sqrt{q}-1)}\left[1 + \frac{4q+9-12\sqrt{q}}{4(\sqrt{q}-1)}\right]^{1/2} \tag{16.c}$$

$$\sin\Omega_2 = (3q - 2q\sqrt{q})/6m_2(\sqrt{q}-1)^{3/2},$$

$$\cos\Omega_2 = -q/3m_2(\sqrt{q}-1) \qquad (16.d)$$

$$n_1 = \sqrt{q}/2 \text{ , and } n_2 = 0.$$

(iii) Third-order approximation

Equating third-order powers from (6) we get

$$J(\gamma_c)u_3 = -\omega_2 \frac{\partial}{\partial\tau} u_1 + A_2 L'(\gamma_c)u_1 + \\ + N_3(\gamma_c, u_1, u_2, A_1) \qquad (17)$$

To (17) Fredholm's alternative together with the transversality condition (9) yield

$$A_2 = -\frac{(\sqrt{q}+1)}{8(\sqrt{q}-1)\sqrt{q}} \qquad (18.a)$$

$$\omega_2 = \frac{-1}{8(\sqrt{q}-1)^{1/2}}\left[\frac{5q - 8\sqrt{q}+3}{3} - \frac{(\sqrt{q}-2)(2q+3+3\sqrt{q})}{6(\sqrt{q}-1)}\right] \qquad (18.b)$$

and so on.

Inversion now of (10.a) gives

$$\epsilon = \pm\left(\frac{A-A_c}{A_2}\right)^{1/2} + O(A-A_c)^{3/2} \qquad (19)$$

that put into (10.b) and (10.c) respectively gives

$$u(\theta,\varphi,t) = \pm\left(\frac{A-A_c}{A_2}\right)^{1/2}\begin{pmatrix}\cos\omega t\\ -\left[\frac{\sqrt{q}}{\sqrt{q}-1}\right]^{1/2}\cos(\omega t-\alpha)\end{pmatrix} + \tag{20.a}$$

$$+\left(\frac{A-A_c}{A_2}\right)\begin{pmatrix}m_1\cos(2\omega t+\Omega_1)+n_1\\ m_2\cos(2\omega t+\Omega_2)\end{pmatrix} + O(A-A_c)^{3/2}$$

and

$$\omega = \omega_o + \left(\frac{A-A_c}{A_2}\right)\omega_2 + O(A-A_c)^{3/2} \tag{20.b}$$

in which all parameters (A_c, A_2, ω_o, ω_2, θ, Ω_1, Ω_2, m_1, m_2 and n) are the above given functions of q.

The stability of limit cycle (20) can be assessed by the knowledge of the Floquet exponents. That is, by the eigenvalues β of the following eigenvalue equation problem (6)

$$\omega\frac{\partial}{\partial\tau}\varphi - L(\gamma)\varphi - M(\gamma,u(\tau))\varphi = \beta\varphi \tag{21}$$

in which all operators are as defined above. It follows (6) that

(i) if solution (20) branches supercritical (for $A < A_c$) it is asymptotically orbitally stable, whereas

(ii) if solution (20) branches subcritical (for $A > A_c$) it is unstable.

From (1) we get that $q > 1$, and from (18.a) follows $A_2 < 0$. Thus, (20) branches supercritical and we have stability in at least a small enough neighborhood of A_c

It is remarkable that the diffusion constants D_X, D_Y do not explicitely show up either in (1) or in (20). However, their influence is implicitely accounted for as (i) their values restrict the range of values of q in the linear stability portrait of (1.1) for which bifurcation is possible (see Figure 1 and Reference 1); (ii) their presence in (1.1) yields the consequence that the solution (20) does not show any spatial dependence: the motion of points in the surface S has vanishing phase shifts. Without diffusion the motions will all be independent of each other.

REFERENCES

ARIS, R., 1976, The Mathematical Theory of Diffusion and Reaction in Permeable Catalysts, Vol. II (Clarendon Press, Oxford).

BALSLEV, I. and H. DEGN, 1975, J. Theoret. Biol. 49, 173.

HANUSSE, P., 1972, Compt. Rend. 274C, 1247.

IBAÑEZ, J. L., V. FAIRÉN and M. G. VELARDE, 1976a, Physics Letters 58A, no. 6, 364.

IBAÑEZ, J. L., V. FAIRÉN and M. G. VELARDE, 1976b, Physics Letters 59A, no. 5, 335.

SEGEL, L. A. and J. L. JACKSON, 1972, J. Theoret. Biol. 37, 545.

TYSON, J., 1973, J. Chem. Phys. 59, 4164.

1. The Lorenz model and turbulence

In this part we shall discuss the seemingly stochastic behaviour of a deterministic model proposed by Lorenz [1963]. Though it is not expected that Lorenz' model accurately represents the onset of turbulence, it has, however, a rather intrinsic interest as it may be taken as a counter example to the usual dogma (and its ensuing folklore) in the physicists' community, according to which stochasticity arises either from the interaction of an infinite number of degrees of freedom or from an external noise source (usually chosen gaussian as the randomness is related to an infinite number of degrees of freedom via the central limit theorem). It will appear from the analysis of Lorenz' model that in systems far away from thermodynamic equilibrium, stochasticity or randomness can merely arise from the deterministic dynamics of a few macroscopic degrees of freedom. We may very well agree with the reader that a macroscopic degree of freedom hides almost on every occasion encountered in physics, an infinite number of them at a lower and rather more sophisticated level of description.

The Lorenz' equations are

$$\dot{X} = \sigma(Y - Z) \tag{1.a}$$

$$\dot{Y} = -XZ + rX - Y \tag{1.b}$$

$$\dot{Z} = XY - bZ \tag{1.c}$$

It must be clearly recognized that the behaviour of three-dimensional systems like (1) is not at all as well understood as the behaviour of systems with two degrees of freedom. In the latter case, it is often possible to prove that a well-defined asymptotic state exists, which may be either a limit curve or a stable fixed point as discussed in textbooks on differential equations (see La Salle and Lefshetz [1961] or Coddington and Levinson [1955]). For aystems such as (1) there is actually no detailed description of the geometry of the attractors. The analysis of the behaviour of (1) uses mainly the properties of the linearized motion in the vicinity of points. As shown by Lorenz, for $r > r_T = \frac{\sigma(\sigma+b+3)}{\sigma-b-1}$ $(= \frac{470}{19}$ if $\sigma = 10$, $b = 8/3)$ these points are: two "convection" points $C_{\pm} = (\pm\, b(r-1), \pm\, b(r-1), r-1)$ and one "conduction" point $0 = (0,0,0)$ are unstable to linear perturbations.

The conduction point (0,0,0) is attractive in two directions: one direction in the plane $Z = 0$, and the axis oZ and it is repulsive only in one direction of the plane $Z = 0$. The axis oZ is a possible trajectory, as $X = Y = 0$, $Z = Z_o e^{-bt}$ is a solution of (1). This shows that a point starting close to the conduction point is attracted by the plane of the two stable directions (or "stable manifold") and repelled along the unstable directions. Practically, it moves closer and closer to the unstable line starting from 0. It will move in one of the directions defined by this line, depending on the half-space where it started from. In the neighborhood of the origin, these two half-spaces are separated by the plane defined by the two stable directions. Should this separating surface divide

the whole space like a plane does, the motion of any point would remain in one of these half-spaces; but this is not the case. Let us then look at the vector field generated by $(\dot{X},\dot{Y})$ in any horizontal plane (i.e., at fixed Z). The plane motion of a point corresponding to this field is described by (1) Z being a fixed parameter. The origin is the fixed point of this vector field and any motion around it is very simple, as the equations are linear. For $Z < Z_c = r - 1$, the point (0,0) (actually the vertical axis) is attractive in one direction and repulsive in another. For $Z_c < Z < Z'_c = Z_c + \frac{(\sigma+1)^2}{4}$, the point (0,0) is attractive in any direction and two real trajectories (which are straight lines) go through the origin. For $Z > Z'_c$, these trajectories are no longer real and any point converges toward the origin following a spiralling motion.

This means that below a given height ($Z < Z_c$), a point is repelled by the axis oZ, but if it goes high enough it is attracted instead, either by an almost straight or by a spiralling motion. This will explain that, if during its trajectory a point moves at high Z it may rotate enough around the vertical axis and pass on any side of the separating surface upon descending. Thus, this surface cannot actually separate the trajectories "in the large".

Consider now the neighborhood of the other two fixed points, i.e., the "convection" points $C_\pm = (\pm\sqrt{b(r-1)}, \pm\sqrt{b(r-1)}, r-1)$. For $r > r_T$ they are attractive in one direction and repulsive in a plane. (This is a plane close to C, and becomes more or less curved surface far away, to actually yield the

unstable manifolds of C_+ and C_-). In this plane, the repulsion occurs through a spiralling motion (it corresponds to two complex conjugate eigenvalues of the stability matrix). It is not difficult to understand how a point moves, starting close to one of these convection points, say C_+. It begins to revolve around C_+ by slowly going away and yet pointing at the same time toward the unstable manifold of C_-. When the spiral has grown enough, it is attracted by the axis oZ when $Z > Z_c$ and repelled when $Z < Z_c$. When it reaches the height Z'_c, it rotates around the axis oZ and goes down on the other side of the separating surface passing through the origin. As the origin is repulsive in one direction, the point is "violently" repelled toward the convection point C_- as the two unstable orbits starting from the origin pass close to the convection points (it is likely that they join exactly these convection points, in which case they would constitute the so-called heteroclinic orbits of Poincaré). Then the point begins again to revolve around C_-, and so on.

This qualitative picture of the 3d motion is simplified by restricting oneself to the so-called Poincaré transform. Consider the successive intersection of the upward trajectories with the horizontal plane of the convection point, i.e., the plane $Z = r - 1$. Let $(X_1,Y_1),(X_2,Y_2),\ldots(X_n,Y_n),\ldots$ be these intersections. The Poincaré transform is the law of correspondence (or 2d mapping) that relates (X_n,Y_n) to (X_{n-1},Y_{n-1}).

A first important property of this mapping is that it contracts the 'volume'. Consider an ensemble of initial

conditions filling a volume V(0). As $\frac{\partial \dot{X}}{\partial X} + \frac{\partial \dot{Y}}{\partial Y} + \frac{\partial \dot{Z}}{\partial Z} = -(\sigma+b+1)$, at time t the volume occupied in phase space by the arrival points is $\rho(t)V(o)$ with $\rho(t) = \exp(-\sigma+b+1)t$. As the motion between two crossings with the plane $Z = r - 1$ is more or less similar for a large class of initial points, the quantity $\rho(T)$ defines the contraction factor of the Poincaré mapping, T being the mean period of the motion: an ensemble of points lying on a surface of measure σ, occupies a surface $\sigma\rho(T)$ after one application of the Poincaré transform. This explains that the attractor of Poincaré transform is a set of zero measure, since it is stable (by definition) under this transform, which implies that, if it would occupy a surface σ_o, then

$$\rho(T)\,\sigma = \sigma_o \tag{2}$$

which is satisfied for $\sigma_o = 0$ or ∞ only. The case $\sigma_o = \infty$ is disregarded since, as shown by Lorenz, they are regions of space which are stable by the equations of the motions (what we actually mean here by "stable" will appear at once). For that purpose one considers the ellipsoid of equation

$$\beta X^2 + Y^2 + (Z - r - \sigma)^2 = K \tag{3}$$

with $K >> 1$ and $\beta > 0$.

The scalar product of the velocity of a point (X,Y,Z) on this ellipsoid with the outward normal to the surface is at large K (i.e., by neglecting linear terms):

$$\underset{\sim}{n} \cdot \dot{\underset{\sim}{X}} \approx -\left[X^2\beta\sigma + Y^2 - XY\sigma(\beta-1) + bZ^2\right] \qquad (4)$$

as $X^2\beta\sigma + Y^2 \geq 2XY\sqrt{b\sigma}$, it is possible to choose β (for instance $\beta = 1$) so that $\dot{\underset{\sim}{X}} \cdot \underset{\sim}{n} < 0$ at large K, so that the ellipsoid is "stable" as no point can leave it, and the attractor is inside all the stable ellipsoids constructed in this way.

Following Ruelle [1976], let us call $\Gamma_{\pm}$ the curves which are the intersects of the unstable manifolds of $C_{\pm}$ with the plane $z = r - 1$, and let Σ be the intersect of the stable manifold of the conduction point with the same horizontal plane. The picture is approximately given in Fig. 1. Consider now the successive transform of a point P_1 close to C_-. The first iterates are attracted by Γ_- and repelled along this line, as Γ_- belongs to an unstable manifold of the original equations (in other terms, at each turn around C_-, the point diverges in the direction of the two complex conjugate unstable eigenvectors of C_-). This corresponds, approximately, to the iterates P_1 to P_4 drawn on Fig. 1. In its motion after P_4, we shall assume that the point jumps high enough to rotate around the vertical axis $x = y = 0$, and to go down on the other side of Σ, so that the next iterate, i.e., P_5, is close to C_+. The process begins again: the next iterate moves from P_5 to Σ, jumps to C_-, and so on.

Consider now, instead of a point, a set of points on a surface which is drawn along Γ_- between C_- and Σ. By applying the Poincaré transform to this set of initial points, one finds that at each turn the points closer to are ejected toward C_+, which makes appear a small sheet of arrival points

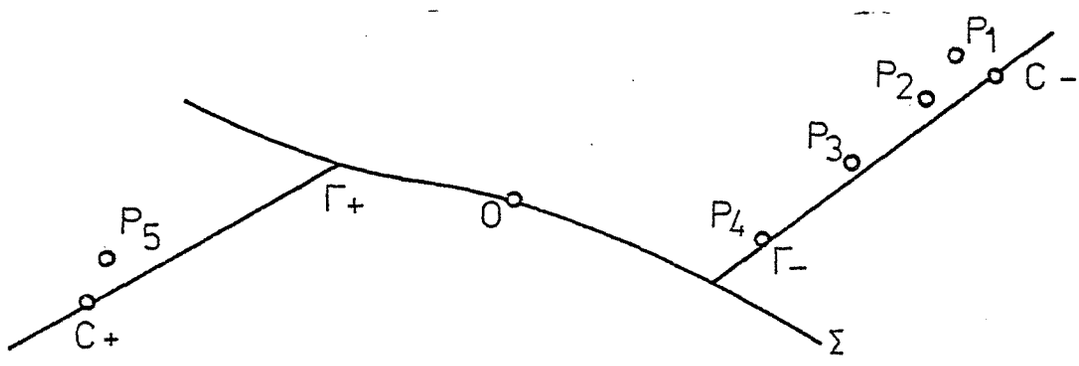

Fig. 1. Poincaré's map generated by the Lorenz model in the plane $Z = r - 1$. $C_{\pm}$ are the 'convection' points, Σ is the stable manifold of the conduction point and $\Gamma_{\pm}$ are the unstable manifolds of $C_{\pm}$.

close to Γ_+. At the next turn, this sheet is stretched along Γ_+ and after a few turns, part of it is ejected again toward C_-. The Poincaré transform is a deterministic mapping as the original equations of the motions. This means that the new sheet appearing close to C_- is approximately parallel and at some distance from the points remaining close to Γ_- (i.e., the points which were close enough to C_- at the beginning, so that after a number of applications of the Poincaré transform, they have not yet been pulled out of Γ_-). On the other hand, after each application of the transform, the area of the ensemble of points occupied by the sheets is reduced by the contraction factor $\rho(T)$. This contraction is mainly due to a thickening perpendicular to the unstable manifolds Γ_+. Thus, if one recapitulates the whole process, starting from a one-sheet system along Γ_-, we now have approximately two parallel sheets with a length of the same order as the one of the original sheets.

Consider now the intersect of these sheets by a line approximately perpendicular to Γ_-. Starting from an ensemble of initial conditions filling a segment on this line, after a few applications of the Poincaré transform, the central part of this segment has been deleted. By continuing the process, we again drop the central part of the remaining segments, and so on. This is the way to generate a Cantor set(*).

(*) A well known Cantor set is obtained by deleting from $|0,1|$ it central part, $|1/3,2/3|$, then by deleting the central part of the two remaining segments, i.e., $|1/9,2/9|$ and $|7/9,8/9|$, and so on. The Cantor set is what remains after an infinite number of applications of this process. To characterize this ensemble, it is useful to write the number between 0,1 on the basis 3 (i.e., by using the digits 0,1,2 only), then any element of this Cantor set is of the form $\sum_{i=1}^{\infty} a_i 3^{-i}$ where a_i = either 0 or 2. This shows that the Cantor set is not denumerable, although it has obviously a zero measure.

The object obtained from the initial sheet after an infinite number of applications of the Poincaré transform is by definition the section of the attractor of the motion with the plane $Z = r - 1$. This explains that the Lorenz attractor is continuous in the direction of the unstable manifolds of $C_{\pm}$ and has a Cantor structure along the normal to this manifold. Let x be a point on the attractor, then a local system of curvilinear coordinates exists such that if (0,0,0) defines x then (u_1,u_2,u_3) belongs to the attractor provided (u_1,u_2) belongs to some finite interval around (0,0) though u_3 belongs to a Cantor (or Cantor-like) set.

The motion defined by the Lorenz equations has the property of mixing, which may be considered as a mathematical version of the general statement: X(t) has an erratic motion for almost any initial condition. Starting from two neighboring points, then after some delay, the arrival points become almost completely uncorrelated namely, shortly after the time of start the two curves become completely different. The explanation of this fact is quite simple: at each turn the point is either ejected toward the other convection point or remains on the same stable manifold. Thus, starting from two close points P_o and P'_o, their distance increases exponentially along the unstable manifold and after a number of turns one of these points will be ejected and the other will not, and the trajectories will become completely different from this instant on.

The mixing property is equivalent to the absence of "long time" correlations or of memory effects, and it may be restated as follows. Let $\psi(x)$ and $\phi(x)$ be any two smooth functions of $X = (X,Y,Z)$, then the time average

$$\left\langle \psi[\underset{\sim}{X}(t)]\, \phi[\underset{\sim}{X}(t+\tau)] \right\rangle \xrightarrow[\tau\to\infty]{} \langle\psi\rangle\langle\phi\rangle \qquad (5)$$

where, by definition

$$\langle f[\underset{\sim}{X}(t)]\rangle = \lim_{\tau\to\infty} \frac{1}{\tau}\int_0^{\tau} f[\underset{\sim}{X}(t)]\, dt \qquad (6)$$

The time correlation functions of the Lorenz equations have indeed this mixing property. Thus, a simple deterministic system with a few degrees of freedom may actually appear as having a random behavior, not originated as the amplification of some random noise.

REFERENCES

CODDINGTON, E. A. and N. LEVINSON, 1955, Theory of Ordinary Differential Equations (McGraw-Hill, New York).

LA SALLE, J. P. and S. LEFSHETZ, 1961, Stability by Liapunov's Direct Method with Applications (Academic Press, New York).

LORENZ, E. N., 1963, J. Atmos. Sci. 20, 130.

RUELLE, D., 1976, preprint.

Acknowledgements

The present work represents the joint effort of the author with C. Normand and Y. Pomeau (C.E.N. de Saclay), R. Pérez Cordón, J.L. Ibáñez, V. Fairén and J. Hernández (Madrid). Fruitful discussions and/or correspondence took place with P. Bergé and M. Dubois-Gance (C.E.N. de Saclay) and E.L. Koschmieder (University of Texas at Austin). To all of them the author of this report wishes to express his sincere appreciation and thanks.

Parts I and III, written with C. Normand and Y. Pomeau belong to an already accepted paper in Reviews of Modern Physics, to appear in 1977. Part II accounts for two published notes (Physics Letters 58A (1976) 364, and 59A (1976) 335) and a third paper to be published in the Journal of Non-equilibrium Thermodynamics. The latter three have been written with J.L. Ibáñez and V. Fairén. The part on the non-periodic (strange) attractor belongs also to a paper by J.L. Ibáñez and Y. Pomeau due to appear in the Journal of Non-equilibrium Thermodynamics.

J.E.N. 379

Junta de Energía Nuclear, Departamento de Tecnología de Reactores, Madrid

"Inestabilidades en capas fluidas y en sistemas de reacción-difusion: Estados estacionarios, ciclos límites, atractores no periodicos y otros fenómenos no lineales convectivos o no".

GARCIA VELARDE, M. (1977) 144 pp. 9 figs. 105 refs.

En este trabajo se estudian las inestabilidades termoconvectivas de capas fluidas con especial hincapié en el problema de Rayleigh-Bénard. En la aproximación de Boussinesq-Oberbeck se presentan tanto soluciones estacionarias como dependientes del tiempo (tales como las oscilaciones de relajación) y asimismo se discute la transición a la turbulencia.

También se estudian las soluciones estacionarias, ciclos límites y estructuras espaciales inhomogéneas (ordenadas: estructuras disipativas) en sistemas sencillos de reacción-difusión.

J.E.N. 379

Junta de Energía Nuclear, Departamento de Tecnología de Reactores, Madrid.

"Inestabilidades en capas fluidas y en sistemas de reacción-difusion: Estados estacionarios, ciclos límites, atractores no periodicos y otros fenómenos no lineales convectivos o no".

GARCIA VELARDE, M. (1977) 144 pp. 9 figs. 105 refs.

En este trabajo se estudian las inestabilidades termoconvectivas de capas fluidas con especial hincapié en el problema de Rayleigh-Bénard. En la aproximación de Boussinesq-Oberbeck se presentan tanto soluciones estacionarias como dependeintes del tiempo (tales como las oscilaciones de relajación) y asimismo se discute la transición a la turbulencia.

También se estudian las soluciones estacionarias, ciclos límites y estructuras espaciales inhomogéneas (ordenadas: estructuras disipativas) en sistemas sencillos de reacción-difusión.

J.E.N. 379

Junta de Energía Nuclear, Departamento de Tecnología de Reactores, Madrid.

"Inestabilidades en capas fluidas y en sistemas de reacción-difusión: Estados estacionarios, ciclos límites, atractores no periódicos y otros fenómenos no lineales convectivos o no".

GARCIA VELARDE, M. (1977) 144 pp. 9 figs. 105 refs.

En este trabajo se estudian las inestabilidades termoconvectivas de capas fluidas con especial hincapié en el problema de Rayleigh-Bénard. En la aproximación de Boussinesq-Oberbeck se presentan tanto soluciones estacionarias como dependientes del tiempo (tales como las oscilaciones de relajación) y asimismo se discute la transición a la turbulencia.

También se estudian las soluciones estacionarias, ciclos límites y estructuras espaciales inhomogéneas (ordenadas: estructuras disipativas) en sistemas sencillos de reacción-difusión.

J.E.N. 379

Junta de Energía Nuclear, Departamento de Tecnología de Reactores, Madrid.

"Inestabilidades en capas fluidas y en sistemas de reacción-difusión: Estados estacionarios, ciclos límites, atractores no periódicos y otros fenómenos no lineales convectivos o no".

GARCIA VELARDE, M. (1977) 144 pp. 9 figs. 105 refs.

En este trabajo se estudian las inestabilidades termoconvectivas de capas fluidas con especial hincapié en el problema de Rayleigh-Bénard. En la aproximación de Boussinesq-Oberbeck se presentan tanto soluciones eatacionarias como dependientes del tiempo (tales como las oscilaciones de relajación) y asimismo se discute la transición a la turbulencia.

También se estudian las soluciones estacionarias, ciclos límites y estructuras espaciales inhomogéneas (ordenadas: estructuras disipativas) en sistemas sencillos de reacción-difusión.

Por último, se construye el atractor no periódico (o anómalo) que aparece para altos números de Rayleigh en el modelo de Lorenz de ecuaciones de Boussinesq-Oberbeck truncadas y se discute asimismo el fenómeno de la turbulencia.

CLASIFICACION INIS Y DESCRIPTORES: A14. A11. Convective instabilities. Lyapunov method. Chemical reaction kinetics. Landau fluctuations. Hydrodynamics. Nonlinear problems.

Por último, se construye el atractor no periódico (o anómalo) que aparece para altos números de Rayleigh en el modelo de Lorenz de ecuaciones de Boussinesq-Oberbeck truncadas y se discute asimismo el fenómeno de la turbulencia.

CLASIFICACION INIS Y DESCRIPTORES: A14. A11. Convective instabilities. Lyapunov method. Chemical reaction kinetics. Landau fluctuations. Hydrodynamics. Nonlinear problems.

Por último, se construye el atractor no periódico (o anómalo) que aparece para altos números de Rayleigh en el modelo de Lorenz de ecuaciones de Boussinesq-Oberbeck truncadas y se discute asimismo el fenómeno de la turbulencia.

CLASIFICACION INIS Y DESCRIPTORES: A14. A11. Convective instabilities. Lyapunov method. Chemical reaction kinetics. Landau fluctuations. Hydrodynamics. Nonlinear problems.

Por último, se construye el atractor no periódico (o anómalo) que aparece para altos números de Rayleigh en el modelo de Lorenz de ecuaciones de Boussinesq-Oberbeck truncadas y se discute asimismo el fenómeno de la turbulencia.

CLASIFICACION INIS Y DESCRIPTORES: A14. A11. Convective instabilities. Lyapunov method. Chemical reaction kinetics. Landau fluctuations. Hydrodynamics. Nonlinear problems.

J.E.N. 379

Junta de Energía Nuclear, Departamento de Tecnología de Reactores, Madrid

"Instabilities in fluid layers and in reaction-diffusion systems: Steady states, time-periodic solutions, non-periodic attractors, and related convective and otherwise non-linear phenomena".

GARCIA VELARDE, M. (1977) 144 pp. 9 figs. 105 refs.

Thermoconvective instabilities in horizontal fluid layers are discussed with emphasis on the Rayleigh-Bénard model problem. Steady solutions and time-dependent phenomena (relaxation oscillations and transition to turbulence) are studied within the nonlinear Boussinesq-Oberbeck approximation.

Homogeneous steady solutions, limit cycles, and inhomogeneous (ordered) spatial structures are also studied in simple reaction-diffusion systems.

Lastly, the non-periodic attractor that appears at large Rayleigh numbers in the truncated Boussinesq-Oberbeck model of Lorenz, is constructed, and a discussion of

J.E.N. 379

Junta de Energía Nuclear, Departamento de Tecnología de Reactores, Madrid

"Instabilities in fluid layers and in reaction-diffusion systems: Steady states, time-periodic solutions, non-periodic attractors, and related convective and otherwise non-linear phenomena".

GARCIA VELARDE, M. (1977) 144 pp. 9 figs. 105 refs.

Thermoconvective instabilities in horizontal fluid layers are discussed with emphasis on the Rayleigh-Bénard model problem. Steady solutions and time-dependent phenomena (relaxation oscillations and transition to turbulence) are studied within the nonlinear Boussinesq-Oberbeck approximation.

Homogeneous steady solutions, limit cycles, and inhomogeneous (ordered) spatial structures are also studied in simple reaction-diffusion systems.

Lastly, the non-periodic attractor that appears at large Rayleigh numbers in the truncated Boussinesq-Oberbeck model of Lorenz, is constructed, and a discussion of

J.E.N. 379

Junta de Energía Nuclear, Departamento de Tecnología de Reactores, Madrid.

"Instabilities in fluid layers and in reaction-diffusion systems: Steady states, time-periodic solutions, non-periodic attractors, and related convective and otherwise non-linear phenomena".

GARCIA VELARDE, M. (1977) 144 pp. 9 figs. 105 refs.

Thermoconvective instabilities in horizontal fluid layers are discussed with emphasis on the Rayleigh-Bénard model problem. Steady solutions and time-dependent phenomena (relaxation oscillations and transition to turbulence) are studied within the nonlinear Boussinesq-Oberbeck approximation.

Homogeneous steady solutions, limit cycles, and inhomogeneous (ordered) spatial structures are also studied in simple reaction-diffusion systems.

Lastly, the non-periodic attractor that appears at large Rayleigh numbers in the truncated Boussinesq-Oberbeck model of Lorenz, is constructed, and a discussion of

J.E.N. 379

Junta de Energía Nuclear, Departamento de Tecnología de Reactores, Madrid.

"Instabilities in fluid layers and in reaction-diffusion systems: Steady states, time-periodic solutions, non-periodic attractors, and related convective and otherwise non-linear phenomena".

GARCIA VELARDE, M. (1977) 144 pp. 9 figs. 105 refs.

Thermoconvective instabilities in horizontal fluid layers are discussed with emphasis on the Rayleigh-Bénard model problem. Steady solutions and time-dependent phenomena (relaxation oscillations and transition to turbulence) are studied within the nonlinear Boussinesq-Oberbeck approximation.

Homogeneous steady solutions, limit cycles, and inhomogeneous (ordered) spatial structures are also studied in simple reaction-diffusion systems.

Lastly, the non-periodic attractor that appears at large Rayleigh numbers in the truncated Boussinesq-Oberbeck model of Lorenz, is constructed, and a discussion of

turbulent behavior is given.

INIS CLASSIFICATION AND DESCRIPTORS: A14. A11. Convective instabilities. Lyapunov method. Chemical reaction kinetics. Landau fluctuations. Hydrodynamics. Nonlinear problems.

turbulent behavior is given.

INIS CLASSIFICATION AND DESCRIPTORS: A14. A11. Convective instabilities. Lyapunov method. Chemical reaction kinetics. Landau fluctuations. Hydrodynamics. Nonlinear problems.

turbulent behavior is given.

INIS CLASSIFICATION AND DESCRIPTORS: A14.A11. Convective instabilities. Lyapunov method. Chemical reaction kinetics. Landau fluctuations. Hydrodynamics. Nonlinear problems.

turbulent behavior is given.

INIS CLASSIFICATION AND DESCRIPTORS: A14.A11. Convective instabilities. Lyapunov method. Chemical reaction kinetics. Landau fluctuations. Hydrodynamics. Nonlinear problems.